RADICAL POLYMERIZATION KINETICS OF BIO-RENEWABLE BUTYROLACTONE MONOMERS IN AQUEOUS SOLUTION

by

Sharmaine Beatrice Luk

A thesis submitted to the Department of Chemical Engineering

in conformity with the requirements for

the degree of Master of Applied Science

Queen's University

Kingston, Ontario, Canada

(August, 2017)

Abstract

In this study, a bio-derived monomer, γ-methyl-α-methylene-γ-butyrolactone (MeMBL) was saponified with sodium hydroxide (NaOH) to make the water-soluble monomer sodium 4-hydroxy-4-methyl-2-methylene butanoate (SHMeMB), that was copolymerized via radical polymerization in aqueous solution with acrylamide (AM) and crosslinker to synthesize superabsorbent hydrogels. Absorbency of these hydrogels was shown to be much higher than sodium acrylate hydrogels, with mechanical properties varying with molar composition and crosslinking content. Reactivity ratio of SHMeMB:AM at 50°C and 15 wt% were estimated using low conversion data (r_{SHMeMB}=0.12 and r_{AM}=1.10), and the integrated Mayo-Lewis equation (r_{SHMeMB}=0.17 and r_{AM}=0.95). However, *in-situ* NMR results showed that SHMeMB:AM copolymerizations proceed at a slower rate than of a similar system of AM copolymerized with sodium 4-hydroxy-2-methylene butanoate (SHMB), a similar monomer produced by ring-opening of α-methylene-γ-butyrolactone (MBL). Pulsed-laser polymerization coupled with size exclusion chromatography (PLP-SEC) studies were done for both systems at 60°C and 10 wt% monomer concentration. Homopolymerization k_p values were estimated to be 25 and 165 L/mol·s for SHMeMB and SHMB, respectively, confirming that SHMeMB is less reactive than SHMB.

Further kinetic studies of SHMeMB:AM copolymerization and homopolymerization of SHMeMB were conducted at elevated temperatures. SHMeMB conversions achieved a limiting value which decreased at higher temperatures, suggesting that polymerization rate was limited by depropagation. Comonomer composition drift also increased with temperature, with more AM incorporated into the polymer while SHMeMB underwent depropagation. Homopolymerization of SHMeMB with added sodium chloride (NaCl) showed a decrease in polymerization rate explained by an increase in propagation rate coefficient (k_p) but an even greater increase in termination rate coefficient (k_t) as supported by parameter estimation done using PREDICI. Even with added salt, however, depropagation was the dominant mechanism at higher temperatures. Lastly, the kinetic parameters estimated were implemented in a copolymerization model used

to estimate the variation of k_t with composition in SHMeMB:AM copolymerizations. It was found that the overall termination rate coefficient was dominated by the presence of SHMeMB, with as the estimate for $k_{t,SHMeMB}$ of the same order of magnitude as k_t of another ionized water-soluble monomer, sodium methacrylic acid.

Co-Authorship

During the time I spent at the Polymer Institute of the Slovak Academy of Sciences, I worked in Dr. Igor Lacik and Dr. Jaroslav Mosnáček's groups for the work described in Chapter 4. The kinetics research was supervised by Dr. Igor Lacík, who provided guidance and reviewed the PLP-SEC results. Additionally, I collaborated with Dr. Jozef Kollár in synthesizing the superabsorbent hydrogels, as he had experience synthesizing the SHMB:AM hydrogels. We worked together on preparing samples and injecting them into the sealed glass cells to make the hydrogels. He also helped me in conducting the swelling tests in water. Jozef and I reviewed our hydrogel synthesis results with Dr. Jaroslav Mosnáček, who helped analyze SHMeMB ring-closure mechanisms and hydrogel synthesis. Jozef sent the hydrogel samples to Miroslav Mrlík in Czech Republic for mechanical testing and SEM imaging, and he assisted in interpreting these results.

Acknowledgements

I would like to thank Dr. Robin Hutchinson, my supervisor, for advising me in the last three years during both my Master's degree and undergraduate thesis. I especially appreciate Robin's generosity in funding me to go to several international conferences and working abroad in Bratislava, Slovakia for 3 months. His attention to detail motivates me to be more comprehensive in my own research.

I am grateful for the hospitality from Dr. Igor Lacík and Dr. Jaroslav Mosnáček's groups at the Polymer Institute at the Slovak Academy of Sciences (PISAS) in Bratislava, Slovakia. Igor brought me to the Polymer Conference in the High Tatras of Slovakia, so I got to see more than just Bratislava. Anna Chovancová went above and beyond in helping me settle in a foreign city, as well as training me in using the laboratory equipment for PLP-SEC. Dr. Jozef Kollár is another great mentor and collaborator, who I very much enjoyed working with. I am very glad to have made many international friends at PISAS, even with the language barrier!

I'd also like to thank my colleagues and friends in the Hutchinson/Cunningham lab groups for their helpful insight and scientific discussions, particularly the PhDs who I've known since fourth year of my undergraduate degree.

To all my friends that I made during my undergraduate and master degrees, some who were here for both, I thank you for the good times and support in and out of school. Knowing you certainly made my experience at Queen's University unforgettable and I will leave here with friendships that will last a long time.

Lastly, I want to thank my parents for their support while I stayed in school. I'm sure you would like me to go on to real world soon and become completely financially independent, but hopefully you're not too disappointed I'm going to do a PhD.

Table of Contents

Abstract ii

Co-Authorship iv

Acknowledgements v

List of Figures ix

List of Tables xv

List of Abbreviations xvii

1 Introduction 1

2 Literature Review 5

2.1 PLP-SEC: Theory and Technique 5

2.2 Effect of ionization and monomer concentration on k_p in aqueous solution 7

2.3 In-situ NMR method 13

2.4 Depropagation: Background 16

2.5 Summary 22

3 Experimental Methods 23

3.1 Materials 23

3.2 Synthesis and Techniques 23

3.2.1 Ring-opening saponification of MBL and MeMBL 23

3.2.2 Superabsorbent Hydrogel Synthesis and Absorption 24

3.2.3 Preparation for *in-situ* NMR studies 25

3.2.4 Preparation for PLP-SEC studies 26

3.2.5 Kinetic parameters for PREDICI parameter estimation 27

4 Superabsorbent Hydrogel Characterization and Kinetics 30

4.1 Ring-closure of SHMB and SHMeMB 30

4.2 Superabsorbent Hydrogel Absorption 31

4.3 Kinetic studies using in-situ NMR 38

4.4 PLP-SEC studies 41

4.5 Summary 48

5 Investigating the influence of depropagation and ionic strength on SHMeMB (co)polymerization 49

5.1 Copolymerization of SHMeMB:AM at different temperatures 49

5.2 Homopolymerization kinetics of SHMeMB 52

5.3 Reactivity ratio estimations for SHMeMB:AM copolymerizations 57

5.4 Parameter estimation for SHMeMB homopolymerizations 60

5.5 Parameter estimation for SHMeMB:AM copolymerizations with depropagation 68

6 Conclusions and Recommendations 73

7 References 76

8 Appendices 86

A. Characterization of MeMBL and SHMeMB 86

B. Ring-closure of SHMeMB under acidic conditions 90

C. PLP-SEC experiments 92

D. Monomer concentration of SHMeMB and AM at different temperatures 94

E. 3:7 SHMeMB:AM copolymerizations at with V-50 and V-86 96

F. SHMeMB:AM conversion profiles with parameter estimation 97

List of Figures

Figure 1: MMD (–) and the first derivate of the distribution (⋯) of poly(dodecyl acrylate) produced at -4°C, 200 bar, and laser pulse repetition rate of 100 Hz from dodecyl acrylate in solution with 36 wt% CO_2. Reprinted with permission from [43], © 2001 Elsevier Ltd. 6

Figure 2: a) Dependence of k_p on non-ionized acrylic acid concentration in aqueous solution at 2, 10, and 20°C. The solid lines were calculated based on correlations in reference [24]. Reprinted with permission from [24], © 2003 American Chemical Society. b) Dependence of k_p on non-ionized methacrylic acid concentration in aqueous solution at 25°C. Reprinted with permission from [26], © 2006 American Chemical Society. 8

Figure 3: Dependence of k_p as a function of a) degree of ionization and b) pH of acrylic acid in aqueous solution at [AA]=0.69 mol/L and 6°C. Reprinted with permission from [25], © 2004 Wiley-VCH Verlag GmbH & Co. 10

Figure 4: Ratio of $k_{p(\alpha)}$ to $k_{p(\alpha=0)}$ as a function of degree of association for MAA at 5 wt% monomer at various temperatures and AA at 5 wt% and 6°C. Reprinted with permission from [27], © 2009 American Chemical Society. 11

Figure 5: The variation in k_p as a function of MAA monomer concentration from 5 to 40 wt% at various degrees of ionization done at 50°C, as fit to PLP-SEC data. Reprinted with permission from [27], © 2009 American Chemical Society. 13

Figure 6: a) Cumulative polymer composition as a function of initial monomer composition estimated at 5 (filled symbols) and 10% (empty symbols) conversion at 5 (◆,◇), 20 (■,□) and 40 (▲,△) wt% monomer. The curve was fitted to give reactivity ratios $r_{AA} = 1.27 \pm 0.26$ and $r_{AM} = 0.54 \pm 0.21$. b) Monomer composition drift as a function of conversion for initial $f_{AA} = 0.3$, 0.5, and 0.8 at 5 (◇), 20 (□), and 40 (△) wt% monomer with 0.217 wt% V-50 and 40ºC. The best-fit reactivity ratios were calculated to be r_{AA} =

1.24 ± 0.02 and r_{AM} = 0.55 ± 0.01. Reprinted with permission from [32], © 2013 Wiley-VCH Verlag GmbH & Co. 15

Figure 7: Chemical structure of a) SHMeMB, b) α-methyl styrene, c) methyl ethacrylate, d) dimethyl itaconate, e) dibutyl itaconate, and f) dicyclohexyl itaconate. 18

Figure 8: a) F_{MEA} vs. f_{MEA} plot of MEA and ST copolymer at 30 and 80°C b) Reactivity ratios of MEA and ST at 30 and 80°C with 95% confidence intervals. Reprinted with permission from [38], © 2000 Elsevier Ltd. 21

Figure 9: a) F_{BMA} vs. f_{BMA} plot of BMA and STY copolymers at 165°C and $[M]_{tot}$=0.7 mol/L (●) and b) at 182°C with $[M]_{tot}$=0.9 mol/L (▲) and $[M]_{tot}$=3.5 mol/L (■). Curves were calculated using Mayo-Lewis with no depropagation kinetics (- -), Lowry's approach (···), and Wittmer's approach (–). Reprinted with permission from [34], © 2006 American Chemical Society. 22

Figure 10: Ring-opening saponification of MBL (top) and MeMBL (bottom) using 1:1 molar ratio of NaOH to butyrolactone ring at 95°C for 2 hours. 24

Figure 11: 2:8 SHMeMB:AM hydrogel with 1.5 mol% crosslinker after swelling (left) and before, i.e. as prepared (right). 34

Figure 12: Swelling ratios of AM:SHMeMB hydrogels made with 0.4 mol% V-50 at 30 wt% monomer for 16 h at varying initial comonomer ratios and BIS crosslinker content, as indicated. 35

Figure 13: Stress vs. strain curves of hydrogels made with a) 1.0 mol% BIS and b) 1.5 mol% BIS and initial comonomer molar ratios of f_{SHMeMB} = 0.2, 0.4, and 0.6 with 30 wt% monomer and 0.4 mol% V-50 in aqueous solution for 16 h at 50°C. 36

Figure 14: Storage (G', filled symbols) and loss (G'', open symbols) moduli measured as a function of frequency for SHMeMB:AM hydrogels produced with monomer molar ratios of 2:8 (top), 4:6 (middle), and 6:4 (bottom) with (left) 1.0 and (right) 1.5 mol% of BIS. 37

Figure 15: SEM images of freeze-dried cross-sections of the SHMeMB:AM hydrogels synthesized at a molar ratio of f_{SHMeMB} = 0.2 with a) 1.0 mol% and b) 1.5 mol% BIS; a molar ratio of f_{SHMeMB} = 0.4 with c)

1.0 mol% and d) 1.5 mol% BIS; and a molar ratio of f_{SHMeMB} = 0.6 with e) 1.0 mol% and f) 1.5 mol% BIS. Hydrogels were synthesized from 30 wt% monomer and 0.4 mol% V-50 for 16 h at 50°C. 38

Figure 16: Overall monomer conversion profiles for polymerization of $f_{SH(Me)MB}$ = 0.2 (left) and $f_{SH(Me)MB}$ = 0.4 (right) initial molar ratios of SHMeMB:AM and SHMB:AM at 50°C with 15 wt% monomer and 1.3 mol% V-50 initiator in D_2O. 39

Figure 17: SHMeMB monomer composition (f_{SHMeMB}) as a function of conversion at varying feed molar ratios of SHMeMB:AM at 15 wt% monomer and 0.5 wt% V-50 at 50°C. Lines represent monomer composition drift computed using the integrated form of the Mayo-Lewis equation with best fit reactivity ratios of r_{SHMeMB}=0.17 and r_{AM}=0.95. 40

Figure 18: (Right) Mayo-Lewis curves for SHMB:AM [23] (solid line) and SHMeMB:AM (points are experimental data and dashed line is best-fit curve) radical copolymerization at 15 wt% monomer and 50°C, where the x-axis represents SH(Me)MB molar fraction in the monomer mixture and the y-axis represents the SH(Me)MB molar fraction in the copolymer at low conversion. (Left) Mayo-Lewis curves for SHMeMB:AM copolymerization calculated using best-fit reactivity ratios estimated from both low conversion data (dashed line, r_{SHMeMB}=0.12 and r_{AM}=1.10) and the integrated form of Mayo-Lewis equation (solid line, r_{SHMeMB}=0.17 and r_{AM}=0.95). 41

Figure 19: Polymer molar mass distributions (left) and first derivative plots (right) produced by PLP of SHMeMB:AM mixtures of varying compositions at 10 wt% monomer, 6.8 mmol/L LiTPO, and 60°C. PLP-SEC experiments for f_{SHMeMB}=0.10 were done with number of pulses=100, and f_{SHMeMB}=0.05 and 0.15 were done with number of pulses=50. 43

Figure 20: Molecular weight distributions and first derivative results of SHMB:AM copolymers at varying compositions with number of pulses=50, 10 wt% monomer, 6.8 mmol/L LiTPO, and at 60°C. 45

Figure 21: k_p^{cop} of SHMeMB:AM and SHMB:AM at varying molar ratios at 10 wt% monomer, 60°C and 6.8 mmol/L LiTPO with error bars representing standard deviation of the data set. The dashed line

represents the terminal model estimating k_p^{cop} for all molar compositions of SHMB:AM and SHMeMB:AM. 46

Figure 22: Overall monomer conversion profiles for copolymerizations at 3:7 (left) and 4:6 (right) initial SHMeMB:AM molar ratios at varying temperatures with 15 wt% monomer and 0.5 wt% V-50. 50

Figure 23: Monomer composition drift with conversion for copolymerization with an initial 3:7 SHMeMB:AM molar ratio, 15 wt% monomer and 0.5 wt% V-50 initiator (left) and 1.67 wt% V-86 initiator (right) at varying temperatures (90°C experiment was conducted with 0.5 wt% V-86). Monomer composition was normalized by initial monomer composition to eliminate the influence of slight variations in the comonomer mixture composition. 51

Figure 24: Monomer conversion profiles obtained by homopolymerization of SHMeMB at 15 and 30 wt% at 75°C and 1 wt% KPS. 53

Figure 25: Monomer conversion profiles obtained by homopolymerization of SHMeMB at 15 and 30 wt% at 75°C and 1 wt% V-86. 54

Figure 26: Monomer conversion profiles obtained from homopolymerization of SHMeMB with 15 wt% monomer and 1 wt% V-86 in aqueous solution at 75 and 90°C. 55

Figure 27: Monomer conversion profiles obtained from homopolymerizations of SHMeMB at 15 wt% with added NaCl salt at 75°C and 1 wt% V-86. 56

Figure 28: Monomer conversion profiles obtained from homopolymerization of SHMeMB at 15 wt% monomer, 1 wt% V-86, and 90°C with added NaCl at 1:0.5 [SHMeMB]:[NaCl] molar ratio. 57

Figure 29: Monomer composition drift for copolymerizations of 3:7 molar ratio of SHMeMB:AM with 15 wt% monomer and 0.5 wt% V-50 at 70 (left) and 80°C (right). The solid line represents parameter estimation with r_{AM} fixed at 0.951 (best-fit value at 50°C), and the dotted line represents parameter estimation to determine both r_{AM} and r_{SHMeMB}. 58

Figure 30: Fit of homopolymerization SHMeMB model assuming no depropagation to monomer conversion profiles obtained at 75°C with 1 wt% V-86 at different monomer concentrations (left) at

different temperatures with 1 wt% V-86 and 15 wt% monomer (right). Solid lines represent model output, with experimental results indicated by data points. 61

Figure 31: $k_p/k_t^{0.5}$ vs conversion profile of SHMeMB homopolymerization at 75°C with 15 and 30 wt% monomer concentration and at 90°C with 15 wt% monomer and 1 wt% V-86 for 15 hours. 62

Figure 32: Conversion profile of SHMeMB homopolymerization at 75°C with 1 wt% V-86 and 15 wt% monomer. The solid line represents parameter estimation using existing experimental data, and the dashed line represents parameter estimation using an extended conversion profile capturing the depropagating behaviour..... 63

Figure 33: Monomer conversion profiles for the homopolymerization of SHMeMB at 90°C with 1 wt% V-86 and 15 wt% monomer. The solid line represents the estimated conversion profile using parameter estimation..... 64

Figure 34: Monomer conversion profiles for the homopolymerization of SHMeMB at 75°C with 1 wt% V-86 and 30 wt% monomer. The solid line represents the estimated conversion profile using parameter estimation..... 65

Figure 35: Monomer conversion profiles from homopolymerization of SHMeMB with different concentrations of added NaCl salt at 75°C with 1 wt% V-86 and 15 wt% monomer. The solid lines represent the conversion profiles using parameter estimation..... 66

Figure 36: k_t of SHMeMB:AM copolymers estimated for copolymerizations done at 50°C with 0.5 wt% V-50 and 15 wt% monomer. 70

Figure 37: Simulated SHMeMB monomer composition drift of SHMeMB:AM copolymerization at initial monomer fraction f_{SHMeMB}=0.3 (left) and f_{SHMeMB}=0.6 (right) with 15 wt% monomer and 0.5 wt% V-50. 72

Figure A. 1: NMR spectra (500 MHz) of MeMBL in DMSO solvent (4.7 ppm) at room temperature and pH=7. 86

Figure A. 2: NMR spectra (500 MHz) of SHMeMB in D_2O (4.7 ppm) at room temperature and pH=7… 87

Figure A. 3: NMR spectra (500 MHz) of equimolar SHMeMB and AM at 25°C (bottom) and 50°C (top) in D_2O (4.7 ppm) and pH=7. 89

Figure A. 4: NMR analysis of SHMeMB homopolymerizations at pH=5 after 16 hours and 15 wt% monomer at 50°C with 1 wt% V-50 (top) and 75°C with 1 wt% KPS (bottom). The red spectra is of the water-soluble phase in D_2O and the green spectra is of the organic phase in DMSO. 91

Figure A. 5: NMR analysis of SHMeMB homopolymerizations at pH=4 after 16 hours and 15 wt% monomer at 50°C with 1 wt% V-50 (top) and 75°C with 1 wt% KPS (bottom). The red spectra is of the water-soluble phase in D_2O and the green spectra is of the organic phase in DMSO. 92

Figure A. 6: PLP-SEC results of SHMeMB:AM copolymers with f_{SHMeMB}=0.1, number of pulses=1000, 10 wt% monomer, 3.4 mmol/L LiTPO, and 60°C. 93

Figure A. 7: PLP-SEC results of SHMeMB:AM copolymers with f_{SHMeMB}=0.1, number of pulses=1000, 10 wt% monomer, 6.8 mmol/L LiTPO, and 60°C. 93

Figure A. 8: SHMeMB and AM concentration as a function of reaction time at 3:7 and 4:6 SHMeMB:AM molar ratios at 15 wt% monomer and 0.5 wt% V-50 at varying temperatures. 95

Figure A. 9: SHMeMB:AM copolymerizations at 15 wt% monomer at varying temperatures to compare composition drift between V-50 and V-86 initiators. 96

Figure A. 10: Conversion profiles of SHMeMB:AM copolymerizations at 15 wt% monomer concentration and 0.5 wt% V-50 at different molar compositions. The solid line represents simulated conversion to estimate k_t. 98

List of Tables

Table 1: Heat of polymerizations and ceiling temperatures of various monomers. T_c calculations were done with [M]=1 mol/L and ΔS= -120 J/mol·K. *T_c of methyl ethacrylate was calculated at bulk monomer concentration, [M]=8.35 mol/L..... 19

Table 2: Reaction mechanisms for copolymerization of SHMeMB and AM..... 28

Table 3: Known rate expressions used in PREDICI for parameter estimation..... 29

Table 4: Total monomer conversions of SHMB:AM copolymerizations conducted with 15 wt% initial monomer [1] and SHMeMB:AM copolymerizations with 15 and 30 wt% initial monomer in aqueous solution at varying feed molar fractions of SHMB (f_{SHMB}) and SHMeMB (f_{SHMeMB}) at 50°C. 32

Table 5: Individual comonomers conversions (X_{AM} and X_{SHMeMB}) molar fractions of monomers incorporated into the final polymer (F_{AM} and F_{SHMeMB}) and total monomers conversion (X) calculated from ^{1}H NMR for linear polymers, and yield of crosslinked polymer (X_{gel}) based on gravimetric analysis of crosslinked polymers prepared with various initial molar fractions of monomers, f_{AM} and f_{SHMeMB} at 50°C. 33

Table 6: PLP-SEC conditions and results for SHMeMB:AM copolymers at 60°C, 6.8 mmol/L LiTPO and 10 wt% monomer. 44

Table 7: PLP-SEC conditions and results of SHMB:AM copolymers at 60°C, 6.8 mmol/L LiTPO and 10 wt% monomer. 46

Table 8: PLP-SEC conditions and results of SHMeMB:AM copolymers at 60°C, 6.8 mmol/L LiTPO and 20 wt% monomer. 48

Table 9: Reactivity ratios estimates from copolymerization of 3:7 molar ratio of SHMeMB:AM with 15 wt% monomer and 0.5 wt% V-50 at 70 and 80°C. The "1 parameter" method estimates r_{SHMeMB} with r_{AM} fixed at 0.951, and the "2 parameter" method estimates both r_{AM} and r_{SHMeMB}. 59

Table 10: Estimated values for k_t and k_{dep} for homopolymerization of SHMeMB at 75°C with 1 wt% V-86 and 15 wt% monomer with 95% confidence interval values. These values are estimated assuming k_p of 25 L/mol·s. 63

Table 11: Estimated values for k_p and k_t for homopolymerizations of SHMeMB with added salt at 75°C with 1 wt% V-86 and 15 wt% monomer. Results are shown for reactions done with 1:0.5 and 1:1 molar ratios of [SHMeMB]:[NaCl]. These values were estimated using a k_{dep} value of 25 s^{-1}. 67

Table 12: Estimated k_t and k_{dep} values using constant k_p=25 L/mol·s compared to values calculated using an assumed E_A value of 12.4 kJ/mol for propagation. 68

Table A. 1: Proton assignment of MeMBL NMR spectra in Figure A. 1. 87

Table A. 2: Proton assignment of SHMeMB NMR spectra in Figure A. 2. 88

Table A. 3: Proton assignment of AM protons at 50°C in Figure A. 3. 89

Table A. 4: Copolymer composition of SHMeMB:AM copolymers (F_{SHMeMB}) at low conversion (<10%) at from batch studies with varying feed comonomer compositions (f_{SHMeMB}). 94

Table A. 5: Propagation rate coefficients of acrylamide calculated as a function of AM concentration for SHMeMB:AM copolymerization at 15 wt% and 50°C. 99

Table A. 6: Simulated SHMeMB and AM radical species concentration for estimation of k_t of SHMeMB:AM copolymerizations at 15 wt% with 0.5 wt% V-50 at 50°C. 99

List of Abbreviations

AA – acrylic acid

ACVA – 4,4'-azobis(4-cyano-valeric acid)

AM – acrylamide

BIS – *N*,*N*'-methylenebis(acrylamide)

BMA – butyl methacrylate

D_2O – deuterated water

DMSO – dimethyl sulfoxide

GPC – gel permeation chromatography

HCl – hydrochloric acid

HEA – 2-hydroxyethyl acrylate

KPS – potassium persulfate

LiTPO – Lithium monoacylphosphine oxide

MAA – methacrylic acid

MALLS – multi-angle laser light scattering

MBL – α-methylene-γ-butyrolactone

MEA – methyl ethacrylate

MeMBL – γ-methyl-α-methylene-γ-butyrolactone

MMA – methyl methacrylate

MMD – molecular mass distribution

MVL – α-methylene-δ-valerolactone ring

NaAA – sodium acrylic acid (fully ionized acrylic acid)

NaCl – sodium chloride

NaOH – sodium hydroxide

NMR – nuclear magnetic resonance

PLP-SEC – pulsed-laser polymerization coupled with size exclusion chromatography

PMBL – poly(α-methylene-γ-butyrolactone)

PMMA – poly(methyl methacrylate)

RI – refractive index

SHMB – sodium 4-hydroxy-2-methylene butanoate

SHMeMB – sodium 4-hydroxy-4 methyl-2-methylene butanoate

ST – styrene

TMAEMC – [2-(methacryloyloxy)ethyl]trimethylammonium chloride

TS – transition state

VOCs – volatile organic compounds

1 Introduction

Water-soluble polymers are used in many applications including drug delivery [1], flocculation for water recovery in oil sand tailings [2], and metal ion recovery [3]. A major use for water-soluble polymers is in personal products for hair care [4] and detergents [5], and crosslinked materials are used for absorbent hydrogels in diapers or feminine products [6]. Synthesizing these materials in aqueous solution provides the additional benefit of eliminating the use of volatile organic compounds (VOCs) and their associated adverse impact on health [7] and the environment [8]. The environmental impact of these materials can be lessened further by using alternative and renewable feedstocks, as the extraction of crude oil also contributes to VOCs in the atmosphere [9] and depends largely on political and economic factors [10]. Some bio-sourced polymers that are currently commercialized are sugar-based poly(lactic acid) [11] and poly(hydroxyalkanoate) [12], with other bio-sourced monomers, including β-myrcene and limonene, that are terpene-based [13].

Tulipalin A, formally known as α-methylene-γ-butyrolactone (MBL), can be derived from 6-tuliposides found in tulips at levels of 0.2 – 2 wt% [14]. Alternatively, MBL can be synthesized from biomass sugar-based itaconic anhydride [15] or pyruvate using acetyl coenzyme A [16]. A similar monomer, γ-methyl-α-methylene-γ-butyrolactone (MeMBL), was synthesized in a catalytic two-step process using bio-derived levulinic acid [17]. Both monomers are lactone rings with an exocyclic double bond amenable to radical attack and have been successfully polymerized to make transparent and hard thermoplastics similar to poly(methyl methacrylate) (PMMA), but with higher glass transition temperature (T_g) and solvent resistance [18] [19]. While the homopolymers demonstrated promising properties, their brittleness led to a focus on radical copolymerization with monomers such as styrene (ST) and methyl methacrylate (MMA) [20] [21]. Both MBL and MeMBL were more reactive compared to ST, and even more so compared to MMA.

These radical polymerizations were all done in bulk or organic solution, with the monomers in their closed-ring form. It was demonstrated that poly(α-methylene-γ-butyrolactone) (PMBL) could be hydrolyzed in the presence of a strong base to open the lactone ring and form poly(α-methylene-γ-hydroxybutyric acid) [18]. In the presence of potassium hydroxide at 100°C, however, the resulting polymer was not completely water-soluble and closure of the lactone rings occurred when acid was added at room temperature. Only when hydrolyzed with a very strong base, such as hydrazine, was the polymer completely water-soluble. The disadvantage of post-polymerization saponification is the incomplete ring-opening of the lactone rings, as also seen in emulsion polymerization of MBL and acrylic acid with crosslinker saponified to make superabsorbent hydrogel particles [22].

More recently, Kollár *et al.* demonstrated that saponification of MBL monomer with sodium hydroxide proceeds rapidly and completely, resulting in a water-soluble monomer [23]. The resulting sodium 4-hydroxy-2-methylene butanoate (SHMB) was then copolymerized with acrylamide (AM) in aqueous solution at different molar ratios in the presence of *N*,*N*'-methylenebis(acrylamide) (BIS) crosslinker to make superabsorbent hydrogels. These new materials exhibited a significantly higher degree of swelling in water than conventional sodium acrylate:AM hydrogel materials [23]. The same study also provided some information regarding the radical polymerization kinetics, reporting reactivity ratios of the system and demonstrating that the homopolymerization rate of SHMB was very slow compared to AM. However, copolymerization of SHMB and AM and homopolymerization kinetics of SHMB in aqueous solution are still not well-understood.

There are previous kinetic studies examining the radical polymerization of various aqueous monomers like non-ionized to fully ionized acrylic and methacrylic acids [24] [25] [26] [27] and acrylamide [28]. Propagation rate coefficients (k_p) were determined for these aqueous systems using pulsed-laser polymerization coupled with size exclusion chromatography (PLP-SEC), an IUPAC recommended method for determining k_p [29]. Water-soluble monomers exhibit different polymerization kinetics than the same

monomers in most organic solutions. Non-ionized acrylic acid and methacrylic acid have higher k_p values in water than in methanol and dimethyl sulfoxide (DMSO) [30], and monomer concentration was found to greatly influence the magnitude of propagation rate coefficients of acrylic acid [25], methacrylic acid [27], and acrylamide [31] in aqueous solution. The dependence of k_p on monomer concentration was attributed to hydrogen-bonding effects between water, monomer, and radical species. Although k_p was dependent on monomer concentration, it was found that the reactivity ratios of AM and non-ionized acrylic acid copolymerization were constant with concentration using an *in-situ* NMR technique [32]. It should be noted that hydrogen-bonding effects are not only present in aqueous solution, but also influence reactivity ratios of butyl methacrylate (BMA) and 2-hydroxyethyl acrylate (HEA) copolymerization in organic solution, as the relative reactivity of the two monomers is dependent on solvent choice [33].

Another kinetic effect that will be considered in this study is depropagation. In free radical polymerization, monomer addition to a growing macroradical (propagation) can usually be considered as an irreversible reaction. However, depropagation, the process by which a single monomer unit is released from the growing radical chain, can also occur if there is steric hindrance near the radical site. Therefore, the propagation and depropagation mechanisms become a reversible reaction pair, with the relative rates (and hence overall rate of polymerization) a function of temperature and monomer concentration. Some monomers that are known to depropagate are butyl methacrylate [34], itaconates [35], methyl ethacrylate [36], and α-methyl styrene [37]. In the presence of appreciable rates of depropagation, the polymerization does not reach full monomer conversion and the reaction can also influence copolymer composition as well as rate, as seen with methyl ethacrylate and styrene copolymerization [38]. In comparison to the homopolymerization of MBL, the similar monomer α-methylene-δ-valerolactone ring (MVL) exhibits effects of depropagation, with an estimated ceiling temperature of 83°C [39]. Depropagation of MVL was attributed to its non-planar structure that hinders the radical center, but MBL does not depropagate because it is planar in structure.

Currently, MBL is only available in small scale for research purposes and it is extracted from renewable resources. However, MeMBL was synthesized in a more cost-efficient way by DuPont [17], also from bio-derived sources, and the scale-up to commercial production has been investigated. Therefore in this work, MeMBL was saponified to make sodium 4-hydroxy-4-methyl-2-methylene butanoate (SHMeMB) and copolymerized with AM and BIS crosslinker to make similar superabsorbent hydrogels as those produced from SHMB. Properties of the SHMeMB:AM and SHMB:AM hydrogels were compared, with the differences between the two systems motivating studies to understand their relative reactivities using *in-situ* NMR. In addition, the k_p^{cop} of SHMB:AM and SHMeMB:AM were determined using a specialized kinetic technique, pulsed-laser polymerization combined with size exclusion chromatographic analysis of the resulting polymer (PLP-SEC). As the polymerization kinetics of the fully ionized and water-soluble SHMeMB monomer have not previously been studied, further experiments were done to examine effects of monomer concentration and added salt on homopolymerization. Possible effects of depropagation in both homopolymerization and copolymerization kinetics with AM were also considered, using models implemented in PREDICI to estimate both depropagation and termination rate coefficients for the system, and as tools to better understand the SHMeMB homopolymerization and SHMeMB:AM copolymerization experimental data acquired from *in-situ* NMR and PLP-SEC studies.

2 Literature Review

2.1 PLP-SEC: Theory and Technique

Pulsed-laser polymerization coupled with size exclusion chromatography (PLP-SEC) is the IUPAC recommended method for accurately determining propagation rate coefficient (k_p) in free radical polymerizations [29]. Knowing the rate coefficients can help model rates of polymerization, relative reactivity of monomer in copolymerization, and the molar mass distributions of the polymer products. These all contribute to influence the end-use properties of the materials, which can be tailored to different applications by varying the reaction conditions and component ratios. Prior to the development of the PLP-SEC technique, k_p estimates were too scattered to provide a systematic understanding of radical polymerization kinetics. The IUPAC Working Party on 'Modeling kinetics and processes of polymerization' established benchmark k_p data sets using PLP-SEC for several well-studied monomers like styrene [40], methyl methacrylate [41], and alkyl acrylates [42]. The series of publications also provided Arrhenius parameters to represent the temperature dependency of k_p over a broad range of reliable and consistent data obtained from different laboratories.

PLP-SEC consists of pulsing a laser beam through the reaction mixture at a known repetition rate to generate populations of radicals, and measuring the molar mass distribution of the resulting polymer product to determine k_p from characteristic features controlled by the pulsed-initiation profile. Each laser pulse instantaneously generates a new radical population by activating the photoinitiator added to the system. Between laser pulses, these radical chains grow via propagation during the dark period, with some radical termination also occurring. The next pulse generates a new radical population that increases the instantaneous probability of chain termination to create a significant population of dead polymer chains of a specific length (corresponding to the chain lifetime between the two pulses) observable in the polymer molar mass distribution (MMD). Any growing radicals that survive may continue to propagate until the next laser pulse when they are again exposed to a high probability of termination, with the resulting polymer

chains creating a second observable peak in the MMD. Some radicals can survive for more than two consecutive pulses to form higher order peaks in the MMD. A PLP structured polymer MMD is shown in Figure 1 from k_p determination of dodecyl acrylate done at a repetition rate of 100 Hz at -4°C, with monomer in solution containing 36 wt% CO_2 [43]. Taking the derivative of the wlog(M) vs log(M) plot (acquired from SEC analysis) can more easily identify the inflection points of the MMD used to determine the value of k_p.

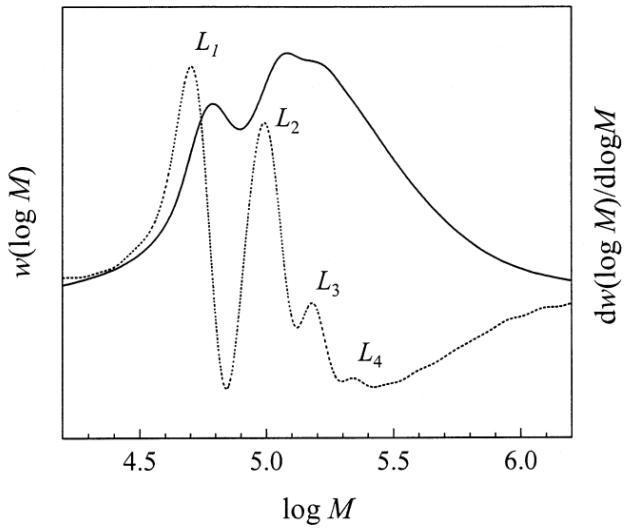

Figure 1: MMD (–) and the first derivate of the distribution (⋯) of poly(dodecyl acrylate) produced at -4°C, 200 bar, and laser pulse repetition rate of 100 Hz from dodecyl acrylate in solution with 36 wt% CO_2. Reprinted with permission from [43], © 2001 Elsevier Ltd.

The molar mass at each inflection point correlates linearly with the propagation rate coefficient, k_p, according to Equation 1. L_1 represents the first inflection point from the MMD related to polymer chains with a lifetime corresponding to the time between two consecutive laser pulses, and L_2, L_3, … etc. are higher order inflection points of growing radical chains that survived for two dark periods or more. L_i represents polymer chain length, however SEC gives molar mass results, therefore $L_i = M_i/M_{mon}$ where M_i is molecular mass of polymer chain and M_{mon} is molar mass of monomer. Monomer concentration, c_M, can be assumed

to be constant, as fractional monomer conversion is kept very low (generally less than 3%) during the experiment. The time between pulses, t_0, is the reciprocal of the laser pulse repetition rate.

$$L_i = i\, k_p c_M t_0 \qquad i = 1, 2, 3, \ldots \tag{1}$$

The PLP-SEC technique is an IUPAC recommended method because it provides a measure of k_p without needing to accurately determine radical concentrations, and because of self-consistency checks for reliable determination of k_p [29]. The same k_p should always be observed regardless of photoinitiator concentration, repetition rate, or laser pulse energy, and the PLP-structured MMD should have at least a second inflection point that is twice the molecular weight of the first inflection point to confirm the linear correlation between molecular weight and the chain lifetime controlled by repetition rate [43]. If there is a significant level of chain transfer of radical to monomer, then polymer average chain-length is no longer controlled by the laser pulses. This leads to a wide molecular weight distribution without inflection points, as chain-transfer, rather than the periodic radical initiation/termination profile controlled by the laser, controls the polymer chain length distribution. Therefore, PLP conditions should be optimized in order to determine k_p accurately, as too much or too little termination between pulses can also lead to unimodal MMDs without the distinctive features shown in Figure 1.

2.2 Effect of ionization and monomer concentration on k_p in aqueous solution

The study of radical polymerization kinetics in aqueous solution has lagged behind that of polymerizations in bulk or organic solution. It was found that the k_p values of common monomers such as styrene and methyl methacrylate did not vary greatly with solvent choice or concentration, with a difference of less than 20% between bulk and 1:1 monomer to solvent mixtures [44]. However, the influence of solvent choice was greater for monomers with increased polarity: non-ionized acrylic acid (AA) and methacrylic acid (MAA) had significantly higher k_p values in water than in methanol or dimethyl sulfoxide (DMSO) [30]. While variation in MAA k_p values with monomer concentration was also found to be small in organic solvents [30], the PLP-SEC technique has revealed that both monomer concentration and ionization has significant

effects on k_p for both AA [25] and MAA [27] in an aqueous environment. Furthermore, the polymerization rate of fully ionized (meth)acrylic acid in water was found to be an order of magnitude lower than the non-ionized system [45].

The effect of monomer concentration on k_p values for non-ionized AA in aqueous solution is apparent from the data shown in Figure 2a [24]. The propagation rate coefficient reached a maximum at 3 wt% monomer, but decreased when monomer concentration was above or below 3 wt%. The decreasing trend of k_p where monomer concentration is >3 wt% has been attributed to hydrogen bonding. At higher monomer concentrations, there is less hydrogen bonding of water molecules with the carboxylate group on the growing radical chains. The adsorption of water provides a fluidizing effect that enhances the internal rotation of the transition state, therefore increasing k_p at lower monomer concentrations [28]. Furthermore, there are stronger dipolar intermolecular interactions at higher monomer concentrations that decrease internal rotation of the growing radical species.

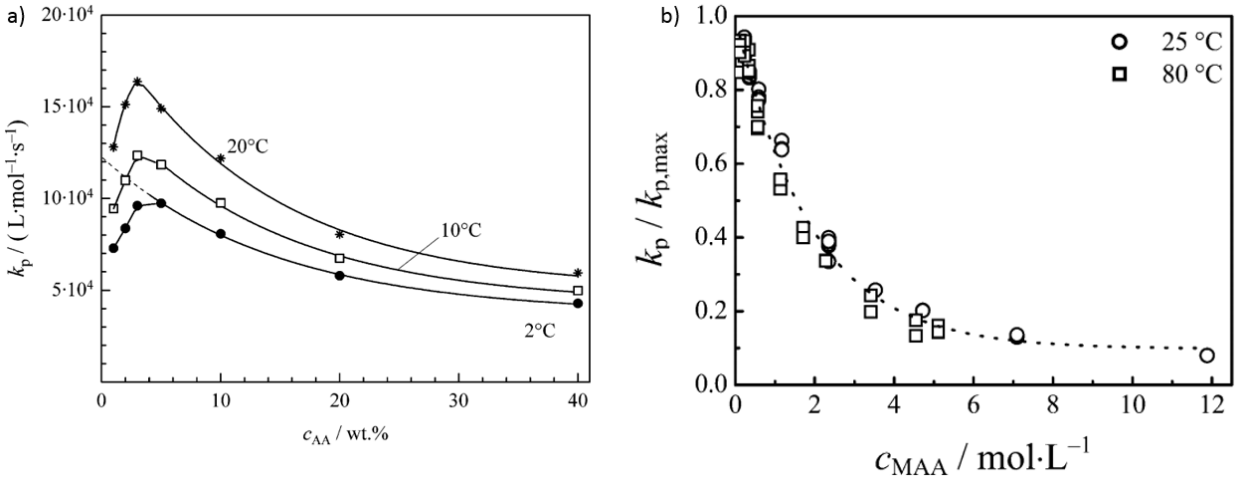

Figure 2: a) Dependence of k_p on non-ionized acrylic acid concentration in aqueous solution at 2, 10, and 20°C. The solid lines were calculated based on correlations in reference [24]. Reprinted with permission from [24], © 2003 American Chemical Society. b) Dependence of k_p on non-ionized methacrylic acid concentration in aqueous solution at 25°C. Reprinted with permission from [26], © 2006 American Chemical Society.

In the region <3 wt%, the decrease in non-ionized AA k_p was initially explained by the adsorption of acrylic acid monomers onto the growing chain, hence decreasing the local monomer concentration at the radical site. This amount of monomer adsorption is very small and is negligible at higher monomer concentrations relative to other effects. However, a decrease in monomer concentration at the local radical site was not a sufficient explanation because a maximum k_p was not observed for MAA, as shown in Figure 2b [26]. Furthermore, the difference between concentration at the radical site and in bulk would have to be very large to cause k_p to differ by a factor of 20 at low monomer concentrations from non-ionized to fully ionized systems [27]. Another explanation for the decrease in the apparent k_p value for AA was backbiting, a side-reaction known for acrylates (and AA) that creates a mid-chain radical (MCR) that is located on a tertiary rather than a secondary C-atom [46]. Propagation is slowed down in the presence of the more stable MCR population, with increasing influence at higher temperatures and lower monomer concentrations. Backbiting does not occur with methacrylates because the methyl group provides a more stable tertiary chain-end radical. Therefore, the decrease in k_p at monomer concentration <3 wt% for AA was attributed to backbiting effects.

Non-ionized AA describes the acrylic acid molecule with a protonated carboxylic group, and the carboxylic groups become ionized when sodium hydroxide (NaOH) is added to the solution. The degree of ionization (α) of AA at lower monomer concentration (5 wt%) increases from non-ionized to fully ionized by changing the pH of the solution by adding NaOH. In Figure 3, k_p was shown to decrease by an order of magnitude as α (or equivalently pH) of AA increases to unity, and to increase again when α is greater than one [25]. The decrease in k_p was attributed to electronic repulsion of the ionized carboxylic groups as α approaches one, while at $\alpha > 1$, the excess counterions screened the charges of the ionized monomers, therefore increasing k_p again.

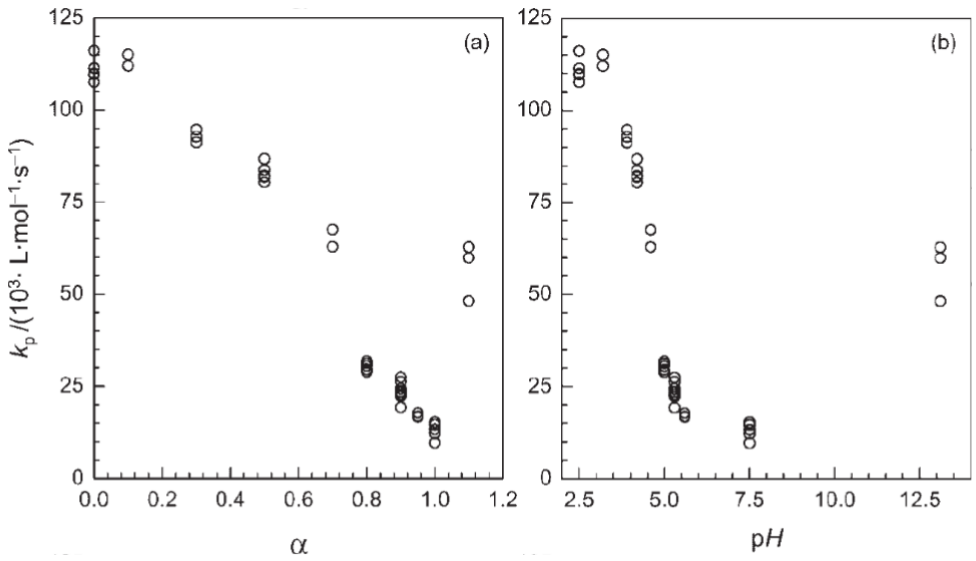

Figure 3: Dependence of k_p as a function of a) degree of ionization and b) pH of acrylic acid in aqueous solution at [AA]=0.69 mol/L and 6°C. Reprinted with permission from [25], © 2004 Wiley-VCH Verlag GmbH & Co.

As AA polymerization conditions go from partially to fully ionized, there are four propagation scenarios to consider [25]: A) non-ionized radical + non-ionized monomer, B) non-ionized radical + ionized monomer, C) ionized radical + ionized monomer, and D) ionized radical + non-ionized monomer. Scenario D was neglected because the idea of "non-ionized" monomer in a fully ionized system, where charge of ionized monomers are screened by counterions, was not considered. In other words, only conditions where $0 \leq \alpha \leq 1$ were considered. From Figure 3, k_p where α=0 ($k_{p(\alpha=0)}$) is 110 000 L/mol·s and represents scenario A where monomer and polymeric radical species are non-ionized. Scenario C is represented by $k_{p(\alpha=1)}$=13 000 L/mol·s, where all species are ionized. Scenario B, a partially ionized system, is represented by $k_{p(ionic/non-ionic)}$. By fitting the experimental k_p values as a function of ionization, $k_{p(ionic/non-ionic)}$ was determined using Equation 2, in which the fraction of non-ionized species is represented by (1-α). The value of $k_{p(ionic/non-ionic)}$ should be between $k_{p(\alpha=0)}$ and $k_{p(\alpha=1)}$, therefore $k_{p(ionic/non-ionic)}$ was expressed as $f \cdot k_{p(\alpha=0)}$, where f is between 0 and 1. It was determined that an f factor of 0.8-0.9 gave the best fit of experimental data.

$$k_p = \alpha^2 k_{p(\alpha=1)} + (1-\alpha)^2 k_{p(\alpha=0)} + 2\alpha(1-\alpha) k_{p(ionic/non-ionic)} \quad (2)$$

The derived equation for k_p as a function of α gave a good representation of AA polymerization at 5 wt%. At this low monomer concentration, the observed k_p values differed by an order of magnitude between α=0 and 1 [27]. The effect of ionization on MAA relative k_p values (scaled to the value at α=0) at the same low monomer concentration was similar to AA, as shown in Figure 4, and the relative change was also found to be independent of temperature from 6 to 80°C [27].

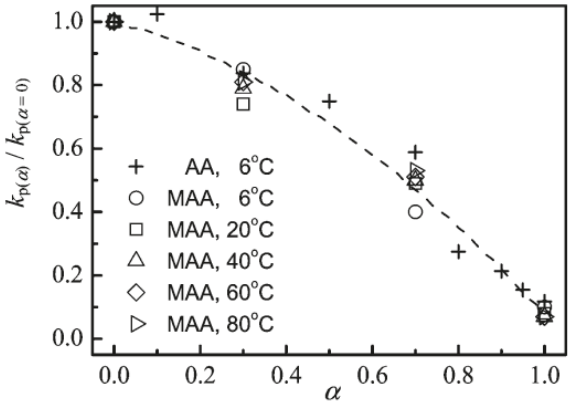

Figure 4: Ratio of $k_{p(\alpha)}$ to $k_{p(\alpha=0)}$ as a function of degree of association for MAA at 5 wt% monomer at various temperatures and AA at 5 wt% and 6°C. Reprinted with permission from [27], © 2009 American Chemical Society.

The same study found that the addition of NaCl at different MAA concentrations did not affect k_p as a function of degree of ionization [27], suggesting that it was not the effect of electrostatic repulsion of the ionized carboxylic group that was decreasing k_p, as the addition of salt would screen the charges of the ionized groups. Arrhenius fits of the k_p data at different monomer concentrations and degrees of ionization showed that activation energy (E_A) remained constant, but the pre-exponential factor (A) decreased with increasing α [27]. The decrease in pre-exponential factor indicates a decrease in internal rotation of the transition state (TS). Therefore, the decrease in k_p was attributed to a restricted internal rotation due to attractive forces between the ionized carboxylic group and counter ions in solution.

Because of the lower propagation rates of MAA, and also because no backbiting occurs, it proved possible to use the PLP-SEC technique to measure k_p over a range of monomer concentrations and temperatures.

Equation 2 only had one adjustable parameter (*f*) and was only applicable for lower monomer concentrations. The series of MAA data was used to derive an equation for k_p as a function of MAA concentration ($0.05 \leq w^0_{MAA} \leq 0.40$), degree of ionization ($0 \leq \alpha \leq 1$), and temperature ($6 \leq T$ (°C) ≤ 80) as shown in Equation 3.

$$k_p(\alpha, w^0_{MAA}, T) = 4.1 \times 10^6 \exp\left(-\frac{1.88 \times 10^3}{T}\right)(0.08 + (1 - 0.08)$$

$$\exp(-5.3w^0_{MAA})) \left[(-0.202w^0_{MAA} - 0.553)\alpha^2 + (2.283w^0_{MAA} - 0.475)\alpha + 1\right] \quad (3)$$

Using Equation 3, k_p was calculated at different degrees of ionization as a function of MAA concentration at 50 °C, as summarized in Figure 5 [27]. It was found that the influence of ionization on the value of k_p diminished with increasing monomer concentration. Thus, as α increased from 0 to 0.8, the effect of MAA concentration on k_p became less prominent. This result was explained in terms of the restricted internal rotation of the TS due to monomer concentration becoming less prominent with increased ionic strength (*i.e.*, monomer concentration) at a constant α [47]. The increase of k_p with MAA concentration found at α=1 is contrary to the observed trends for non- and partially ionized MAA, a result attributed to an increase in radical chain flexibility from charge screening of ionized MAA species as monomer concentration increased from 5 to 40 wt% [47]. At a high MAA concentration of 40 wt%, degree of ionization did not have a large influence on k_p, suggesting that the decrease in hydrogen-bonding and fluidizing effect of water had a similar effect as increased attractive forces of ionized species on the internal rotation of TS at high monomer concentration [47].

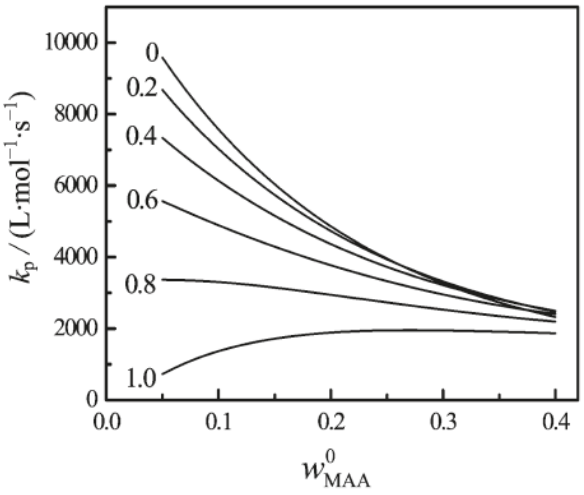

Figure 5: The variation in k_p as a function of MAA monomer concentration from 5 to 40 wt% at various degrees of ionization done at 50°C, as fit to PLP-SEC data. Reprinted with permission from [27], © 2009 American Chemical Society.

2.3 In-situ *NMR method*

The *in-situ* NMR method was previously applied in our lab to study the copolymerization of AM and non-ionized AA in aqueous solution over a range of monomer concentrations up to 40 wt% [32]. Previous studies of batch AM and AA copolymerizations were conducted in larger reaction volumes, but they were limited to low monomer concentrations due to high viscosities and poor mixing at high monomer concentrations [48] [49] [50]. However, higher monomer concentrations are used in industry to increase production rate. Hence, it is important to study polymerizations at industrially relevant conditions because k_p can vary with monomer concentration and k_t can vary with viscosity as it is diffusion-controlled. *In-situ* NMR allows for online tracking of polymerization rate, as well as monomer composition drift up to high conversions. AM homopolymerization in aqueous solution had been previously studied using this method [51], which can be reliably implemented as long as: 1) reaction rate is less than scanning rate, 2) the polymer formed remains soluble, and 3) distinguishable monomer and polymer peaks are available for determination of monomer composition and conversion.

Copolymerization of AA and AM was studied using *in-situ* NMR to estimate reactivity ratios at 40°C with varying initial monomer concentrations and monomer compositions [32]. The reactivity ratios for the system were first estimated assuming the terminal model using experimental data at <10% conversion. Assuming terminal copolymerization kinetics, the copolymer molar composition (F_i) is related to monomer molar composition (f_i) according to the Mayo-Lewis equation (Equation 4), where r_i is the reactivity ratio of species *i* defined by the ratio of propagation rate coefficients describing addition of monomer-*i* to radical-*i* ($k_{p,ii}$) compared to the addition of monomer-*j* to radical-*i* ($k_{p,ij}$), such that $r_i = k_{p,ii}/ k_{p,ij}$ [52].

$$F_1 = \frac{r_1 f_1^2 + f_1 f_2}{r_1 f_1^2 + 2 f_1 f_2 + r_2 f_2^2} \tag{4}$$

The polymer and monomer composition data obtained at low conversion was fitted to this equation using parameter estimation algorithms in PREDICI to yield reactivity ratios estimates of $r_{AA} = 1.27 \pm 0.26$ and $r_{AM} = 0.54 \pm 0.21$ (Figure 6a) [32]. However, more precise estimates can be obtained by using the measure of monomer composition drift as a function of conversion obtained from *in-situ* NMR using the integrated Mayo-Lewis equation [53]. The latter method estimated best-fit reactivity ratios to be $r_{AA} = 1.23 \pm 0.02$ and $r_{AM} = 0.58 \pm 0.01$ (Figure 6b) [32]. Reactivity ratios estimated using both methods showed good agreement, while the best-fit estimates using the monomer composition drifts as a function of conversion had much smaller error. It is interesting to note that, while homopropagation k_p values for both monomers decrease with increasing monomer concentration, the comonomer composition drift (and hence values of reactivity ratios) are independent of monomer concentration. However, reactivity ratios proved to change with both monomer concentration and degree of ionization when the study was extended to the copolymerization of AM with partially and fully ionized AA [54].

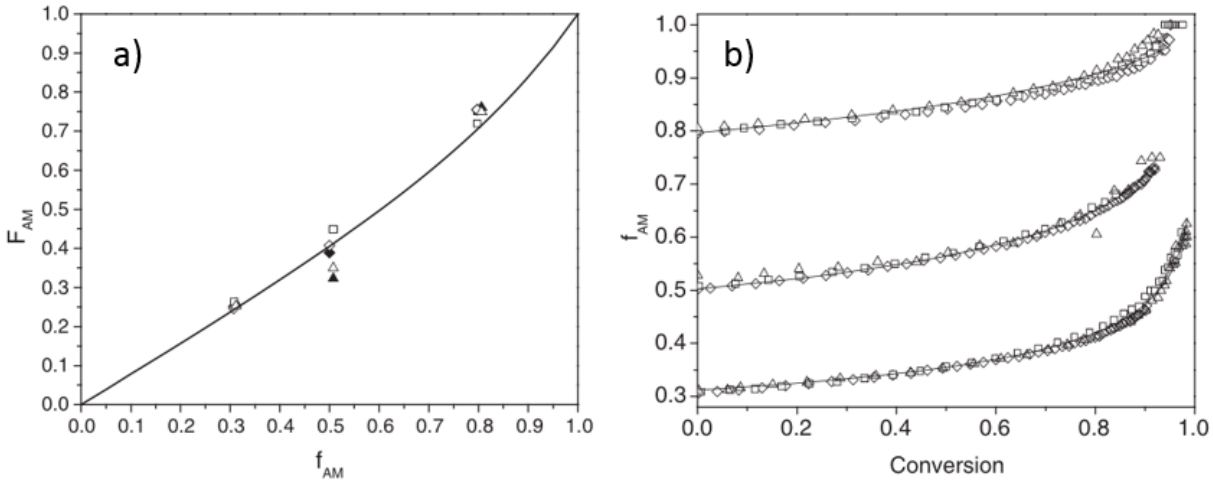

Figure 6: a) Cumulative polymer composition as a function of initial monomer composition estimated at 5 (filled symbols) and 10% (empty symbols) conversion at 5 (◆,◇), 20 (■,□) and 40 (▲,△) wt% monomer. The curve was fitted to give reactivity ratios r_{AA} = 1.27 ± 0.26 and r_{AM} = 0.54 ± 0.21. b) Monomer composition drift as a function of conversion for initial f_{AA} = 0.3, 0.5, and 0.8 at 5 (◇), 20 (□), and 40 (△) wt% monomer with 0.217 wt% V-50 and 40°C. The best-fit reactivity ratios were calculated to be r_{AA} = 1.24 ± 0.02 and r_{AM} = 0.55 ± 0.01. Reprinted with permission from [32], © 2013 Wiley-VCH Verlag GmbH & Co.

The *in-situ* NMR technique also provides a measure of the overall rate of (co)monomer conversion in the system. While the PLP-SEC studies of AM [31] and AA [24] showed that homopolymerization k_p values decreased with increasing monomer concentration for both monomers, it was found that the homopolymerization rates increased with an increased initial monomer concentration in aqueous solution [32]. Combined with independent measures of termination rate coefficients (k_t) for AA [55] and AM [56], it was concluded that the decreased rate at low monomer concentrations was caused by the backbiting side reaction that is known to happen during radical polymerization of AA [55] and also AM [57], but to a lesser extent. Less reactive mid chain radicals are formed as the radical chains undergo intramolecular chain transfer, therefore the observed overall rate of conversion is lowered, especially at low monomer concentrations. Data obtained by the *in-situ* NMR method (including final polymer MMDs measured by SEC) was used to test kinetic models developed to represent the AA [46] and AM [31] homopolymerization

systems based on individually measured rate coefficients (k_p, k_t, backbiting), as well as a model developed to represent the batch radical copolymerization of AM and AA [58].

2.4 Depropagation: Background

The essential mechanisms of all radical polymerizations are initiation, propagation, and termination, as shown in Scheme 1. Initiators generate the primary radicals in the system, which then propagate rapidly through multiple monomer additions to form long polymer chains, with all growing radical chains subjected to unavoidable radical-radical termination to form the "dead" polymer chains sold as products. There can also be transfer of radicals to monomer or solvent, limiting the polymer molar mass that can be achieved. As mentioned in Chapter 1, the propagation step is normally assumed to be irreversible, as it is exothermic in nature. However, this assumption is not valid under certain polymerization conditions (low monomer concentrations and higher temperatures), dependent on the heat of polymerization associated with the monomer. Depropagation, also included in Scheme 1, occurs when a single monomer unit comes off the growing radical chain to regenerate a monomer unit.

Initiation	$I \xrightarrow{2fk_d} 2fP_1$
Propagation	$P_n + M \xrightarrow{k_p} P_{n+1}$
Depropagation	$P_{n+1} \xrightarrow{k_{dep}} P_n + M$
Termination	
By combination	$P_n + P_m \xrightarrow{k_{tc}} D_{n+m}$
By disproportionation	$P_n + P_m \xrightarrow{k_{td}} D_n + D_m$

Scheme 1: Initiation, propagation, depropagation, and termination reaction steps in free radical polymerization. (*I* is initiator, k_d is decomposition rate coefficient of initiator, *f* is initiator efficiency, P_n represents radical species of *n* length, *M* is monomer, k_p is propagation rate coefficient, k_{dep} is depropagation rate coefficient, k_{tc} is termination by combination rate coefficient, and k_{td} is termination by disproportionation rate coefficient.

Several monomers are known to depropagate due to steric hindrance that inhibits the propagation step and lowers the heat of reaction. Examples of depropagating monomers include butyl methacrylate [34], itaconates [35], methyl ethacrylate [36], and α-methyl styrene [37], as shown in Figure 7. These monomers are all di-substituted at the α-carbon of the methylene group. The substituents are fairly bulky, especially in the case of the itaconates. However, even addition of an extra methyl group as a substituent in α-methyl styrene and methyl ethacrylate, as opposed to the analogous styrene and methyl methacrylate, respectively, can greatly contribute to a monomer's propensity for depropagation.

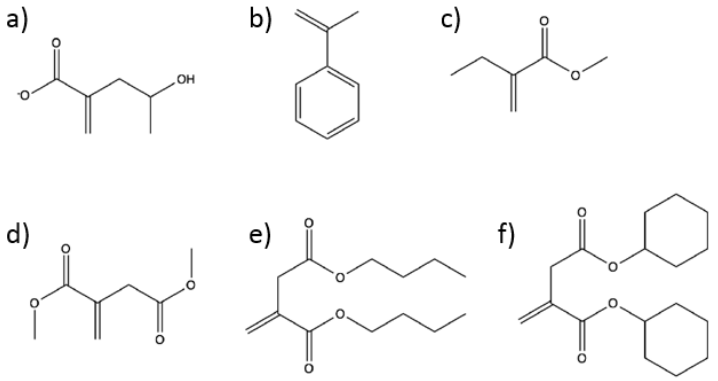

Figure 7: Chemical structure of a) SHMeMB, b) α-methyl styrene, c) methyl ethacrylate, d) dimethyl itaconate, e) dibutyl itaconate, and f) dicyclohexyl itaconate.

When depropagation occurs, the propagation rate approaches equilibrium and the effective propagation rate coefficient depends on both k_p and k_{dep} (Equation 5). At high monomer concentrations, the k_{dep} term is generally negligible, but the influence of depropagation becomes more significant at low monomer concentration. The Gibb's free energy at equilibrium, defined in Equation 6, is dependent on the ceiling temperature (T_c), and the equilibrium monomer concentration ($[M]_{eq}$) [59]. The Gibb's energy or rate of polymerization could approach zero in two ways: at a constant monomer concentration as temperature approaches T_c, or at a constant temperature as monomer concentration approaches its equilibrium value.

$$k_p^{eff} = k_p - \frac{k_{dep}}{[M]} \tag{5}$$

$$\Delta G^0 = -RT_c\left(\frac{k_p}{k_{dep}}\right) = -RT_c \ln[M] = -RT \ln[M]_{eq} \tag{6}$$

Gibb's free energy can also be defined in terms of heat of polymerization, ΔH_p, and entropy, ΔS, (Equation 7) leading to the definition of ceiling temperature in Equation 8. As the activation energy for depropagation is directly related to ΔH_p by Equation 9, the importance of the reaction is increased for systems with lowered heats of reaction (always exothermic), which also lowers T_c.

$$\Delta G^0 = \Delta H_p - \Delta S\, T_c \tag{7}$$

$$T_c = \frac{\Delta H_p}{\Delta S - R \ln[M]} \quad (8)$$

$$\Delta H_p = E_p - E_{dep} \quad (9)$$

The importance of depropagation can be studied by comparing values of ΔH_p and T_c for various monomers as summarized in Table 1. As noted, the calculation of T_c assumes that the change in entropy for propagation is a constant value, independent of monomer structure [59]. ΔH_p of styrene is -73 kJ/mol [37], but by adding a methyl group in α-methyl styrene, ΔH_p decreased to -35 kJ/mol [37]. Consequently, T_c lowers from 335°C to 19°C. Similarly, methyl methacrylate has a ΔH_p of -56 kJ/mol, and methyl ethacrylate has a side chain that is one carbon longer and has a value of -35 kJ/mol. The itaconates, however, do not have as low ΔH_p values as the other depropagating monomers considering their substituents are much larger. Out of the three itaconates, dibutyl itaconate has the lowest ΔH_p, even though dicyclohexyl itaconate has the bulkiest substituents.

Table 1: Heat of polymerizations and ceiling temperatures of various monomers. T_c calculations were done with [M]=1 mol/L and ΔS= -120 J/mol·K. *T_c of methyl ethacrylate was calculated at bulk monomer concentration, [M]=8.35 mol/L.

	$-\Delta H_p$ (kJ/mol)	T_c (°C)	Reference
Styrene	73	335	[37]
Methyl methacrylate	56	194	[37]
Methyl acrylate	80	394	[37]
α-methyl styrene	35	19	[37]
Methyl ethacrylate	31	82*	[36]
Dibutyl itaconate	42	77	[35]
Dimethyl itaconate	60.5	231	[35]
Dicyclohexyl itaconate	53.5	173	[35]

In a copolymerization system in which one monomer is known to depropagate but the other does not, the apparent reactivity ratios can be affected by reaction temperature, due to the influence of depropagation on

the incorporation rate of the depropagating monomer. The set of terminal model propagation reactions in which one of the two monomers (monomer A) depropagates is shown in Scheme 2. The terminal model assumes that the reactivity of the radical chain is controlled only by the type of monomeric unit at the radical end of the growing chain, and is not affected by the penultimate monomer unit. Depropagation is assumed to only occur when monomer A has added on to a radical growing chain that is terminated by another monomer A unit to form an AA diad. P_{n+1}^{A} and P_{n+1}^{B} represent radical chains of *n* length with A or B monomer unit, respectively, in the terminal position.

$$P_n^A + A \underset{k_{dp,AA}}{\overset{k_{p,AA}}{\rightleftharpoons}} P_{n+1}^A$$

$$P_n^A + B \xrightarrow{k_{p,AB}} P_{n+1}^B$$

$$P_n^B + B \xrightarrow{k_{p,BB}} P_{n+1}^B$$

$$P_n^B + A \xrightarrow{k_{p,BA}} P_{n+1}^A$$

Scheme 2: Propagation mechanisms where depropagation is assumed to only occur for homopolymerization of monomer A.

The effect of depropagation on copolymer composition has been examined in a number of studies. Methyl ethacrylate (MEA) was copolymerized with styrene (ST) at 30 and 80°C and a difference in apparent reactivity ratios was observed. The reactivity ratios at 30°C were r_{MEA}=0.782 and r_{ST}=0.224 and at 80°C they were r_{MEA}=0.0974 and r_{ST}=0.532 [38], with the values estimated assuming that no depropagation occurs; i.e., using the Mayo-Lewis equation (Equation 4). Methyl ethacrylate has a ceiling temperature of 82°C in bulk polymerization [36], and as these copolymerizations were done in solution polymerization the ceiling temperature of MEA in this system would be even lower. Thus, the effects of MEA depropagation in MEA:ST copolymerization was observed at 80°C as shown in Figure 8a, where less MEA was incorporated into the polymer at 80°C due to depropagation, lowering the effective value of r_{MEA}. The

difference in reactivity ratios exceeded the 95% confidence intervals of the estimates (Figure 8b), indicating the real effect of depropagation on the copolymerization kinetics.

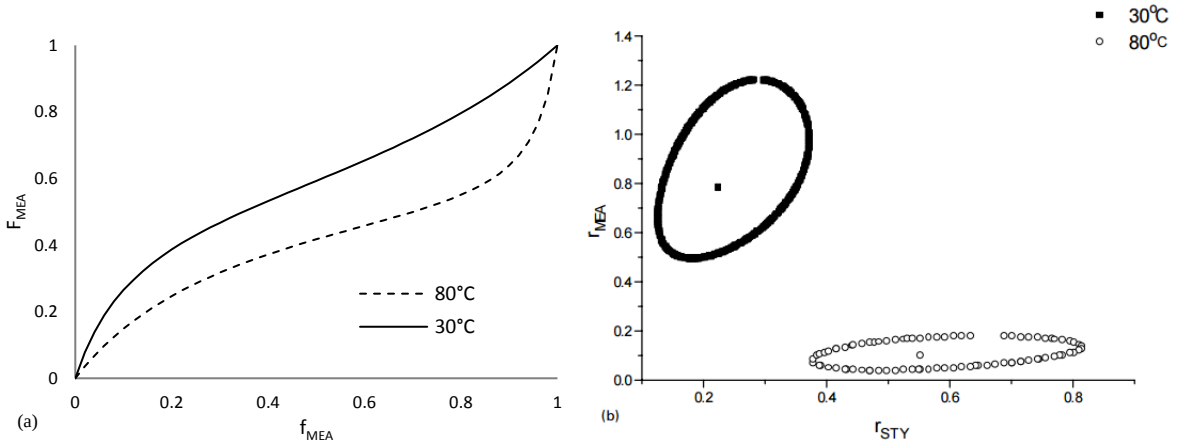

Figure 8: a) F_{MEA} vs. f_{MEA} plot of MEA and ST copolymer at 30 and 80°C b) Reactivity ratios of MEA and ST at 30 and 80°C with 95% confidence intervals. Reprinted with permission from [38], © 2000 Elsevier Ltd.

The effects of depropagation were also observed at high temperatures and low monomer concentration conditions for copolymerization of butyl methacrylate (BMA) with ST. There was negligible temperature dependency in the reactivity ratio estimates between 50 and 150°C, but the copolymer composition was affected at higher temperatures [34]. Experimental data was fitted with different models: 1) terminal model with no depropagation, 2) Lowry's approach where depropagation occurs when the radical contains the depropagating monomer at the penultimate and terminal position [60], and 3) Wittmer's approach where BMA also depropagates with ST in the penultimate position [61]. With a combination of low concentration and high temperatures, BMA and ST copolymerization fitted with Lowry's depropagation model in Figure 9. Note that if monomer concentration was high, the influence of depropagation was negligible, even at high temperatures as shown in Figure 9 b). This work validated the assumption that depropagation only occurs when the depropagating monomer is at the terminal and penultimate positions, as indicated in Scheme 2.

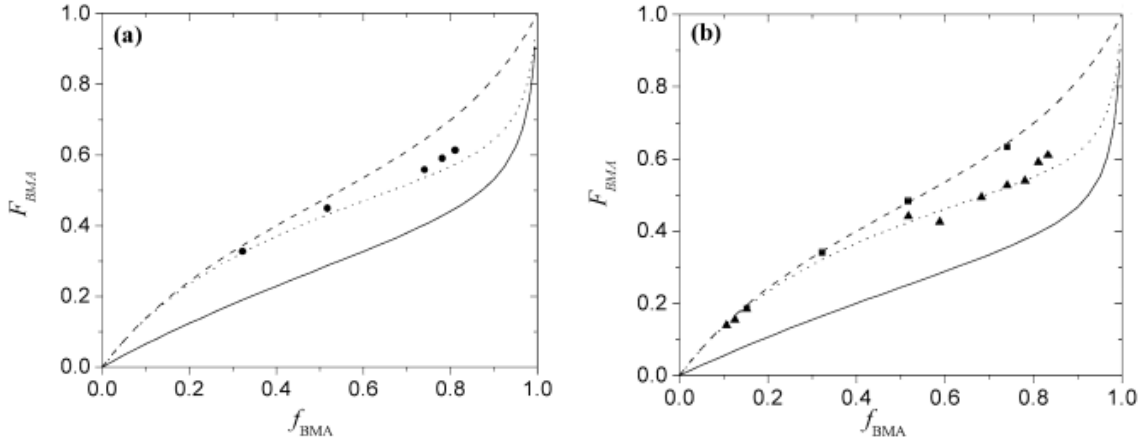

Figure 9: a) F_{BMA} vs. f_{BMA} plot of BMA and STY copolymers at 165°C and $[M]_{tot}$=0.7 mol/L (●) and b) at 182°C with $[M]_{tot}$=0.9 mol/L (▲) and $[M]_{tot}$=3.5 mol/L (■). Curves were calculated using Mayo-Lewis with no depropagation kinetics (- -), Lowry's approach (⋯), and Wittmer's approach (–). Reprinted with permission from [34], © 2006 American Chemical Society.

2.5 Summary

The techniques and background information summarized in this literature review are applied in this study to analyze and better understand the polymerization kinetics of SHMeMB homopolymerization and SHMeMB:AM copolymerization in aqueous solution. PLP-SEC is a reliable technique in determining k_p so long as the conditions were optimized to achieve multiple inflection points in the MMD. The *in-situ* NMR method provides detailed conversion profiles, as well as monomer composition with conversion, which are used for determining reactivity ratios of SHMeMB:AM copolymerization. SHMeMB is water-soluble and ionized, similar to (meth)acrylic acid, therefore previous knowledge in MAA and AA polymerization kinetics are useful, especially when studying effects of added salt and monomer concentration on polymerization. Depropagation is also considered, as SHMeMB has substituents on either side of the methylene α-carbon that could hinder the radical site. Models are developed and parameter estimation used to gain a better understanding of these mechanisms on the polymerization behaviour during the synthesis of SHMeMB homopolymers and SHMeMB:AM copolymers.

3 Experimental Methods

3.1 Materials

The following chemicals were purchased from Sigma-Aldrich, Canada and used as received: α-methylene-γ-butyrolactone (MBL, 97%), acrylamide (AM, >98%), *N,N'*-methylenebis(acrylamide) (BIS, 99%), deuterated dimethyl sulfoxide (DMSO, 99.9% D), 2,2'-azobis(2-methyl-propionamidine) dihydrochloride (V-50 initiator, 97%), 4,4'-azobis(4-cyano-valeric acid) (ACVA initiator, >98%), potassium persulfate (KPS initiator, >99%), sodium hydroxide (NaOH, >97%). 2,2'-Azobis[2-methyl-N-(2-hydroxyethyl)propionamide] (V-86 initiator) was purchased from Wako Pure Chemicals Ltd., USA. Deuterated water (D_2O, 99.8% D) and hydrochloric acid (HCl, 36.5% w/w) were purchased from Fisher Scientific, Canada and the γ-methyl-α-methylene-γ-butyrolactone (MeMBL, >97%) was provided by DuPont Central Research Laboratories. Ultrapure water was obtained from Ultrapure Water System NW Series (Heal Force Bio-Meditech Holdings, Ltd., China). Lithium monoacylphosphine oxide (LiTPO), the photoinitiator used in the PLP-SEC experiments, was provided by Prof. Robert Liška's research group from Technische Universität Wien, Austria.

3.2 Synthesis and Techniques

3.2.1 Ring-opening saponification of MBL and MeMBL

The procedure for the ring-opening of MBL and MeMBL (Figure 10) for in-situ NMR studies follows that previously developed for MBL [23]. For 1 g of MBL or MeMBL, 10 mol% excess of NaOH was measured and dissolved in 1 g of D_2O in a small vial with a stir-bar. The saponification reaction took place in an oil bath at 95°C for 2 hours, after which the solution was cooled to room temperature and 1 M HCl was added until a pH of 7 was reached. The SHMB or SHMeMB mixture was then diluted with D_2O to a final monomer concentration of 40 wt% (including mass of sodium ions). A similar procedure was done for the PLP-SEC and hydrogel studies, except that ultrapure water was used instead of deuterated water. This stock solution was mixed with other components to achieve desired concentrations for the *in-situ* NMR, PLP-SEC, or

hydrogel studies. The structure of MeMBL was confirmed by NMR (Figure A. 1), and NMR was also used to confirm that the ring structures were completely opened to make SHMeMB (Figure A. 2).

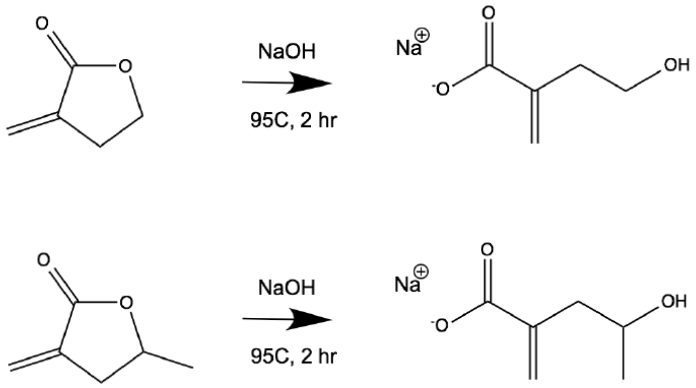

Figure 10: Ring-opening saponification of MBL (top) and MeMBL (bottom) using 1:1 molar ratio of NaOH to butyrolactone ring at 95°C for 2 hours.

3.2.2 Superabsorbent Hydrogel Synthesis and Absorption

Hydrogels were prepared using three molar ratios of SHMeMB:AM 2:8, 4:6, and 6:4, corresponding to f_{SHMeMB} of 0.2, 0.4 and 0.6, respectively, with 0.4 mol% of V-50, 1 or 1.5 mol% of BIS, and either 15 or 30 wt% monomer content in H_2O. After purging with nitrogen for 10 min, the mixture was injected into a sealed glass cell that was held at 50 °C for 16 h to yield a hydrogel of 1 mm in thickness and about 5 cm in width and length. The circular piece of hydrogel 13 mm in diameter was cut and immersed in ultrapure water at room temperature and water absorption was determined using analytical balance. The swollen hydrogel was removed from solution, patted dry to remove excess water and weighed at set intervals; fresh ultrapure water was added after each measurement. Measurements were less frequent for hydrogels that had lower mechanical strength in order to minimize breakage. It was assumed that this process leached all residual monomer from the hydrogel after 24 h, which was shown to be sufficient time for the swollen hydrogel to reach its equilibrium absorbency in the previous study [23]. The swollen samples were then freeze dried to remove the water and then weighed to determine the mass of the dried crosslinked polymer.

The gel yield (X_{gel}) and swelling ratio (%) were calculated using Equation 10 and 11, respectively,

$$X_{\text{gel}} = \frac{m_{\text{dry}}}{m_{\text{initial}} w_{\text{M}}} \tag{10}$$

$$Swelling\ Ratio\ [\%] = \frac{m_{\text{wet}} - m_{\text{dry}}}{m_{\text{dry}}} \times 100\% \tag{11}$$

where m_{initial} and m_{dry} are the masses of as prepared hydrogel sample and sample after lyophilization, respectively, w_{M} is the weight fraction of monomer in the initial reaction mixture and m_{wet} is the mass of hydrogel sample measured at various time points during the swelling study.

Stress vs. strain curves of the swollen hydrogels were obtained at 25 ± 0.1°C using an MCR-502 instrument (Anton Par, Austria) and Peltier accessories with a PP10 upper plate, with a solvent trap used to keep samples from dehydration. The mechanical tests were done in compression mode at a compression rate of 0.6 mm/s. Values shown in the plots were averaged from eight separate measurements. Storage and loss moduli measurements were also done with the same setup in the linear viscoelastic region varying the frequency from 0.1 to 10 Hz. In addition, the swollen hydrogel samples were frozen with liquid nitrogen in order to obtain the cross section for scanning electron microscopy (SEM) imaging using a Nova NanoSEM instrument (FEI Quanta, Japan).

3.2.3 Preparation for *in-situ* NMR studies

The in-situ NMR method was used to measure overall monomer conversion profiles, as well as the variation of monomer and polymer composition with conversion, following procedures described by Preusser and Hutchinson [32]. These studies were conducted without BIS crosslinker, over a range of SHMB:AM and SHMeMB:AM initial molar ratios and total monomer concentrations in D_2O, with initiator content specified as weight percent of the total mixture (monomers + D_2O).

Overall conversion $X(t)$ was calculated from the decrease in monomer peak integrations relative to the HOD reference peak using Equation 12, where $A_{\text{SHMeMB}}(0)$ and $A_{\text{SHMeMB}}(t)$ are the areas of the SHMeMB proton peak at time=0 and time=t, respectively, and $A_{\text{AM}}(0)$ and $A_{\text{AM}}(t)$ are the areas of the corresponding AM proton peaks. The proton peak assignments for SHMeMB and AM are shown in Figure A. 3. Individual

conversions of SHMeMB and AM, calculated using Equation 13 and Equation 14 were used to calculate f_{SHMeMB}, the mole fraction of SHMeMB in the monomer (Equation 15), with F_{SHMeMB}, the SHMeMB mole fraction in the copolymer, calculated from mass balance according to Equation 16.

$$X(\mathrm{t}) = \frac{(A_{\mathrm{SHMeMB}}(0) - A_{\mathrm{SHMeMB}}(t)) + (A_{\mathrm{AM}}(0) - A_{\mathrm{AM}}(t))}{A_{\mathrm{SHMeMB}}(0) + A_{\mathrm{AM}}(0)} \tag{12}$$

$$X_{\mathrm{SHMeMB}}(t) = \frac{A_{\mathrm{SHMeMB}}(0) - A_{\mathrm{SHMeMB}}(t)}{A_{\mathrm{SHMeMB}}(0)} \tag{13}$$

$$X_{\mathrm{AM}}(t) = \frac{A_{\mathrm{AM}}(0) - A_{\mathrm{AM}}(t)}{A_{\mathrm{AM}}(0)} \tag{14}$$

$$f_{\mathrm{SHMeMB}}(t) = \frac{A_{\mathrm{SHMeMB}}(t)}{A_{\mathrm{AM}}(t) + A_{\mathrm{SHMeMB}}(t)} \tag{15}$$

$$F_{\mathrm{SHMeMB}}(t) = \frac{X_{\mathrm{SHMeMB}}(t) A_{\mathrm{SHMeMB}}(0)}{X_{\mathrm{SHMeMB}}(t) A_{\mathrm{SHMeMB}}(0) + X_{\mathrm{AM}}(t) A_{\mathrm{AM}}(0)} \tag{16}$$

3.2.4 Preparation for PLP-SEC studies

PLP experiments were performed using an excimer laser (ExciStar XS 500, Coherent, Inc.) operated at 351 nm with corona preionization and an all-solid-state-pulser. Pulse repetition rate was varied between 1-5 Hz with 3 mJ of laser energy per pulse. Appropriate molar ratios of monomers in ultrapure water with LiTPO photoinitiator were prepared. Reaction mixtures of 1 mL were placed in 110 OS cell (Hellma GmbH & Co. KG, Germany) with a path length of 10 mm. Prior to PLP, cells were purged with nitrogen for 2 min and sealed with a PTFE stopper, then heated for 20 min up to reaction temperature. It is important to keep reaction mixtures in a dark area to avoid initiation of the photoinitiator. A beam expander BXUV-10.0-3X (CVI Melles Griot, USA) was placed between the laser and the cell to evenly distribute the laser beam throughout the cell. After PLP, the polymer solutions were transferred into vials containing small amounts of hydroquinone monomethyl ether to inhibit further reaction. Polymer solutions were transferred into 3500 Da dialysis tubes (Spectra/Por 6, Spectrum Laboratories, Inc., Compton, CA) in ultrapure water for 3 days (with frequent changes of water), then freeze-dried using Mini-Lyotrap (LTE Scientific, Greenfield, UK).

Polymer molar mass analysis was performed using a Waters size-exclusion chromatograph with pump 515, a column heater, and 2414 refractive index indicator. Polymer samples (1-2 mg/mL) were dissolved in eluent (0.1 M Na_1HPO_4 and 100 ppm NaN_3) with added ethylene glycol as flow marker, and stirred for 24-48 h. The aqueous polymer solutions were filtered using 0.45 μm nylon membrane filters (Millex-HN, Millipore, Ireland) before being injected into the system with a flow rate of 1.0 mL/min. The columns (Polymer Standards Service, Mainz, Germany) used were 8 x 50 mm guard Suprema column, and three 8 x 300 mm Suprema columns with 10 μm particle size and pore sizes of 100, 1000, and 3000 Å maintained at 60°C. Polyacrylamide standards (American Polymer Standards Corp.) with peak molar masses between 2950 and 950 000 Da were used for calibration, with data analysis done using PSS WinGPC Unichrom software. Polymer molar mass distributions are reported relative to polyacrylamide. However, the values should still be reasonably accurate, as the AM-rich copolymers contained only 5-15 mol% of SHMeMB or SHMB.

True molecular weight of these copolymers can be determined using the multi-angle laser light scattering (MALLS) detector in the SEC. Samples of SHMeMB homopolymers at different concentrations were made to determine a dn/dc calibration curve using the refractive index (RI) detector. The dn/dc value was determined to be 0.165 and would then be used to calibrate the MALLS signal to find true molecular weight of SHMeMB. Due to technical issues with the MALLS detector, only RI detector was used to measure molecular weights of most SHMeMB:AM and SHMB:AM copolymers. Molecular weight of these samples were calibrated using an AM homopolymer calibration curve for the RI signal, and true molecular weights were not reported. However, their molecular weights should still be reasonably accurate because there were only 5-15 mol% of SHMeMB and SHMB in the copolymers.

3.2.5 Kinetic parameters for PREDICI parameter estimation

The parameter estimations for SHMeMB homopolymerizations and SHMeMB:AM copolymerizations were done based on the reaction mechanisms listed in Table 2. It was assumed that all termination occurs by combination. For SHMeMB:AM copolymerizations, k_t represents an averaged value for all three

termination mechanisms. Values were estimated from individual experimental monomer conversion profiles, to provide a perspective on how the rate coefficient varied with monomer composition. Depropagation was also considered in the model. Based upon previous work described in Chapter 2, it was assumed to only occur if both the penultimate and terminal monomer units of the growing radical chain are SHMeMB.

Table 2: Reaction mechanisms for copolymerization of SHMeMB and AM

Reaction mechanisms		
Initiator decomposition		$I \xrightarrow{k_d f} 2R_o^*$
Initiation		$R_0^* + SHMeMB \xrightarrow{k_i} SHMeMB_1^*$
		$R_0^* + AM \xrightarrow{k_i} AM_1^*$
Propagation	SHMeMB homopolymerization	$SHMeMB_n^* + SHMeMB \xrightarrow{k_{p1,1}} SHMeMB_{n+1}^*$
	Copolymerization	$SHMeMB_n^* + AM \xrightarrow{k_{p1,2}} AM_{n+1}^*$
	Copolymerization	$AM_n^* + SHMeMB \xrightarrow{k_{p2,1}} SHMeMB_{n+1}^*$
		$AM_n^* + AM \xrightarrow{k_{p2,2}} AM_{n+1}^*$
Termination (by combination)	SHMeMB homopolymerization	$SHMeMB_n^* + SHMeMB_m^* \xrightarrow{k_t} P_{n+m}$
	Copolymerization	$AM_n^* + SHMeMB_m^* \xrightarrow{k_t} P_{n+m}$
		$AM_n^* + AM_m^* \xrightarrow{k_t} P_{n+m}$
Depropagation		$SHMeMB_n^* \xrightarrow{k_{dep}} SHMeMB_{n-1}^* + SHMeMB$

The rate coefficients for initiator decomposition and propagation of AM are shown in Table 3. Initiator efficiency of V-50 was assumed to be 0.8, and for V-86 it was assumed to be 0.38 as determined in a previous study [62]. The propagation rate expression for AM homopolymerization was determined [28] and modelled [31] previously as a function of both monomer concentration and temperature, yielding a $k_{p,AM}$ value of 86 037 L/mol·s for 15 wt% AM in aqueous solution at 50°C. Although AM concentration changes with SHMeMB:AM comonomer composition (keeping total monomer content at 15 wt%), the value of $k_{p,AM}$ in the model was kept constant. This assumption is reasonable, as k_p^{cop} is dominated by the

low value of $k_{p,SHMeMB}$ and not sensitive to small changes in $k_{p,AM}$. As shown in Appendix F, $k_{p,AM}$ values were calculated at different total AM wt% (while maintaining 15 wt% monomer concentration) and the estimated values for k_t remained the same. In this work, a first estimate for $k_{p,SHMeMB}$ was obtained, but only at 60°C and 15 wt% monomer.

Table 3: Known rate expressions used in PREDICI for parameter estimation

Reaction	**Rate expression**	**References**
Decomposition of V-50	$k_d = 9.385 \times 10^{14} \exp(-14890/T(K))$	[63]
	$f = 0.8$	
Decomposition of V-86	$k_d = 1.24 \times 10^{13} \exp(-14800/T(K))$	[62]
	$f = 0.38$	
Propagation of AM	$k_p^0 = 9.5 \times 10^7 \exp(-2189/T\ (K))$	[28]
	$k_p = k_p^0 \exp(-0.01\ c_{AM}(0.0016T + 1.015))$	

4 Superabsorbent Hydrogel Characterization and Kinetics

4.1 Ring-closure of SHMB and SHMeMB

Before proceeding with hydrogel formation and in-situ NMR studies, it was necessary to verify that SHMeMB does not undergo side reactions under synthesis conditions. In the previous study there was evidence of SHMB ring-closure to form MBL during homopolymerization: insoluble polymer was observed after a 16 h polymerization of 30 wt% SHMB monomer with 0.2 mol% ACVA at 75°C and a pH of 7, and 4 mol% of the monomer remaining in solution was determined by NMR to be MBL rather than SHMB [23]. As the MBL amount increased as pH was lowered, it was concluded that the ring-closure was catalyzed in acidic conditions, and that the resulting precipitate was evidence of poly(MBL), which is insoluble in water. The study also found that homopolymerization of SHMB in water was very slow [23], especially relative to rates of radical polymerization of MBL in organic solution [20]. As it is well known that values of k_p in water are significantly higher than in organic solution (for example, as seen for methacrylic acid [30]), it is likely that MBL formed from ring-closure of SHMB was quickly polymerized to form poly(MBL).

Similar experiments were done in this study to determine if ring-closure of SHMeMB to form MeMBL occurred. Homopolymerizations were conducted at pH=7 with both V-50 and ACVA initiators at 15 wt% monomer and 50 and 75°C. There was no evidence of MeMBL monomer peaks observed in the NMR spectra after a reaction time of 16 h, and no polymer precipitate was observed. Thus, it can be concluded that, contrary to SHMB homopolymerization with ACVA, SHMeMB did not undergo ring-closure. Further investigations found that polymer precipitate was observed under more acidic conditions, i.e., with pH decreased to 4 and 5 using 1 M HCl and homopolymerizations conducted at both 50 (1 wt% V-50) and 75°C (1 wt% KPS) for 16 h; the amount of precipitate increased at lower pH and higher temperature. NMR was used to verify this trend; as shown in Figure A. 4 and Figure A. 5, the amount of MeMBL dissolved in

the water phase at the end of the 16 h reaction at 75°C was less than 3 mol% at pH=5 and about 9 mol% at pH=4. While the cause of the differences between the two monomers is not certain and was not the aim of this study, it can be concluded that ring-closure of both SHMB and SHMeMB does not occur if pH is greater than 7, conditions maintained throughout the remainder of this study.

4.2 Superabsorbent Hydrogel Absorption

Superabsorbent hydrogels were synthesized by copolymerizing SHMeMB and AM with small amounts of BIS crosslinker at varying molar ratios of SHMeMB:AM, similar to conditions used to produce SHMB:AM hydrogels in the study of Kollár et al. [23]. The initial reactions were conducted with solutions containing 0.2 mol% V-50 and 15 wt% monomer in water at 50°C for 4 h. The resulting hydrogels, however, lacked mechanical strength (i.e., visually very soft and jelly like and difficult to handle), with a significant amount of unreacted monomer remaining in solution, unlike SHMB:AM hydrogels made at the same conditions. It was also observed qualitatively that the fragility of the swollen hydrogels increased as the SHMeMB content was increased from 20 to 60 mol% in the formulations.

The increased fragility of SHMeMB:AM relative to SHMB:AM hydrogels was contrary to the expectation that the fragility would decrease with the bulkier side group in the polymer chain. In a study regarding properties of (meth)acrylate crosslinked polymers, it was found that both the length of the ester side group and the addition of the α-methyl side group increased T_g [64]. Nonetheless, the increasing mechanical strength found with increasing AM is consistent with the relative properties of crosslinked poly(AM) and poly(sodium acrylate) homopolymers [65]: poly(AM) has a higher shear modulus, and poly(sodium acrylate) chains are more extended due to repulsion of the charged species. Increasing the initial monomer concentration during synthesis is also known to affect properties of the crosslinked polymer, as chain transfer to polymer is more likely to occur with increased conversion, giving rise to branching and self-crosslinking and therefore hydrogels of higher rigidity [66]. Thus, the monomer concentration in this study

was increased from 15 wt% to 30 wt% and reaction time from 4 to 16 h in order to achieve a sufficient conversion for subsequent swelling experiments.

To better understand these results, the experiments were repeated in D_2O solution without crosslinker in order to determine the final monomer conversion using NMR and to compare to results for SHMB:AM copolymerization reported by Kollár *et al.* [23]. As shown in Table 4, conversion decreased with decreasing AM content for both systems, indicating that both SHMB and SHMeMB slow the overall copolymerization kinetics. SHMeMB:AM copolymers reached a lower conversion than SHMB:AM for all 3 molar ratios.

Table 4: Total monomer conversions of SHMB:AM copolymerizations conducted with 15 wt% initial monomer [23] and SHMeMB:AM copolymerizations with 15 and 30 wt% initial monomer in aqueous solution at varying feed molar fractions of SHMB (f_{SHMB}) and SHMeMB (f_{SHMeMB}) at 50°C.

f_{SHMB}	**0.2**			**0.4**			**0.6**		
V-50 mol%	0.2	-	-	0.2	-	-	0.2	-	-
M/H_2O wt./wt.	15/85			15/85			15/85		
Reaction time (hrs)	4	-	-	4	-	-	4	-	-
Conversion	97%	-	-	92%	-	-	59%	-	-
f_{SHMeMB}	**0.2**			**0.4**			**0.6**		
V-50 mol%	0.2	0.2	0.4	0.2	0.2	0.4	0.2	0.2	0.4
M/H_2O wt./wt.	15/85	30/70	30/70	15/85	30/70	30/70	15/85	30/70	30/70
Reaction time (hrs)	16	16	16	16	16	16	16	16	16
Conversion	72%	84%	97%	44%	50%	66%	35%	40%	44%

Increased reaction time, initiator levels and overall monomer concentration provides sufficient conversion for subsequent hydrogel testing. Thus, the swelling experiments and testing of mechanical properties were performed on hydrogels synthesized with 0.4 mol% of V-50 for 16 h at 30 wt% monomer concentration. Conversions of monomer to gel (gel yield), calculated from weight of the dry hydrogel using Equation 10

were in good agreement with the conversions estimated by NMR from copolymerizations performed in D_2O without addition of crosslinker (Table 5) except for f_{SHMeMB} = 0.6. Higher gel yield of f_{SHMeMB} = 0.6 samples may be due to very fast moisture absorption of dry hydrogel after the lyophilization procedure.

Table 5: Individual comonomers conversions (X_{AM} and X_{SHMeMB}) molar fractions of monomers incorporated into the final polymer (F_{AM} and F_{SHMeMB}) and total monomers conversion (X) calculated from ^{1}H NMR for linear polymers, and yield of crosslinked polymer (X_{gel}) based on gravimetric analysis of crosslinked polymers prepared with various initial molar fractions of monomers, f_{AM} and f_{SHMeMB} at 50°C.

f_{AM} / f_{SHMeMB}	F_{AM} / F_{SHMeMB}	X_{AM} (%)	X_{SHMeMB} (%)	X (%)	X_{gel} (%)
0.80 / 0.20	0.81 / 0.19	98	89	97	90±2
0.60 / 0.40	0.71 / 0.29	78	48	66	61±2
0.40 / 0.60	0.60 / 0.40	66	29	44	54±1

As shown in Figure 11 for material synthesized with 1.5 mol% crosslinker and f_{SHMeMB} = 0.2 as an example, the hydrogels swell significantly from their original size of 1 mm in thickness and 13 mm in diameter (Figure 11 right) during the swelling studies. After 24 h, swelling of the hydrogels was assumed to have reached equilibrium (Figure 11 left).

Figure 11: 2:8 SHMeMB:AM hydrogel with 1.5 mol% crosslinker after swelling (left) and before, i.e. as prepared (right).

The absorbency of the complete set of SHMeMB:AM hydrogels is compared in Figure 12. With 1.0 mol% crosslinker, swelling ratios of f_{SHMeMB} = 0.4 and 0.6 samples were 59000% and 33000%, respectively. These values were higher than values found for the corresponding SHMB:AM hydrogels (40000% and 20000% for f_{SHMB} = 0.4 and 0.6, respectively [23]), Interestingly, the lowest content of SHMeMB in the hydrogel (f_{SHMeMB} = 0.2) results in lower water absorption compared to the corresponding SHMB hydrogel (8600% vs 13000%). It should be noted, however, that direct comparison of SHMeMB:AM and SHMB:AM hydrogels is not strictly valid, since they differ in the monomer and initiator contents used during preparation due to the lower SHMeMB:AM reactivity. The higher monomer and initiator content should provide a denser network at a similar monomer conversion, which could lead to lower water absorption observed for f_{SHMeMB} = 0.2. However, the lower monomer conversions achieved with f_{SHMeMB} = 0.4 and 0.6 (copared to SHMB) likely led to lower network densities, providing the higher water absorption observed. Nonetheless, the trend of higher absorbency with increased SHMeMB content is consistent with the results reported for SHMB:AM and conventional poly(sodium acrylate-co-acrylamide) hydrogels, as the carboxylate groups are more hydrophilic than the acrylamide groups [67]. In addition, the crosslinked network becomes more expanded due to electrostatic repulsion of the ionized groups, with the SHMeMB unit providing more hydrophilicity to these hydrogels than sodium acrylate. Increasing the crosslinker

concentration from 1 mol% to 1.5 mol% showed the expected behaviour, with a slight decrease of swelling ratios measured for all samples (Figure 12).

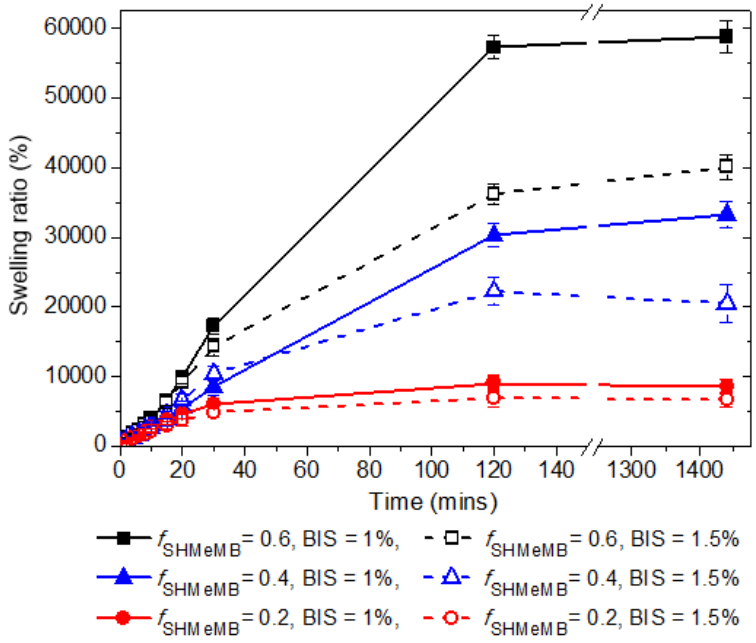

Figure 12: Swelling ratios of AM:SHMeMB hydrogels made with 0.4 mol% V-50 at 30 wt% monomer for 16 h at varying initial comonomer ratios and BIS crosslinker content, as indicated.

The mechanical strength of the hydrogels was quantified from the stress vs. strain curves obtained under compression, as shown in Figure 13. Hydrogels with increased AM content were able to withstand higher compression stress, indicating higher mechanical strength. In addition, higher compression stress was observed for hydrogels prepared with higher crosslinker concentration.

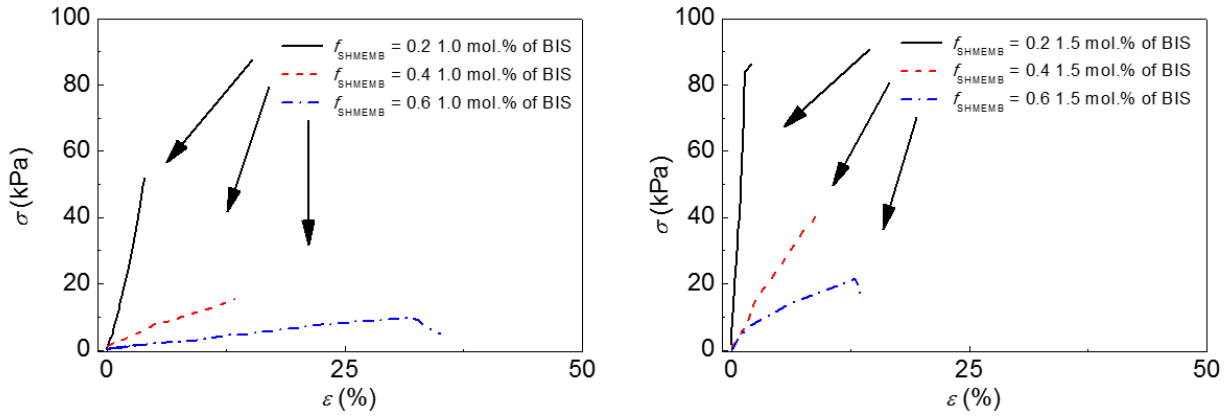

Figure 13: Stress vs. strain curves of hydrogels made with a) 1.0 mol% BIS and b) 1.5 mol% BIS and initial comonomer molar ratios of f_{SHMeMB} = 0.2, 0.4, and 0.6 with 30 wt% monomer and 0.4 mol% V-50 in aqueous solution for 16 h at 50°C.

Storage (G') and loss (G'') moduli are shown as a function of frequency in Figure 14. The storage modulus is constant with frequency, consistent with the expected properties of cross-linked viscoelastic materials. G' increased from 680 Pa to 13100 Pa with increasing AM content in the hydrogels synthesized with 1.0 mol% of BIS, and from 1200 Pa to 32000 Pa with 1.5 mol% of BIS, indicating that AM provides mechanical strength as well as improving the elastic property of the hydrogels. Similarly to the G' behaviour, G'' is also nearly independent of frequency, indicating that the hydrogels were well cross-linked, with relatively low energy dissipation observed especially at higher AM contents. Overall, the mechanical properties of SHMeMB:AM hydrogels are highly tunable and can be tailored by changing the amount of crosslinker and the molar composition of the copolymer. The hydrogels made of higher AM content, having better mechanical properties, could be suitable for a variety of applications such as cell culturing or tissue engineering [68], while those produced with higher SHMeMB content exhibit promise as superabsorbent materials.

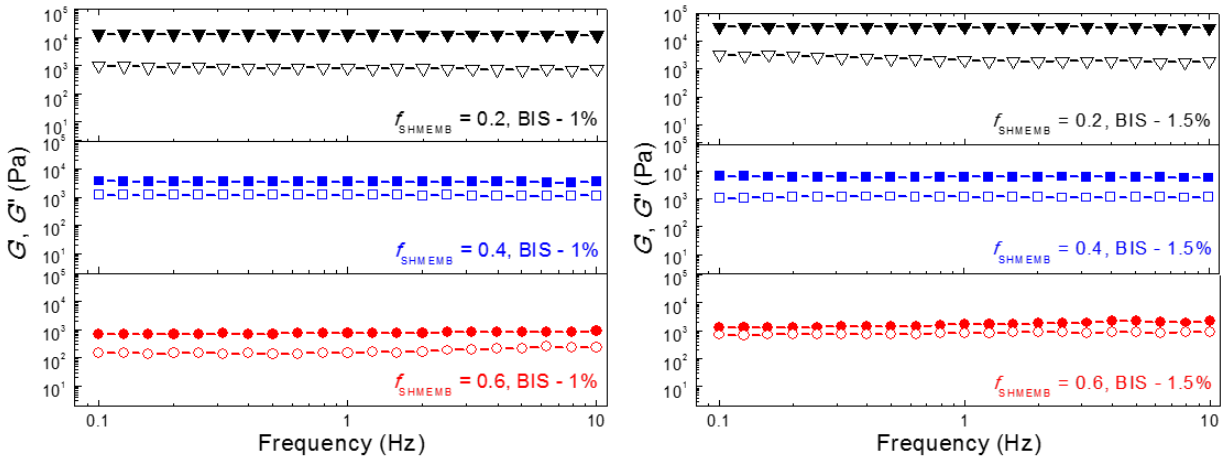

Figure 14: Storage (G', filled symbols) and loss (G'', open symbols) moduli measured as a function of frequency for SHMeMB:AM hydrogels produced with monomer molar ratios of 2:8 (top), 4:6 (middle), and 6:4 (bottom) with (left) 1.0 and (right) 1.5 mol% of BIS.

SEM images of hydrogels are shown in Figure 15. The porosity of the hydrogel is higher with increasing amount of SHMeMB. Porosity decreased at higher crosslinker level, indicating the formation of a denser polymer network consistent with the degree of swelling results. SEM images of poly(sodium acrylate – co – acrylamide/graphene oxide hydrogels also indicated a smoother polymer surface and a denser hydrogel with increasing crosslinker content [69].

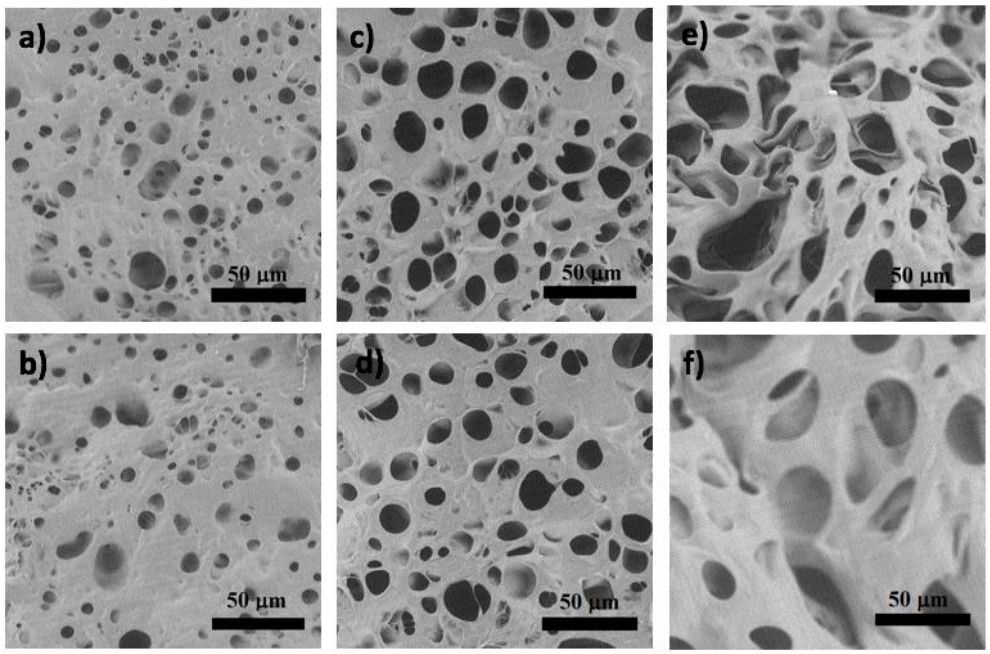

Figure 15: SEM images of freeze-dried cross-sections of the SHMeMB:AM hydrogels synthesized at a molar ratio of f_{SHMeMB} = 0.2 with a) 1.0 mol% and b) 1.5 mol% BIS; a molar ratio of f_{SHMeMB} = 0.4 with c) 1.0 mol% and d) 1.5 mol% BIS; and a molar ratio of f_{SHMeMB} = 0.6 with e) 1.0 mol% and f) 1.5 mol% BIS. Hydrogels were synthesized from 30 wt% monomer and 0.4 mol% V-50 for 16 h at 50°C.

4.3 Kinetic studies using in-situ *NMR*

The decrease in total monomer conversion with increasing SHMeMB content is due to the lower reactivity of SHMeMB, slowing both the overall copolymerization rate and the relative rate of SHMeMB incorporation into the copolymer. Due to the significant difference in reactivity compared to the SHMB:AM system, further kinetic studies were done to better understand and quantify the influence of SHMeMB on the copolymerization system.

Using the *in-situ* NMR method, the consumption of the individual monomers can be monitored by following the change in their proton peak intensities with reaction time, providing both a continuous measure of overall monomer conversion, as well as the change in comonomer (and thus copolymer) composition over the course of the batch reaction. In Figure 16, the increases in overall monomer

conversion of SHMeMB:AM and SHMB:AM systems under identical conditions are shown for both 2:8 and 4:6 initial molar ratios. It is evident that SHMB:AM copolymers have a faster rate of polymerization, in agreement with the observations made during hydrogel synthesis. A comparison of these plots indicates also that the rate of monomer conversion decreases for both systems as the initial AM fraction is decreased.

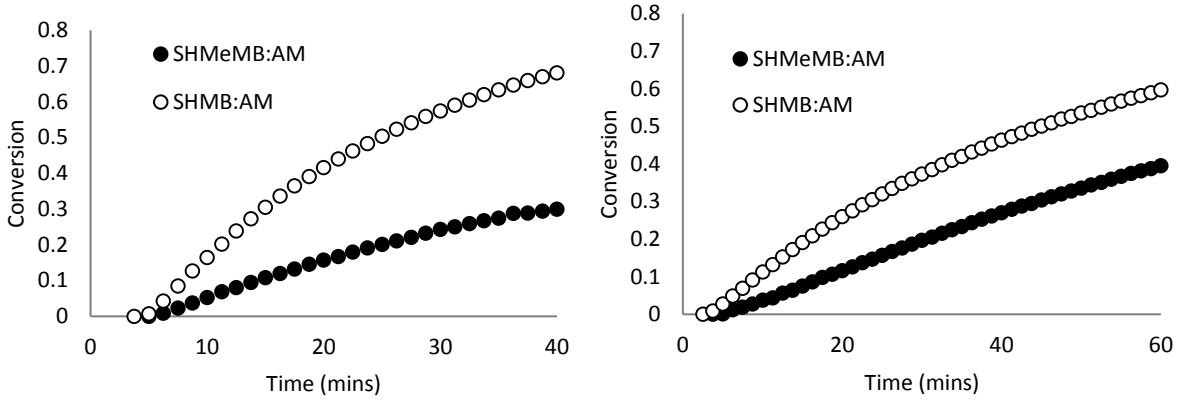

Figure 16: Overall monomer conversion profiles for polymerization of $f_{SH(Me)MB}$ = 0.2 (left) and $f_{SH(Me)MB}$ = 0.4 (right) initial molar ratios of SHMeMB:AM and SHMB:AM at 50°C with 15 wt% monomer and 1.3 mol% V-50 initiator in D_2O.

A series of SHMeMB:AM copolymerizations at various molar ratios were completed at 50°C with 1.3 mol% V-50 and 15 wt% monomer. The drift in monomer composition (molar fraction SHMeMB in time, denoted by f_{SHMeMB} with conversion is shown in Figure 17. Despite the lowering of polymerization rate observed with increasing SHMeMB level, there is only a slight drift in f_{SHMeMB} with conversion, with the increasing value indicating preferential incorporation of AM into the copolymer. Material balances were used to calculate the composition of the copolymer formed at low (<10%) conversion, with results summarized in Table A. 4. The low-conversion data was used to construct a Mayo-Lewis plot to represent the relationship between comonomer and copolymer composition, as shown in Figure 18. Also included on the plot is the previously reported fit for SHMB:AM data obtained by the terminal model with reactivity ratios r_{SHMB}=0.35±0.15 and r_{AM}=1.42±0.40 [23]. From this study the reactivity ratios for SHMeMB:AM were determined to be r_{SHMeMB}=0.12±0.08 and r_{AM}=1.10±0.01. The two sets of data overlap below a

comonomer fraction of 0.4, but the incorporation of SHMeMB is lowered at higher comonomer levels, leading to the significant difference in the reactivity ratio estimates.

As shown in previous work, more precise estimates of reactivity ratios can be obtained by fitting an integrated form of the Mayo-Lewis equation to the drift in monomer composition as a function of conversion [32]. Figure 18 demonstrates that the best-fit values of r_{SHMeMB}=0.17±0.01 and r_{AM}=0.95±0.01, determined using the entire set of composition drift data, provide an excellent representation of the in-situ NMR results. While there is a minor difference between the estimates, both the values determined using the entire monomer composition drift and those fit to the low-conversion data provide a similar representation of copolymer vs comonomer composition, as evidenced by comparing the two curves generated in Figure 18. Although there is no discernable difference in addition rates of AM and SHMeMB monomer to an AM macroradical ($r_{AM} \approx 1$), there is a clear preference for AM monomer to add to the anionic SHMeMB radical compared to SHMeMB monomer addition. A comparison of the two systems indicates there is a lower tendency for SHMeMB to homopolymerize compared to SHMB, most likely due to the presence of the extra methyl group (see Figure 10).

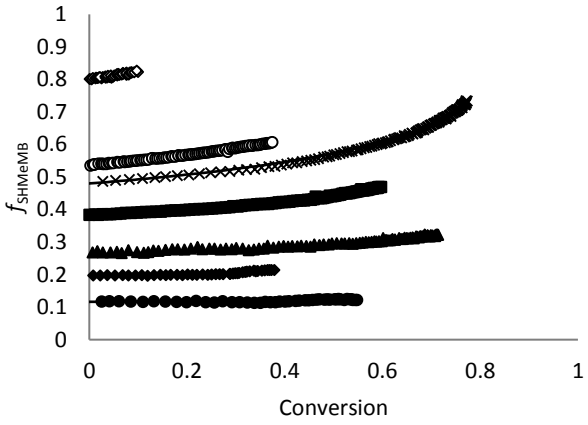

Figure 17: SHMeMB monomer composition (f_{SHMeMB}) as a function of conversion at varying feed molar ratios of SHMeMB:AM at 15 wt% monomer and 0.5 wt% V-50 at 50°C. Lines represent monomer composition drift computed using the integrated form of the Mayo-Lewis equation with best fit reactivity ratios of r_{SHMeMB}=0.17 and r_{AM}=0.95.

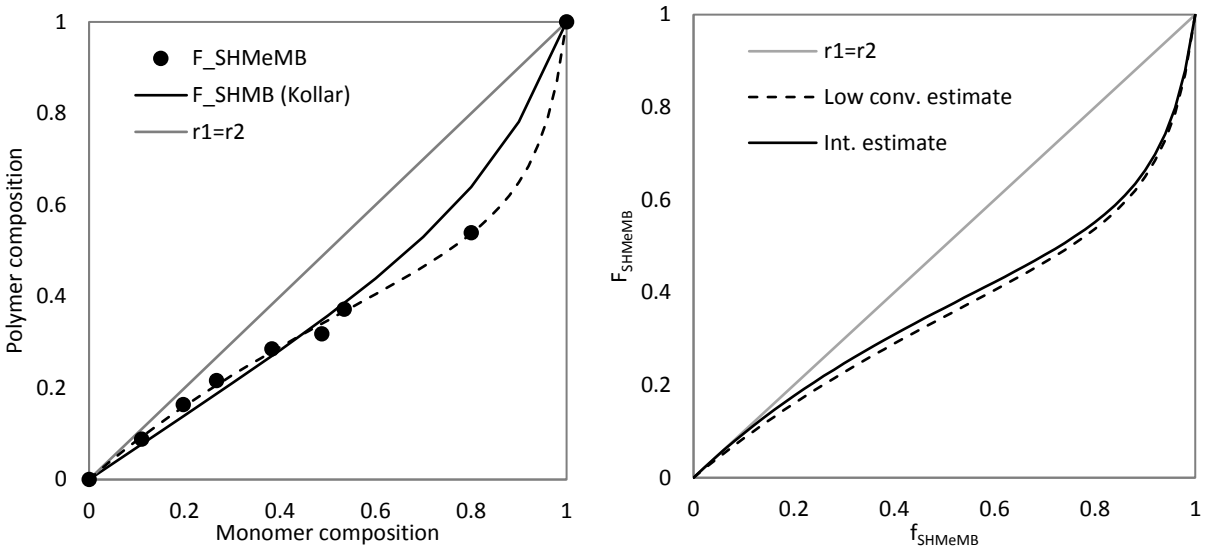

Figure 18: (Right) Mayo-Lewis curves for SHMB:AM [23] (solid line) and SHMeMB:AM (points are experimental data and dashed line is best-fit curve) radical copolymerization at 15 wt% monomer and 50°C, where the x-axis represents SH(Me)MB molar fraction in the monomer mixture and the y-axis represents the SH(Me)MB molar fraction in the copolymer at low conversion. (Left) Mayo-Lewis curves for SHMeMB:AM copolymerization calculated using best-fit reactivity ratios estimated from both low conversion data (dashed line, r_{SHMeMB}=0.12 and r_{AM}=1.10) and the integrated form of Mayo-Lewis equation (solid line, r_{SHMeMB}=0.17 and r_{AM}=0.95).

4.4 PLP-SEC studies

Previous experiments for AM homopolymerization in aqueous solution at 10 wt% and at 60°C resulted in good PLP structures using the pulse repetition rates of 150 and 300 Hz, and the lower number of pulses of100 and 300 pulses; the resulting k_p value under these conditions was 110 000 L/mol·s [28]. Thus, the first PLP-SEC experiments for SHMeMB:AM were done under similar conditions, the only difference being 10 mol% SHMeMB introduced, with total monomer content in water remaining at 10 wt%. Laser frequency was varied between 5 and 300 Hz, and a significantly larger number of pulses (1000 or 1500) was used with 3.4 mmol/L LiTPO. As the hydrogel synthesis demonstrated that SHMeMB is much less reactive than AM, the lower frequencies were used to allow for a longer dark period, with the higher number

of pulses to increase conversion. However, these PLP conditions did not lead to well-structured MMDs (Figure A. 6 and Figure A. 7), as there was no evidence of multiple inflections to accurately determine k_p^{cop}.

Thus, a new set of PLP experiments was done with the pulse repetition rate lowered to between 1 and 5 Hz with 6.8 mmol/L LiTPO, and the number of pulses reduced to 50 and 100 in order to improve the features of the distributions. SHMeMB:AM mixtures of 10 wt% total monomer in water were examined, with 5, 10, and 15 mol% of SHMeMB. The resulting polymer MMDs and their first derivative plots (used to identify the points of inflection L_i) are shown in Figure 19. In most of the cases, there is more than one inflection point, indicating that the experiments can be used to determine k_p^{cop}. As mentioned in the Experimental Methods (Chapter 3.2.4), MMDs were analyzed using PAM calibration, although the copolymers contained up to 15 mol% SHMeMB.

In order to verify the accuracy of the k_p^{cop} values calculated from these PLP structures, the ratio of molecular weights at the first and second inflection points were determined (L_1/L_2). In some cases, the experimental ratios were slightly below the expected value of 0.5, perhaps due to the higher conversion of some experiments, as the decreased monomer concentration can cause small shifts in the distribution. Thus, the conversion was reduced to <10% by lowering the number of pulses from 100 to 50 in later experiments. Due to the limited number of successful experiments, all values were used to estimate k_p^{cop}, as the values determined from experiments at different pulse repetition rates are in good agreement as seen by inspecting the full set of data in Table 6; checks such as these indicate good PLP structure such that k_p^{cop} can be reliably estimated using Equation 1 [40].

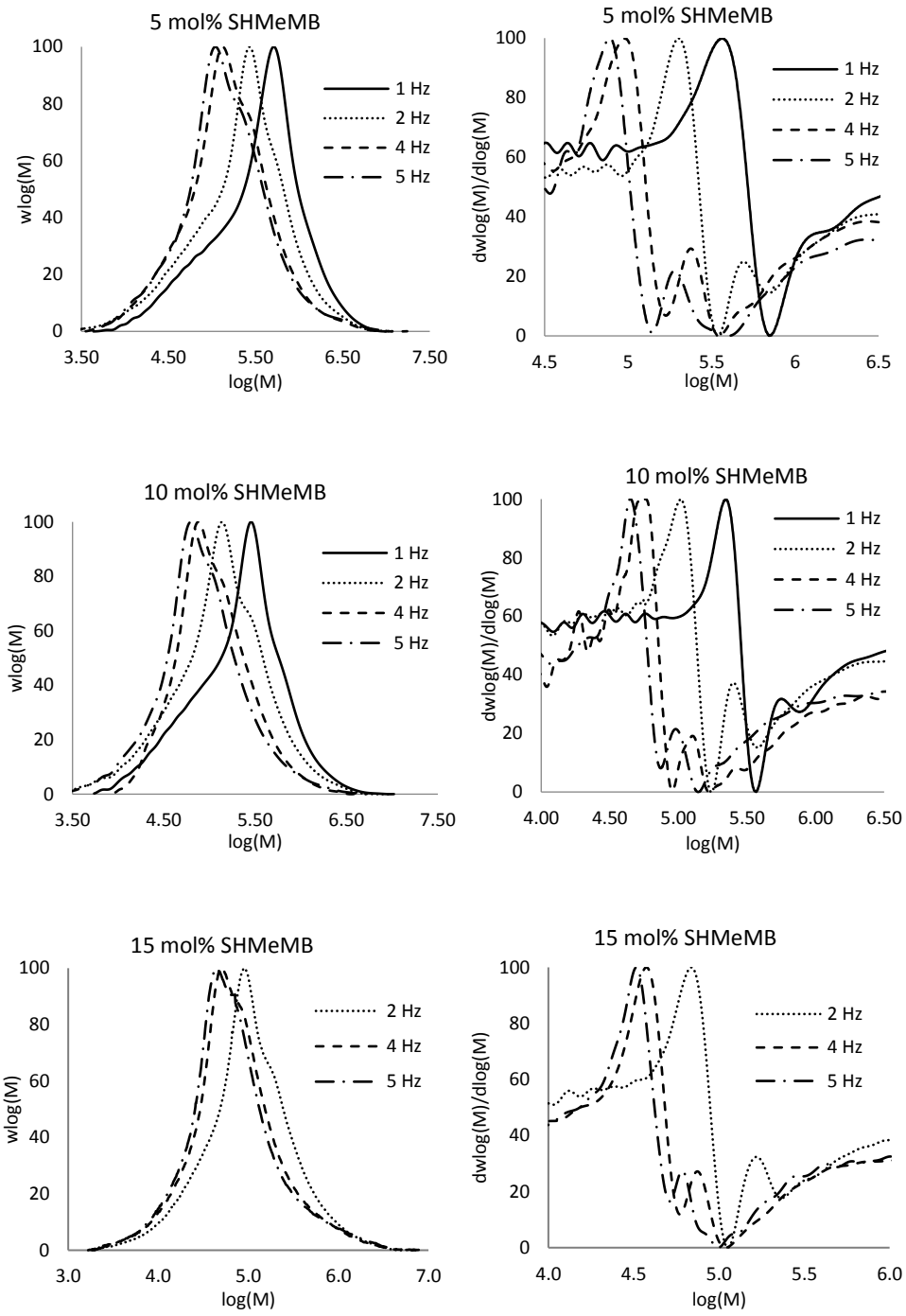

Figure 19: Polymer molar mass distributions (left) and first derivative plots (right) produced by PLP of SHMeMB:AM mixtures of varying compositions at 10 wt% monomer, 6.8 mmol/L LiTPO, and 60°C. PLP-SEC experiments for f_{SHMeMB}=0.10 were done with number of pulses=100, and f_{SHMeMB}=0.05 and 0.15 were done with number of pulses=50.

Table 6: PLP-SEC conditions and results for SHMeMB:AM copolymers at 60°C, 6.8 mmol/L LiTPO and 10 wt% monomer.

mol% SHMeMB	Repetition rate	# of pulses	$\log M_1$	$\log M_2$	M_1/M_2	$k_p^{cop}{}_1$	$k_p^{cop}{}_2$	Conversion
5 mol%	1 Hz	100	5.56	6.05	0.32	3639	5613	19.0%
	2 Hz	100	5.30	5.69	0.41	4020	4941	15.0%
	4 Hz	100	4.98	5.37	0.41	3838	4709	12.4%
	5 Hz	100	4.89	5.28	0.41	3884	4760	7.9%
10 mol%	1 Hz	100	5.35	5.75	0.40	2040	2558	14.3%
	2 Hz	100	5.02	5.40	0.41	1890	2303	11.6%
	4 Hz	100	4.77	5.10	0.46	2133	2304	8.3%
	5 Hz	100	4.65	4.98	0.47	2045	2174	6.8%
15 mol%	2 Hz	50	4.84	5.22	0.41	1374	1662	4.7%
	4 Hz	50	4.57	4.87	0.50	1499	1496	3.1%
	5 Hz	50	4.52	4.78	0.54	1639	1520	3.3%

The same PLP conditions were used for SHMB:AM to produce a direct comparison of k_p^{cop} for the two systems. Their MMDs and first derivative plots are shown in Figure 20 for 5-15 mol% of SHMB in SHMB:AM mixtures of 10 wt%. For the SHMB copolymer system it was the experiments at higher pulse repetition rates of 4 and 5 Hz that yielded more distinct PLP-structured MMDs, unlike the 1 and 2 Hz required for SHMeMB:AM system at the same conditions. With SHMB:AM, the MMDs were broadened at lowered repetition rates, perhaps due to a higher termination rate in the system. Although the data set is limited (Table 7), the k_p^{cop} estimates from SHMB:AM copolymerization provide a useful comparison to the SHMeMB:AM system.

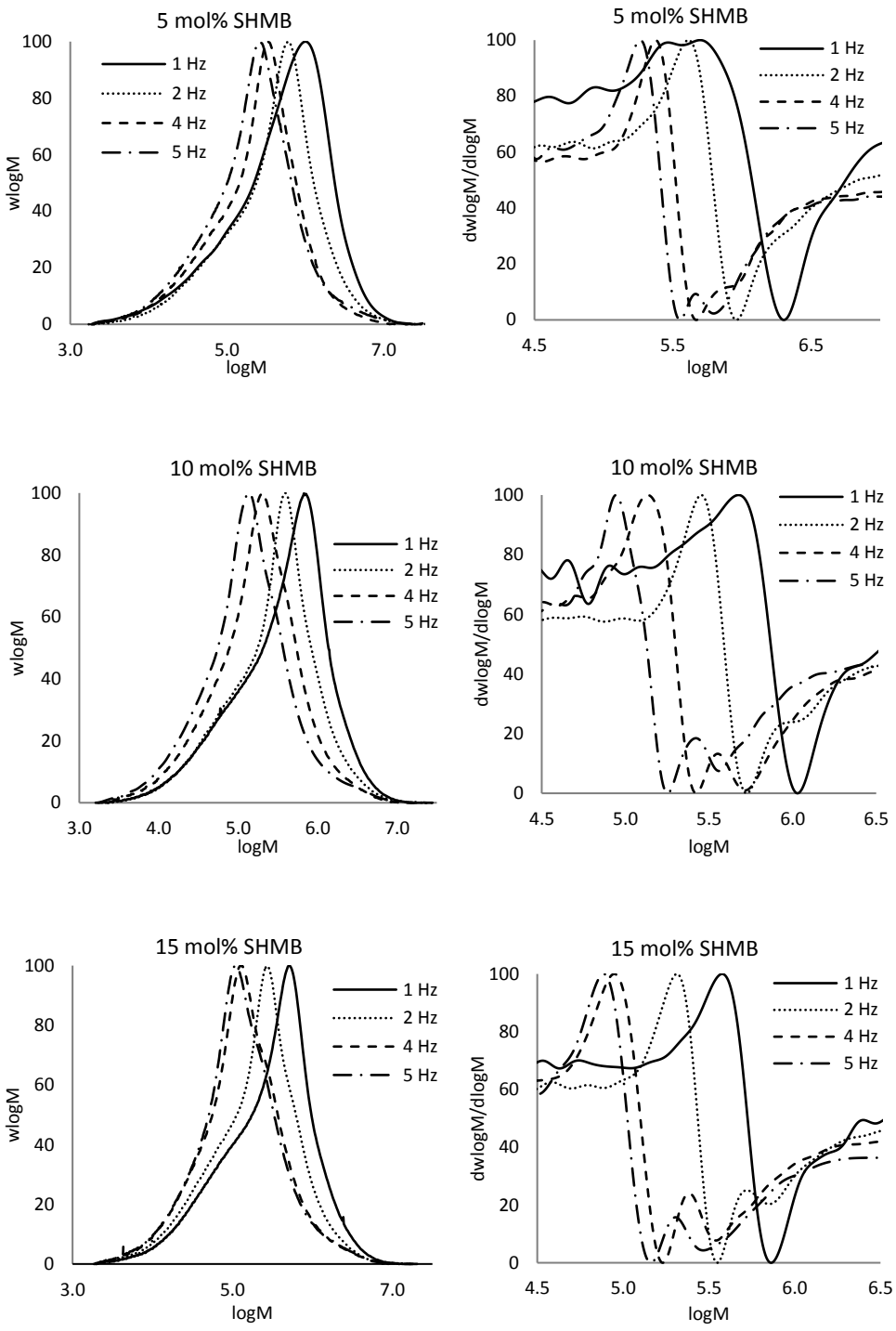

Figure 20: Molecular weight distributions and first derivative results of SHMB:AM copolymers at varying compositions with number of pulses=50, 10 wt% monomer, 6.8 mmol/L LiTPO, and at 60°C.

Table 7: PLP-SEC conditions and results of SHMB:AM copolymers at 60°C, 6.8 mmol/L LiTPO and 10 wt% monomer.

mol% SHMB	Repetition rate	# of pulses	$logM_1$	$logM_2$	M_1/M_2	$k_p^{cop}{}_1$	$k_p^{cop}{}_2$	Conversion
5 mol%	5 Hz	50	5.26	5.68	0.39	9177	11830	10.4%
10 mol%	4 Hz	50	5.13	5.55	0.38	5418	7165	5.2%
	5 Hz	50	4.94	5.42	0.33	4402	6590	4.3%
15 mol%	2 Hz	50	5.31	5.72	0.39	4132	5281	5.1%
	4 Hz	50	4.95	5.39	0.37	3573	4879	4.0%
	5 Hz	50	4.89	5.31	0.38	3872	5071	3.4%

The k_p^{cop} values of SHMeMB:AM and SHMB:AM determined by PLP-SEC are compared in Figure 21, plotted as a function of molar fraction of AM and also as a function of comoonomer molar fraction. For both systems, k_p^{cop} decreases rapidly when the comonomer is added to the AM system. Even 5 mol% of comonomer reduces k_p from the known homopolymerization value of ~110 000 L/mol·s for AM [28] to 10 000 L/mol·s with 5 mol% SHMB and 4300 L/mol·s with 5 mol% SHMeMB. These results also show that the SHMB:AM system is more reactive than SHMeMB:AM by greater than a factor of two.

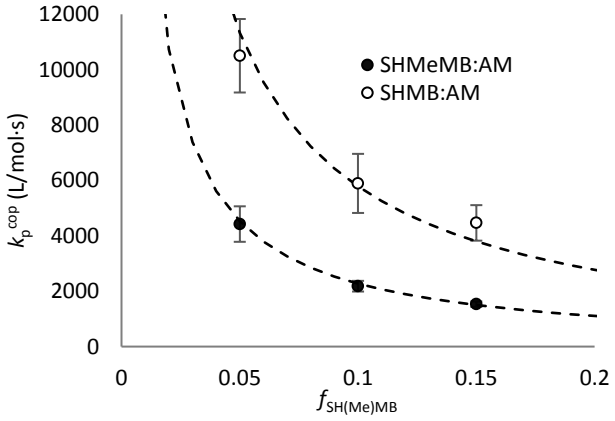

Figure 21: k_p^{cop} of SHMeMB:AM and SHMB:AM at varying molar ratios at 10 wt% monomer, 60°C and 6.8 mmol/L LiTPO with error bars representing standard deviation of the data set. The dashed line represents the terminal model estimating k_p^{cop} for all molar compositions of SHMB:AM and SHMeMB:AM.

PLP structures were not obtained for SHMB or SHMeMB homopolymers (or copolymers formed with f_{SHMB} and f_{SHMeMB} >15 mol%), as propagation for the homo/copolymerizations became too slow. Repetition rate of the laser pulse could not be decreased further to obtain characteristic MMD inflection points. However, assuming the terminal model, k_p of SHMB and SHMeMB homopolymers were estimated using Equation 17 to fit the variation in k_p^{cop} as a function of monomer composition (f_A and $f_B = 1 - f_A$, with A representing AM and B the SHMB or SHMeMB comonomer) using the determined monomer reactivity ratios (r_A and r_B), monomer fractions and homopolymer k_p values.

$$k_p^{cop} = \frac{r_A f_A^2 + 2 f_A f_B + r_B f_B^2}{\frac{r_A f_A}{k_{p,AA}} + \frac{r_B f_B}{k_{p,BB}}} \quad (17)$$

Using the known reactivity ratios of r_{SHMB} and r_{AM} from Kollár *et al*. study [23], r_{SHMeMB} and r_{AM} from this study, and $k_{p,AM}$ of 110 000 L/mol·s [28], the k_p values of SHMB and SHMeMB were estimated to be 165 and 25 L/mol·s, respectively, at 60 °C. While these absolute values have significant uncertainty due to the limited number of data points and the extrapolation of the curve to $f_{SH(Me)MB}$ = 1, the PLP-SEC study indicates clearly that SHMB is more reactive than SHMeMB.

Effects of monomer concentration on k_p^{cop} was explored by doubling the monomer concentration. For fully ionized methacrylic acid, k_p was found to increase with increasing monomer concentration [27], a result explained by charge screening occurring at the increased concentration of counterions to reduce hindrance to internal rotation. The k_p^{cop} of 10 mol% SHMeMB in SHMeMB:AM at 60°C and 6.8 mmol/L LiTPO at 10 vs. 20 wt% were 2181 ± 193 and 2314 ± 233 L/mol·s, respectively. Even though both values are within error of each other, k_p^{cop} at 20 wt% is slightly higher than at 10 wt% and is consistent with the trend of increased k_p with increasing monomer concentration. The quality of the PLP results are verified in Table 8, where M_1/M_2 ratios are close to 0.5 and conversion is <10%.

Table 8: PLP-SEC conditions and results of SHMeMB:AM copolymers at 60°C, 6.8 mmol/L LiTPO and 20 wt% monomer.

mol% SHMB	Repetition rate	# of pulses	$\log M_1$	$\log M_2$	M_1/M_2	$k_p^{cop}{}_1$	$k_p^{cop}{}_2$	Conversion
10 mol%	2 Hz	50	5.34	5.73	0.41	2208	2680	4.7%
	4 Hz	50	5.01	5.38	0.42	2043	2425	3.8%
	5 Hz	50	4.91	5.30	0.41	2055	2477	3.7%

4.5 Summary

MeMBL was successfully saponified to form a water-soluble SHMeMB monomer that does not undergo ring-closure at pH of 7 or greater. The synthesis of lightly crosslinked SHMeMB:AM hydrogels represents a unique approach for the preparation of superabsorbent material. The hydrogels attained an equilibrium degree of swelling in the range of 6,700 – 59,000%, depending on copolymer composition as well as crosslink density, with the swelling capacity significantly increasing with SHMeMB content. The monomer ratio and crosslinker concentration also influenced the porosity and overall mechanical properties of the hydrogels. These characteristics were shown to be highly tunable, allowing the potential to prepare tailored hydrogels suitable for a wide range of applications.

Kinetic studies of SHMeMB:AM and SHMB:AM aqueous-phase radical copolymerization were conducted to investigate their reactivities using in-situ NMR and PLP-SEC techniques. The in-situ NMR studies revealed that SHMeMB:AM mixtures polymerized at slower rates than SHMB:AM, with comonomer composition drifts used to estimate the monomer reactivity ratios as $r_{SHMeMB} = 0.12 – 0.17$ and $r_{AM} = 0.95 – 1.10$. Using PLP-SEC, values for k_p^{cop} of SHMeMB:AM were confirmed to be lower than those of SHMB:AM. The data obtained at high AM content were fit by the terminal model to provide first estimates of the SHMeMB and SHMB homopropagation rate coefficients, albeit with considerable uncertainty. It is clear from the study, however, that the k_p value for SHMeMB is lower than that of SHMB, and that both values are much lower, by three orders of magnitude, than the k_p of AM, explaining the long polymerization times required to produce the hydrogels.

5 Investigating the influence of depropagation and ionic strength on SHMeMB (co)polymerization

The previous chapter looked at the copolymerization of SHMeMB and AM with crosslinker to synthesize superabsorbent hydrogels. Kinetic studies were done on SHMeMB:AM linear copolymers to determine their monomer reactivity ratios. Furthermore, k_p^{cop} values of SHMeMB:AM and SHMB:AM systems were determined using PLP-SEC, and k_p of SHMeMB and SHMB homopolymers were estimated assuming the terminal model of copolymerization chain growth. A significant difference in reactivity was observed between SHMeMB:AM and SHMB:AM systems, both in polymerization rates as seen from *in-situ* NMR results, as well as propagation rate coefficients from PLP-SEC results. Hence, as described in this chapter, further studies were done to better understand the polymerization kinetics. SHMeMB:AM copolymerizations and SHMeMB homopolymerizations were studied at elevated temperatures to explore whether depropagation is present. In addition, homopolymerizations of SHMeMB were done with added salt to observe whether the changes in polymerization rate are similar to those reported for NaAA [70] [71]. The conversion profiles acquired from *in-situ* NMR were modeled in PREDICI to estimate the rate coefficients for termination (k_t) and depropagation (k_{dep}), using the k_p values of SHMeMB estimated from PLP-SEC in the previous chapter. Ultimately, the estimated parameters from SHMeMB homopolymerization were implemented in a copolymerization kinetic model of SHMeMB:AM.

5.1 Copolymerization of SHMeMB:AM at different temperatures

While the majority of the *in situ* batch copolymerizations of SHMeMB and AM were done at 50°C, a few experiments were also performed at elevated temperatures to determine whether polymer composition was affected by temperature. Conversion profiles measured for experiments with initial monomer content of 15 wt% and SHMeMB:AM molar ratios of 3:7 (50-80 °C) and 4:6 (50-70 °C) are shown in Figure 22. It is evident that the initial rate of polymerization increases with temperature, as expected due to the accelerated radical production rate as well as the increased k_p value. However, monomer conversion plateaus at values

of less than 100% at the higher temperatures. This limiting conversion does not result from initiator depletion near the end of the reaction, as 27% of the V-50 is remaining after 3 h at 70°C, based on literature values of V-50 decomposition kinetics [63]. The conversion plateau occurs at a lower conversion as the initial fraction of SHMeMB is increased, as seen by comparing the profiles for 3:7 and 4:6 SHMeMB:AM after 3 h. Thus, the presence of SHMeMB is not only affecting the initial rate of polymerization, but also is causing the copolymerization rate to significantly slow down as higher conversions are reached at the higher temperatures.

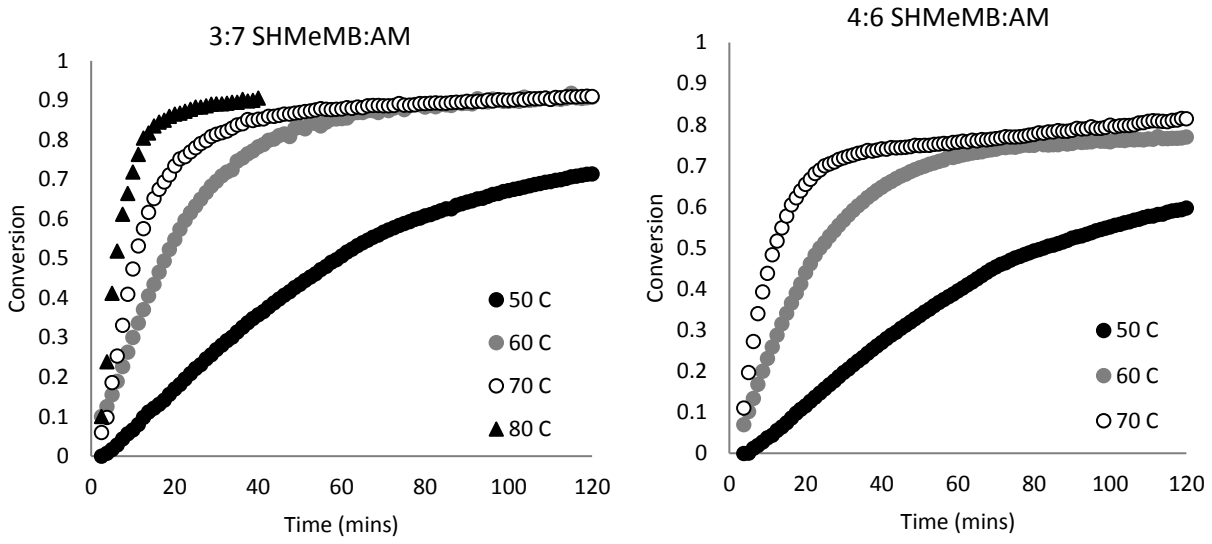

Figure 22: Overall monomer conversion profiles for copolymerizations at 3:7 (left) and 4:6 (right) initial SHMeMB:AM molar ratios at varying temperatures with 15 wt% monomer and 0.5 wt% V-50.

Individual monomer concentration profiles of SHMeMB and AM at 50, 60, and 70°C are presented in Appendix D. The plots show that the rate of SHMeMB consumption becomes very slow at low SHMeMB concentrations reached later in the reactions, while the consumption of AM continues. This behaviour becomes more evident at higher temperatures and increased SHMeMB content, under which conditions the absolute concentration of AM decreases to values below that of SHMeMB, despite its higher initial value.

The limiting SHMeMB conversions suggest that depropagation of SHMeMB monomer may be occurring, leading to a significantly decreased rate of polymerization as AM is consumed.

To further explore this possibility, the comonomer composition drifts with conversion at different temperatures are plotted in Figure 23; the curves are normalized by the initial fraction of SHMeMB in the mixture to provide a better comparison by eliminating slight variations in the initial compositions. If SHMeMB depropagation is important, the value of f_{SHMeMB} would increase more significantly with conversion as temperature is increased due to decreased incorporation of SHMeMB under conditions that favour depropagation, as seen for the MEA/ST [38] and BMA/ST [34] systems described in Chapter 2.4. As shown in Figure 20, this behaviour is indeed observed for the SHMeMB:AM system as temperature increased from 50 to 80°C. At higher conversions, monomer concentration is low and the influence of depropagation on SHMeMB consumption becomes more prominent. Reaction temperature was further increased to 90°C using a different initiator, V-86, as it has a slower rate of decomposition. At 90°C, there was further deviation of the drift in f_{SHMeMB} with conversion compared to 50°C. Reactions with V-50 and V-86 were done at the same temperatures and showed that composition drift was consistent using both initiators (see Appendix E, Figure A. 9).

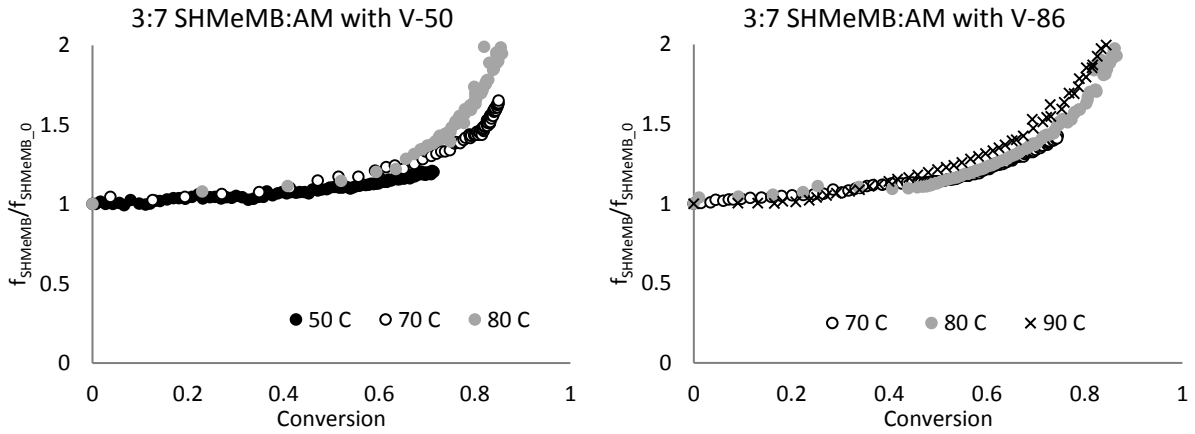

Figure 23: Monomer composition drift with conversion for copolymerization with an initial 3:7 SHMeMB:AM molar ratio, 15 wt% monomer and 0.5 wt% V-50 initiator (left) and 1.67 wt% V-86

initiator (right) at varying temperatures (90°C experiment was conducted with 0.5 wt% V-86). Monomer composition was normalized by initial monomer composition to eliminate the influence of slight variations in the comonomer mixture composition.

5.2 Homopolymerization kinetics of SHMeMB

To investigate depropagation kinetics further, the *in-situ* NMR technique was used to study homopolymerization of SHMeMB at increased temperature and initiator content (75°C and 1 wt% KPS), with reaction times (14 h) considerably extended compared to copolymerizations in order to obtain the conversion profiles shown in Figure 24. It was necessary to switch to KPS as initiator, since at high concentrations of monomer and V-50 initiator (30 wt% and 1 wt%, respectively) the solution was no longer homogeneous; even after sonification, solids remained and did not dissolve. It was suspected that the cationic V-50 initiator coordinated with the anionic SHMeMB monomer and precipitated out of solution. Therefore, the initiator was changed to anionic KPS to avoid ionic interaction between monomer and initiator. At 15 and 30 wt% monomer, conversions after 14 h were 23% and 13% respectively. Note that the homopolymerization of AM is able to reach almost full conversion at varying monomer concentrations in well less than an hour under similar conditions [31], as opposed to a conversion of <25% for SHMeMB after 14 h. If depropagation was occurring, the SHMeMB concentration should eventually decrease to the same equilibrium level; hence starting at a higher initial monomer concentration would result in higher conversion [34]. However, as seen in Figure 24, 30 wt% SHMeMB resulted in a lower conversion than at 15 wt%. This result is contrary to previously reported systems for other depropagating systems [72]; however, as propagation kinetics are concentration dependent in aqueous solution, the same might be true for depropagation.

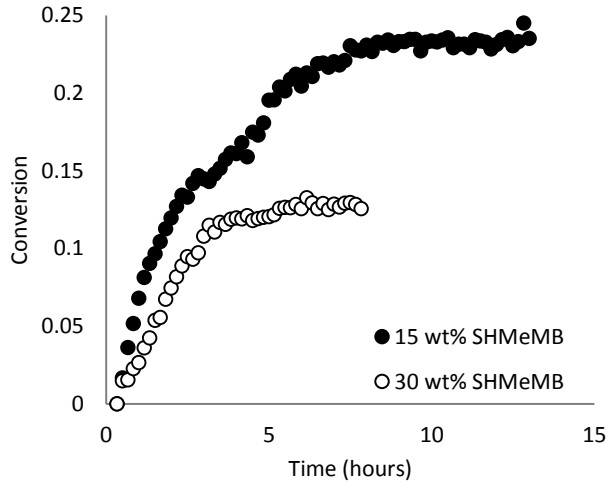

Figure 24: Monomer conversion profiles obtained by homopolymerization of SHMeMB at 15 and 30 wt% at 75°C and 1 wt% KPS.

However, additional problems with initiator choice cannot be ruled out, as literature has reported that decomposition of persulfate initiators is a function of pH, ionization, and monomer concentration. For example, for the polymerization of acrylic acid at 65% ionization at 70°C and 33.8% AA, k_d of sodium persulfate was measured to be 0.20 s^{-1} [73], much higher than the rate coefficient for KPS decomposition in water at 70°C of 3.71×10^{-5} s^{-1} [37]. The potentially enhanced decomposition of KPS in the presence of SHMeMB under the reaction conditions used offers a potential explanation for the observed behaviour: with higher decomposition rates of KPS, radical concentration would decrease to zero much faster than anticipated, leading to the plateau in monomer conversion seen in Figure 24. Thus, the homopolymerizations of SHMeMB were repeated with 1 wt% V-86, a neutral initiator that has a longer half-life that KPS, at 15 and 30 wt% monomer and 75°C (Figure 25). Conversion profiles were the same for both monomer concentrations because decomposition of V-86 was not affected. This is consistent with results reported for other fully ionized aqueous monomers, NaAA [25] and NaMAA [27], systems for which monomer concentration did not have large effects on k_p. However, no difference in the limiting conversion was seen between 15 and 30 wt% SHMeMB monomer concentration – perhaps monomer concentration in

both cases have not yet reached the equilibrium values for depropagation to cause a difference in limiting conversion.

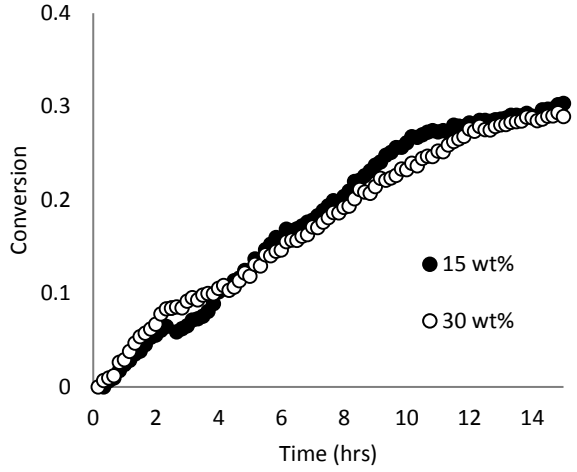

Figure 25: Monomer conversion profiles obtained by homopolymerization of SHMeMB at 15 and 30 wt% at 75°C and 1 wt% V-86.

The possible effects of depropagation on the homopolymerization of SHMeMB was investigated at higher temperatures. In Figure 26, the initial rate of polymerization is seen to be faster at 90°C than at 75°C as expected, but the rate eventually slows down and the final conversion plateaus at a lower value than at 75°C. The decrease in polymerization rate at 90°C is not due to lack of initiator as there is still 25% of initiator left after 16 hrs [74]. This result supports the hypothesis that depropagation is affecting SHMeMB polymerization, and is consistent with the copolymerization of SHMeMB:AM, for which increased incorporation of AM into the copolymer was observed at elevated temperatures.

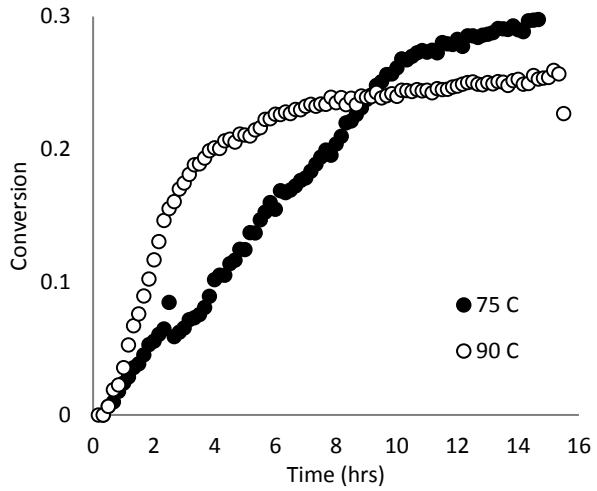

Figure 26: Monomer conversion profiles obtained from homopolymerization of SHMeMB with 15 wt% monomer and 1 wt% V-86 in aqueous solution at 75 and 90°C.

A previous study demonstrated that the polymerization rate of fully ionized acrylic acid was influenced by the addition of a salt, such that at a molar ratio of 1:5.7 [AA^-]:[NaCl] the polymerization rate of fully ionized AA was comparable to that of non-ionized AA [70]. It was proposed that the screening of charges by the added salt reduced the repulsion between the ionized monomers and ionized radical sites, therefore enhancing the polymerization rate of fully-ionized AA. Thus, NaCl was added to SHMeMB homopolymerizations to examine for a similar effect. However, as shown in Figure 27, the polymerization rate at 75°C was found to decrease with added salt, with the rate of polymerization perhaps slightly lower at the 1:1 ratio of SHMeMB]:[NaCl] compared to the 1:0.5 ratio.

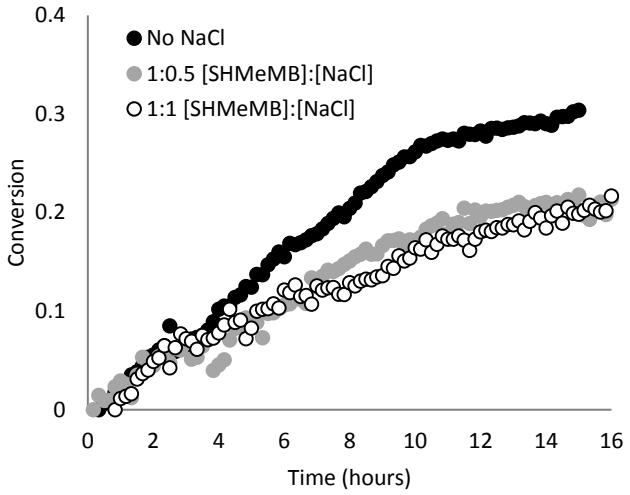

Figure 27: Monomer conversion profiles obtained from homopolymerizations of SHMeMB at 15 wt% with added NaCl salt at 75°C and 1 wt% V-86.

More recent work from Patrick Drawe's Ph.D. thesis [75] looked at the effect of ionic strength on polymerization of fully ionized methacrylic acid (NaMAA). It was found that the rate of monomer conversion increased both with increasing monomer concentration [76] and in the presence of salt [75]. However, rate of conversion is dependent on the ratio of $k_p/k_t^{0.5}$ such that it is necessary to understand the influence of salt on both rate coefficients individually. Separate PLP-SEC results showed that k_p increased with increased ion concentration. Counterions in aqueous solution exist in a dynamic equilibrium between contact-ion pair, solvent-separated ion pair, and free ions, which is determined by the distance between ions (ionic strength) and temperature. Termination was shown to be faster for contact-ion pairs than free ions. It was believed that there were more species in contact-ion pairs at higher NaMAA monomer concentration, therefore increasing k_t [76].

In an unpublished study of polymerization of the cationic monomer [2-(methacryloyloxy)ethyl]trimethylammonium chloride (TMAEMC), the rate of polymerization was unaffected by the addition of salt at 20 wt% monomer at 50°C [77]. However, PLP-SEC studies showed that the TMAEMC k_p value increases with NaCl concentration, which infers that k_t must also increase in

order for the overall polymerization rate to remain constant. Therefore, it can be concluded from these previous studies that k_p and k_t for ionized monomers are both affected (increased) by the presence of salt, but to different extents according to the monomer. Individual estimates are not available for SHMeMB, but the conversion profiles indicate that k_t is enhanced in the presence of NaCl to a greater extent than k_p, hence decreasing the overall rate of polymerization (or $k_p/k_t^{0.5}$ ratio) at 75°C. As shown in Figure 28, the addition of NaCl to the polymerization at 90°C, however, has no effect on the conversion profile. Depropagation is more important at this elevated temperature, complicating the situation; however, the net effect of the added salt on the rate of conversion is minor.

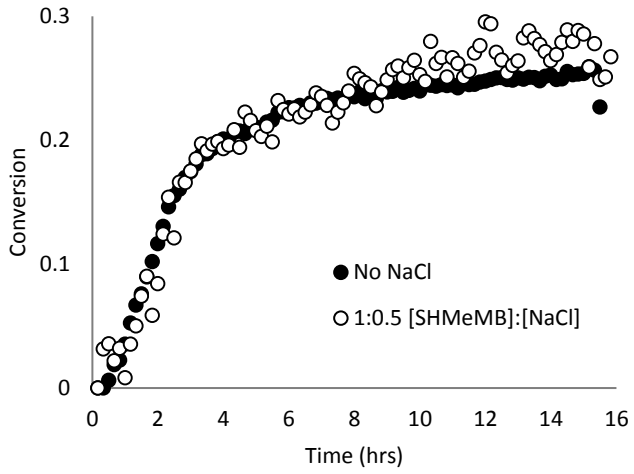

Figure 28: Monomer conversion profiles obtained from homopolymerization of SHMeMB at 15 wt% monomer, 1 wt% V-86, and 90°C with added NaCl at 1:0.5 [SHMeMB]:[NaCl] molar ratio.

5.3 Reactivity ratio estimations for SHMeMB:AM copolymerizations

Reactivity ratios for SHMeMB:AM copolymerizations at 50°C with 0.5 wt% V-50 and 15 wt% monomer was previously determined to be r_{SHMeMB} = 0.169 ± 0.005 and r_{AM} = 0.951 ± 0.007 (see Chapter 4.3). However, as shown in Chapter 5.1, monomer composition drifts vary at higher temperatures, likely due to the effect of depropagation. As a first step to understanding this behaviour, monomer composition drifts

measured with 3:7 molar ratio of SHMeMB:AM copolymerizations at 70 and 80°C were fitted to provide reactivity ratio estimates, with results shown in Figure 29.

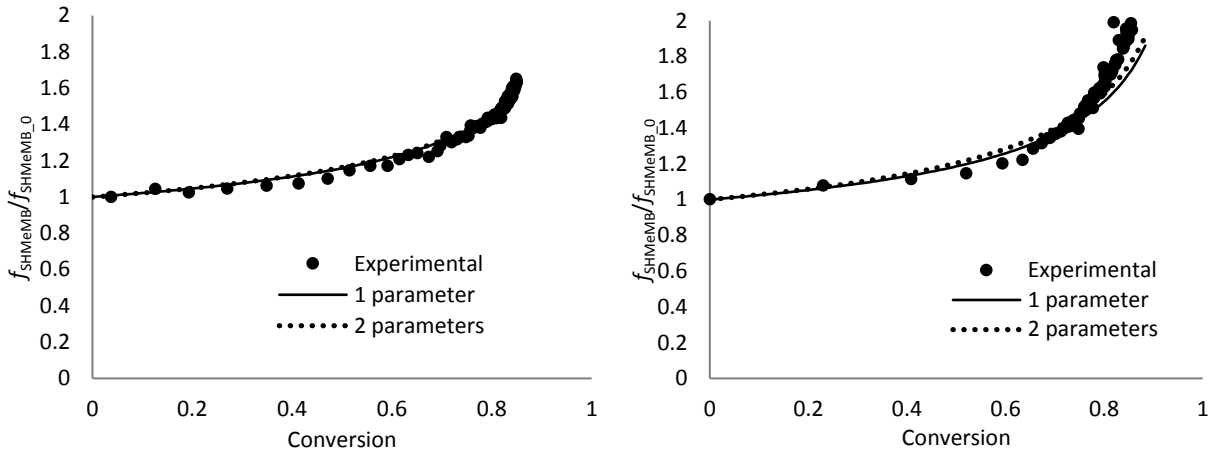

Figure 29: Monomer composition drift for copolymerizations of 3:7 molar ratio of SHMeMB:AM with 15 wt% monomer and 0.5 wt% V-50 at 70 (left) and 80°C (right). The solid line represents parameter estimation with r_{AM} fixed at 0.951 (best-fit value at 50°C), and the dotted line represents parameter estimation to determine both r_{AM} and r_{SHMeMB}.

Two methods were used to fit the experimental data: the first uses the previously determined $r_{AM} = 0.951$ so that only one parameter (r_{SHMeMB}) was estimated, as depropagation should only influence the addition rate of SHMeMB monomer to an SHMeMB radical and thus the effective value of r_{SHMeMB}. For the second fitting, both parameters, r_{AM} and r_{SHMeMB}, were estimated simultaneously. As shown by Figure 29, both methods gave good representations to the experimental data, but with drastically different estimates for r_{SHMeMB}, as summarized in Table 9. When the value of r_{AM} was fixed at 0.951, the parameter estimation forces r_{SHMeMB} to approach zero, with values of 0.0049 ± 0.0079 and $6.64\times10^{-6} \pm 7.49\times10^{-3}$ for 70 and 80°C, respectively. When estimating both r_{SHMeMB} and r_{AM} together, the estimated r_{AM} values did not change very much from the value previously estimated at 50°C, but the r_{SHMeMB} values were significantly lower at 70 and 80°C than at 50°C, with the confidence intervals also encompassing zero.

Table 9: Reactivity ratios estimates from copolymerization of 3:7 molar ratio of SHMeMB:AM with 15 wt% monomer and 0.5 wt% V-50 at 70 and 80°C. The "1 parameter" method estimates r_{SHMeMB} with r_{AM} fixed at 0.951, and the "2 parameter" method estimates both r_{AM} and r_{SHMeMB}.

	70°C		80°C	
	1 parameter	**2 parameters**	**1 parameter**	**2 parameters**
r_{SHMeMB}	0.0049 ± 0.0079	0.120 ± 0.22	6.64×10^{-6} ± 7.49×10^{-3}	0.046 ± 0.172
r_{AM}	-	1.04 ± 0.17	-	1.06 ± 0.21

The terminal model reactivity ratio of monomer 1 (r_1) is defined by Equation 17, where $k_{p,11}$ is the homopropagation rate coefficient for addition of monomer 1 to a monomer 1 radical and $k_{p,12}$ is the cross-propagation rate coefficient for addition of monomer 2 to a monomer 1 radical.

$$r_1 = \frac{k_{p,11}}{k_{p,12}} \tag{17}$$

When only fitting one parameter (r_{SHMeMB}) to the monomer composition drift, the estimation determines a value that indicates that AM monomer addition is greatly favoured over SHMeMB addition to a SHMeMB terminal radical. Estimating r_{SHMeMB} and r_{AM} simultaneously at 70°C gave an r_{AM} value that was close to the value determined at 50°C, and lowered the r_{SHMeMB} value to 0.120 (from 0.169 at 50°C). At 80°C, r_{SHMeMB} decreased to an even lower value of 0.046 due to more prominent depropagation effects at higher temperatures. While these values seem plausible, the uncertainty in the estimates are large. Nonetheless, they are consistent with the expectations of depropagation.

It is important to note that the parameter estimation fits the reactivity ratios based on the terminal model (*i.e.*, no depropagation) assuming that the value of $k_{p,SHMeMB}$ remains constant with conversion. In the case of depropagation, the $k_{p,11}$ value in Equation 17 is effectively k_p^{eff}, which is dependent on k_p, k_{dep} and monomer concentration (Equation 5) such that r_{SHMeMB} would change with conversion. Therefore, parameter estimations need to explicitly consider k_{dep} in order to accurately predict composition drifts for the copolymerization of SHMeMB and AM. Thus, the conversion profiles for SHMeMB

homopolymerizations are first used to estimate k_{dep} before returning to analysis of the copolymerization system.

5.4 Parameter estimation for SHMeMB homopolymerizations

The SHMeMB homopolymerization conversion profiles presented in Section 5.2 are used in this section to estimate both the termination (k_t) and depropagation (k_{dep}) coefficients using the data-fitting tools in PREDICI. The model consists of the mechanisms shown in Table 2 (initiation, propagation, depropagation and termination) of Chapter 3.2.5. As conversion profiles are a function of the ratios of rate coefficients (k_{dep}/k_p and $k_p/k_t^{0.5}$), the strategy employed was to use the previously-estimated propagation coefficient (k_p) of SHMeMB from the PLP-SEC study (Chapter 4.4), and to estimate k_{dep} simultaneously with k_t. For simplicity, the k_p value of 25 L/mol·s estimated at 60°C was used, as the activation energy for propagation is not known. Thus, the qualitative estimates for k_t and k_{dep} at 75 and 90°C are lower than the true values, but could be corrected once the temperature dependency of k_p is determined.

The initial fitting of the SHMeMB homopolymerizations curves, shown in Figure 30, was conducted assuming no depropagation occurs (k_{dep}=0). The model fits the experimental data reasonably well at 75°C until the point at which the rate of polymerization seemed to decrease, around 10 h into the reaction. However, it is evident that the model with no depropagation was not sufficient in fitting the experiment conversion profile at 90°C, predicting a continued increase in conversion not observed experimentally. The best fit value of k_t is 1.3×10^6 L/mol·s at both 75 and 90°C, although the true values would be higher (due to the assumption that k_p remains constant). Furthermore, k_t does not seem to be a large function of temperature, as the same value was able to fit the initial polymerization rate for both 75 and 90°C. These estimates of k_t are higher than recently reported values for ionized AA of ~10^5 L/mol·s [71].

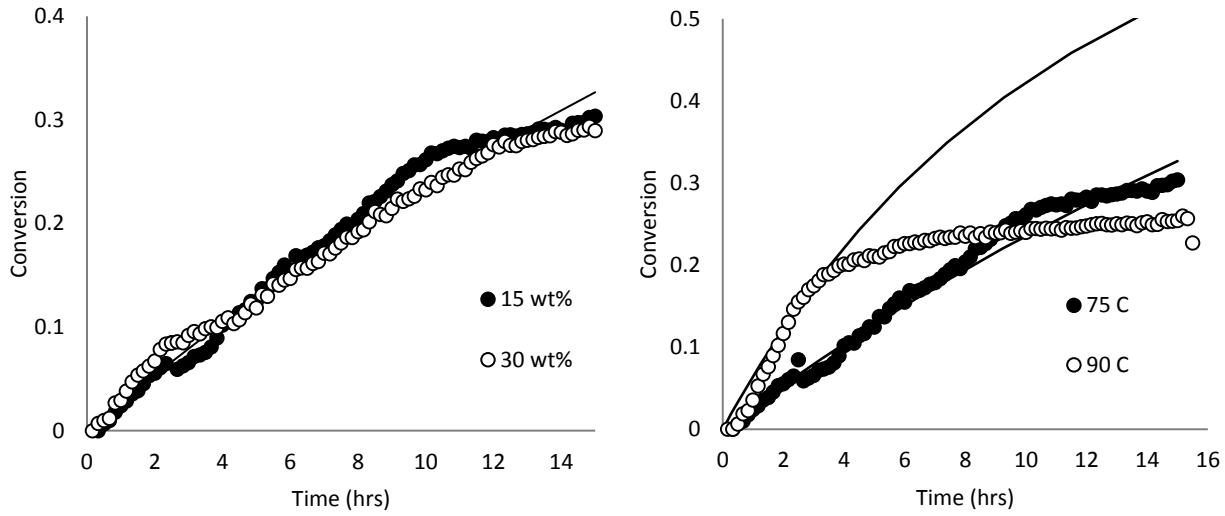

Figure 30: Fit of homopolymerization SHMeMB model assuming no depropagation to monomer conversion profiles obtained at 75°C with 1 wt% V-86 at different monomer concentrations (left) at different temperatures with 1 wt% V-86 and 15 wt% monomer (right). Solid lines represent model output, with experimental results indicated by data points.

The experimental conversion profile of SHMeMB hompolymerization at 75°C was converted using the integrated conversion equation (Equation 18) to generate a $k_p/k_t^{0.5}$ vs conversion plot. In Equation 18, X represents conversion, k_d is decomposition rate coefficient of V-86 initiator, t is reaction time, $[I]_0$ is initial initiator concentration, and f is initiator efficiency.

$$\frac{k_p}{k_t^{0.5}} = \frac{\ln(1-X)}{\exp(0.5k_d t)-1}\sqrt{\frac{k_d}{8[I]_0 f}} \tag{18}$$

In homopolymerizations, where k_p and k_t should be independent of monomer concentration and conversion, the $k_p/k_t^{0.5}$ ratio is directly proportional to rate of polymerization and should be constant. In general, the $k_p/k_t^{0.5}$ ratio calculated from the experimental data at 75°C, as shown in Figure 31, is fairly constant until it reaches a conversion of 25% then starts to decrease, which is also the point where depropagation seems to be evident. Thus, the assumption was made that depropagation was negligible between 0 and 25% conversion. The average value of $k_p/k_t^{0.5}$ in this region was about 0.022 $(L/mol \cdot s)^{0.5}$ and using a k_p value of 25 L/mol·s, k_t was estimated to be 1.30×10^6 L/mol·s. This value is the same as the estimated k_t of 1.3×10^6

L/mol·s at 75 and 90°C when assuming there is no depropagation. It is interesting to note in Figure 31 that where $k_p/k_t^{0.5}$ starts to decrease is the point at which the effect of depropagation starts to become prominent in the reaction. At 75°C between 15 and 30 wt% monomer, it appears that depropagation occurs around the same conversion. At 90°C, the $k_p/k_t^{0.5}$ ratio begins to decrease at a lower conversion which shows that depropagation is more significant at higher temperatures. The $k_p/k_t^{0.5}$ values at <10% conversion were omitted due to scatter of experimental data in the initial stages of the reaction.

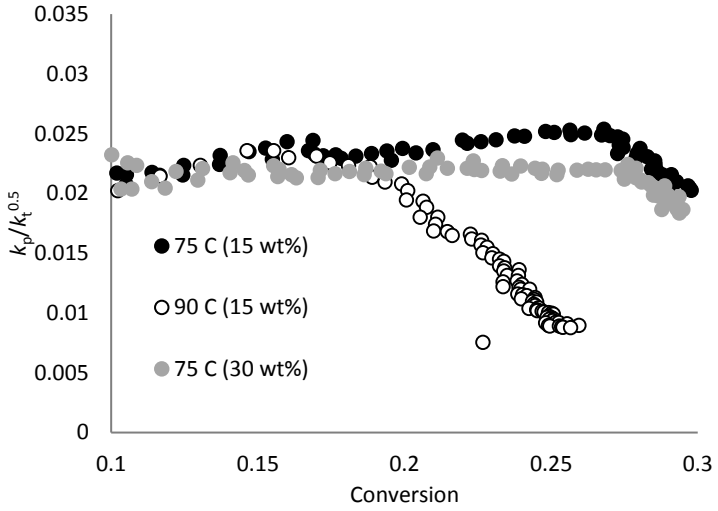

Figure 31: $k_p/k_t^{0.5}$ vs conversion profile of SHMeMB homopolymerization at 75°C with 15 and 30 wt% monomer concentration and at 90°C with 15 wt% monomer and 1 wt% V-86 for 15 hours.

The k_t value of 1.30×10^6 L/mol·s estimated using the $k_p/k_t^{0.5}$ equation assumed depropagation was negligible in the early stages of the reaction, but the true extent of depropagation is still unknown at 75 and 90°C. Using parameter estimation on PREDICI, both k_t and k_{dep} values were simultaneously estimated to be 1.38×10^5 L/mol·s and 21.0 s^{-1}, respectively, at 75°C. The estimated value is an order of magnitude than estimated using $k_p/k_t^{0.5}$ plot. These resulting conversion profiles are shown in Figure 32 and the values with 95% confidence intervals are summarized in Table 10.

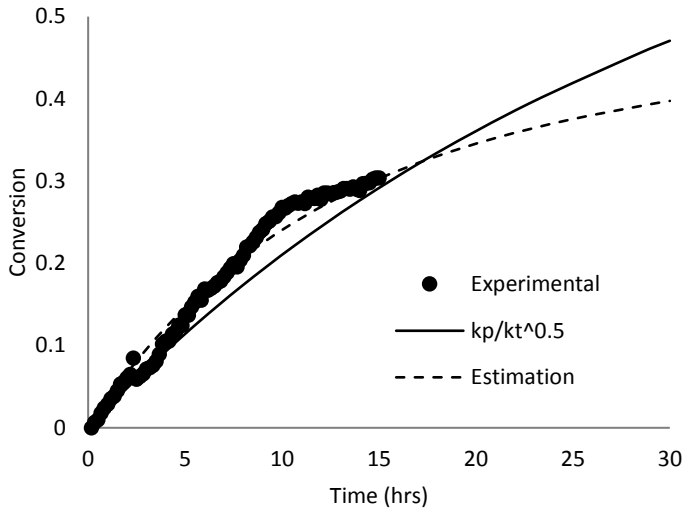

Figure 32: Conversion profile of SHMeMB homopolymerization at 75°C with 1 wt% V-86 and 15 wt% monomer. The solid line represents parameter estimation using existing experimental data, and the dashed line represents parameter estimation using an extended conversion profile capturing the depropagating behaviour.

Table 10: Estimated values for k_t and k_{dep} for homopolymerization of SHMeMB at 75°C with 1 wt% V-86 and 15 wt% monomer with 95% confidence interval values. These values are estimated assuming k_p of 25 L/mol·s.

	$k_p/k_t^{0.5}$ plot		Estimation	
		95% confidence		95% confidence
k_t (L/mol·s)	1.30×10^6	--	1.38×10^5	$\pm 1.81\text{x}10^5$
k_{dep} (s^{-1})	0	--	21.0	± 5.6

The curve generated using the k_t estimated from the $k_p/k_t^{0.5}$ plot was the least accurate representation of the experimental data as seen in Figure 32. As the conversion profile was extended to longer reaction times, a k_t value of 1.30×10^6 evidently did not capture the decrease in polymerization rate after 15 h of reaction. The estimated curve fit the experimental data very well and the k_t value was an order of magnitude lower than k_t value assuming no depropagation. The estimated conversion profile more accurately represents the

change in polymerization rate (plateauing behaviour) as a result of depropagation, which was captured with the estimated k_{dep} value of 21 L/mol·s.

Similarly, k_t and k_{dep} parameters were also estimated from the conversion profile measured at 90°C, with a comparison between the experiment and fitted conversion profiles shown in Figure 33. The values estimated for k_t and k_{dep} ($1.50 \pm 0.78 \times 10^4$ L/mol·s and 30.5 ± 0.7 s^{-1}, respectively) were able to closely fit the experimental data and capture the effect of depropagation on the conversion profile. These values are similar in magnitude compared to the estimates at 75°C, a reasonable result assuming that k_p was kept constant at 25 L/mol·s, independent of temperature. The k_{dep} value estimated at 90°C is higher than at 75°C as expected, as depropagation is enhanced at higher temperatures. However, k_t at 90°C was an order of magnitude smaller than k_t at 75°C, a surprising result as k_t is not normally a strong function of temperature. The estimated k_t at 75°C also had a large error that encompassed zero, therefore it is difficult to comment further on this difference.

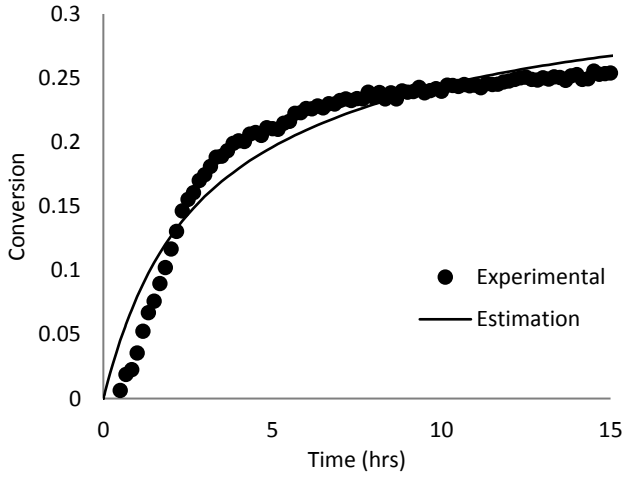

Figure 33: Monomer conversion profiles for the homopolymerization of SHMeMB at 90°C with 1 wt% V-86 and 15 wt% monomer. The solid line represents the estimated conversion profile using parameter estimation.

Termination and depropagation rate coefficients were also estimated at the higher monomer concentration conditions of 30 wt% SHMeMB at 75°C with 1 wt% V-86. From PLP-SEC studies in Chapter 4.4, k_p^{cop} of 10 mol% SHMeMB in SHMeMB:AM mixtures at 10 and 20 wt% were within experimental error. Therefore, a k_p value of 25 L/mol·s was also used for SHMeMB homopolymerization at 30 wt%. The estimated k_t and k_{dep} values were $2.44 \pm 0.57 \times 10^5$ L/mol·s and 35.8 ± 3.3 s^{-1}, respectively, and the fitted curve with experimental conversion profile is shown in Figure 34. Even though the observed conversion profiles at 15 and 30 wt% were nearly identical, the estimated values for k_t and k_{dep} differ significantly. As discussed in Chapter 5.2, k_t of fully ionized NaMAA was shown to increase with monomer concentration (from 5 to 10 wt%) [76], hence the increase in k_t is expected at the higher concentration of SHMeMB. The value of k_{dep} estimated for 30 wt% is slightly higher than that at 15 wt%. Based on studies of depropagation in organic solution, the value of k_{dep} is expected to be constant with monomer concentration, with the influence of depropagation higher at lower monomer concentrations due to a decreased k_p^{eff} in Equation 5. However, as far as we are aware, depropagation kinetics have not yet been studied in aqueous solution. It may be that the difference in the estimates indicates that the rate coefficient for depropagation, like that of propagation, is affected by monomer concentration in the system.

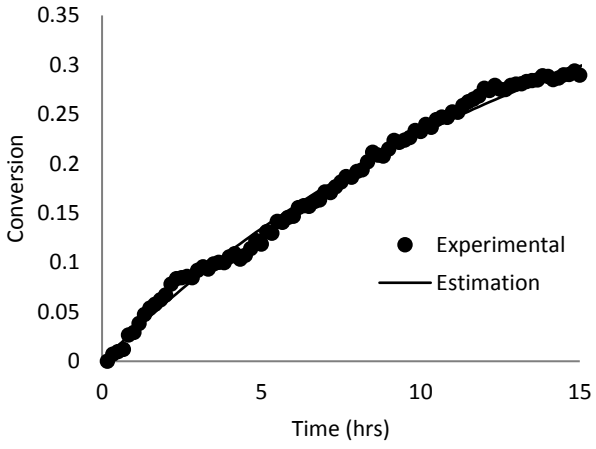

Figure 34: Monomer conversion profiles for the homopolymerization of SHMeMB at 75°C with 1 wt% V-86 and 30 wt% monomer. The solid line represents the estimated conversion profile using parameter estimation.

Parameter estimation was also done for homopolymerizations of SHMeMB with added NaCl at 75°C. As previously stated, k_p for polymerizations of fully ionized monomers with added salt should increase and k_t is also affected independently [75]. Thus, it was assumed that k_{dep} remains the same with added salt (21 s^{-1} as determined previously), with the estimated conversion profiles compared to experimental results in Figure 35. Values of k_p and k_t estimated for 1:0.5 and 1:1 molar ratios of [SHMeMB]:[NaCl] were the same and within their 95% confidence intervals, as summarized in Table 11. The estimated values for k_p did increase with added salt from the value of 25 to ~30 L/mol·s for homopolymerizations with salt, which is consistent with the increase in NaAA k_p reported with added salt [70]. The k_t values are 9.98×10^5 and 1.01×10^6 L/mol·s for 1:0.5 and 1:1 [SHMeMB]:[NaCl], respectively, significantly larger than the value of 1.38×10^5 L/mol·s estimated without salt. Although estimated with high uncertainty, it is interesting to note that these k_t values increased in a similar fashion to the estimate for the 30 wt% SHMeMB homopolymerization, suggesting that charge screening provided from either higher SHMeMB monomer concentration or added salt lowers the electrostatic barrier to radical-radical termination.

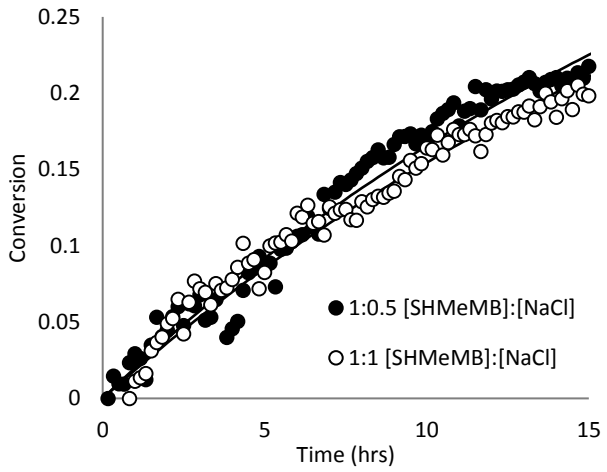

Figure 35: Monomer conversion profiles from homopolymerization of SHMeMB with different concentrations of added NaCl salt at 75°C with 1 wt% V-86 and 15 wt% monomer. The solid lines represent the conversion profiles using parameter estimation.

Table 11: Estimated values for k_p and k_t for homopolymerizations of SHMeMB with added salt at 75°C with 1 wt% V-86 and 15 wt% monomer. Results are shown for reactions done with 1:0.5 and 1:1 molar ratios of [SHMeMB]:[NaCl]. These values were estimated using a k_{dep} value of 25 s^{-1}.

	1:0.5 [SHMeMB]:[NaCl]		1:1 [SHMeMB]:[NaCl]	
		95% confidence		95% confidence
k_p (L/mol·s)	30.3	± 50.9	29.2	± 37.0
k_t (L/mol·s)	9.98×10^5	$\pm 7.96\times10^6$	1.01×10^6	$\pm 6.32\times10^6$

Polymer molecular weight averages were determined for SHMeMB homopolymers made at 75°C with 1 wt% KPS and 15 wt% monomer concentration at varying levels of NaCl. The ability to perform MW analysis was limited due to the lack of suitable instrumentation at Queen's; hence, only a few samples generated early in the study were analyzed using the facilities at PISAS in Bratislava. Note that these are relative molecular weights for the SHMeMB homopolymers, determined using a polyacrylamide calibration curve. Although these homopolymers were made with KPS rather than the V-86 initiator used to generate the conversion profiles for parameter estimation, the results indicate a decrease in MWs with increasing NaCl concentration, where homopolymers made without salt were almost two times (M_w~7×10^3 g/mol) the molecular weight of homopolymers made with salt. This trend is consistent with the lower polymerization rates observed with addition of salt at 75°C, and the estimated higher termination rate coefficient. Furthermore, due to high k_t (~10^5 L/mol·s) relative to k_p (25 L/mol·s) values and the influence of depropagation, molecular weights of SHMeMB homopolymers are fairly low, at ~10^3-10^4 g/mol.

These parameter estimations for SHMeMB homopolymerizations were done assuming k_p is constant with temperature at 25 L/mol·s (obtained from PLP-SEC at 60°C in Chapter 4.4). In order to estimate an Arrhenius equation for k_p of SHMeMB, it was assumed that the activation energy (E_A) is the same as that of a similar monomer, NaMAA (20 wt% and fully ionized) [27]. Using an E_A value of 12.4 kJ/mol, the pre-exponential factor for SHMeMB was calculated to be 2203 L/mol·s. Therefore, k_p at 75 and 90°C were determined to be 30.3 and 36.2 L/mol·s, respectively. These k_p values determined as a function of

temperature were used to estimate new k_t and k_{dep} values at 75 and 90°C as shown in Table 12. Similar trends are seen with increased k_{dep} with temperature, however, estimated k_t values still had large errors and differ by an order of magnitude with temperature.

Table 12: Estimated k_t and k_{dep} values using constant k_p=25 L/mol·s compared to values calculated using an assumed E_A value of 12.4 kJ/mol for propagation.

T (°C)	k_p (L/mol·s)	k_t (L/mol·s)	k_{dep} (s^{-1})	k_p (L/mol·s)	k_t (L/mol·s)	k_{dep} (s^{-1})
75	25	1.38 ± 1.81×10^5	21.0 ± 5.61	30.3	2.20± 2.75×10^5	25.2 ± 6.9
90	25	1.50 ± 0.78×10^4	30.5 ± 0.7	36.2	3.13 ± 1.78×10^4	44.3 ± 1.0

To summarize, despite considerable uncertainty in the parameter estimations, the analysis of the SHMeMB homopolymerization conversion profiles suggest that the system is characterized by similar k_t values as other ionized monomers like NaAA [71] and NaMAA [78] but very low k_p and significant depropagation. A slight increase in k_p and a larger increase in k_t was required to fit the conversion profiles measured with added salt and with increased monomer concentration, consistent with trends observed in NaMAA [76] and TMAEMC polymerizations [77]. Unlike NaMAA and TMAEMC, k_t of SHMeMB increased with ionic strength at a faster rate than the increase of k_p, therefore decreasing the overall rate of monomer conversion. Additionally, homopolymerization of SHMeMB is largely controlled by depropagation such that effect of added salt on rate was decreased at elevated temperatures.

5.5 Parameter estimation for SHMeMB:AM copolymerizations with depropagation

The knowledge gained regarding the kinetic behaviour of SHMeMB is here applied to the interpretation of the experimental SHMeMB:AM copolymerizations. Details of the PREDICI model, which assumes terminal chain-growth kinetics, SHMeMB depropagation, and uses a single k_t value to represent termination

in the two-monomer system, is presented in Section 3.2.5. Using the estimates of reactivity ratios at 50°C from Chapter 4.3 (estimated assuming no depropagation), k_p of SHMeMB (Chapter 4.4) and AM homopolymers [28], and k_{dep} of SHMeMB (21 s^{-1}, as estimated in Chapter 5.4), k_t of the copolymerization system were estimated at 50°C for the different molar ratios of SHMeMB and AM studied experimentally. These values can be compared to the termination rate coefficient for AM ($k_{t,AM}$), which was determined to be a function of monomer concentration and temperature as fit by Equations 19 and 20 [57]. At 50°C, $k_{t,AM}$ values at 10 and 20 wt% were calculated to be 5.20×10^8 and 4.18×10^8 L/mol·s, respectively. Taking the average of the two values gave an estimate of $k_{t,AM}$ at 15 wt% of 4.69×10^8 L/mol·s, several orders of magnitude higher than the k_t of SHMeMB ($k_{t,SHMeMB}$) estimated as $1.38\text{x}10^5$ L/mol·s at 15 wt% and 75°C in Chapter 5.4.

$$\text{At 10 wt\%, } k_{t,AM} = 3.9 \times 10^{11} \exp(-2138/T) \tag{19}$$

$$\text{At 20 wt\%, } k_{t,AM} = 5.0 \times 10^{11} \exp(-2289/T) \tag{20}$$

The fitting of k_t to the SHMeMB:AM copolymerizations at 50°C with 0.5 wt% V-50 and 15 wt% monomer provided a very good representation of the experimental conversion profiles, as seen in Appendix F. The estimated k_t values of SHMeMB:AM copolymers are plotted as a function of f_{SHMeMB} in Figure 36, with $k_{t,AM}$ and $k_{t,SHMeMB}$ included for reference.

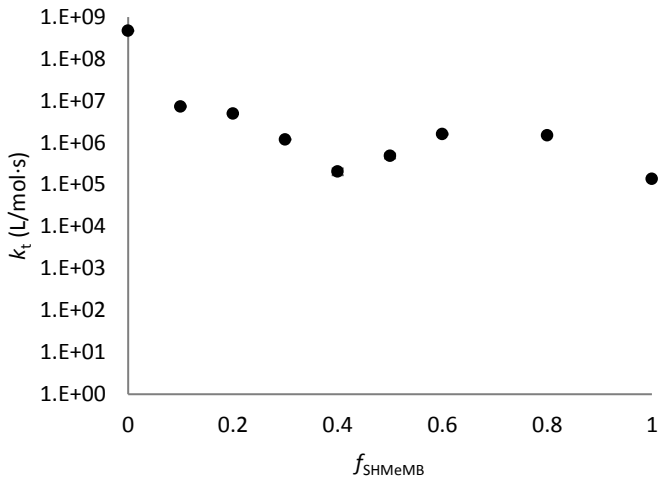

Figure 36: k_t of SHMeMB:AM copolymers estimated for copolymerizations done at 50°C with 0.5 wt% V-50 and 15 wt% monomer.

There is an immediate drop of two orders of magnitude upon addition of SHMeMB as a comonomer to AM, with values further decreasing to ~10^5 L/mol-s as f_{SHMeMB} increases to 0.4. At f_{SHMeMB}=0.5 or higher, however, the k_t values plateaued at this value of 10^5 L/mol·s as it approaches the estimated value for $k_{t,SHMeMB}$ in the previous section, and also the value of 3.6×10^5 L/mol·s reported for homotermination of NaAA at 20 wt% and 50°C in aqueous solution [71]. The structure of SHMeMB has bulky substituents that hinder its radical site, which contribute to depropagation. However, comparable k_t values for SHMeMB and NaAA indicate that the slow termination of two radicals in these systems is dominated by the electrostatic repulsion of the charged species near the radical site, rather than steric hindrance.

The k_t value estimated for the copolymerization is an averaged value that describes all termination events in the SHMeMB:AM copolymerization assuming terminal model kinetics. This averaging is described by Equation 21, where $f_{r,SHMeMB}$ is the fraction of SHMeMB terminal radicals, $f_{r,AM}$ is the fraction of AM terminal radicals, and $k_{t,SA}$ is the rate coefficient describing the cross-termination of SHMeMB and AM radicals [37].

$$k_t = k_{t,SHMeMB} f_{r,SHMeMB}^2 + 2k_{t,SA} f_{r,SHMeMB} f_{r,AM} + k_{t,AM} f_{r,AM}^2 \quad (21)$$

According to Equation 21, k_t must be dominated by value of $k_{t,SHMeMB}$ for it to approach 10^5 and decrease by two orders of magnitude from the value of $k_{t,AM}$ at f_{SHMeMB}=0.1. This large drop indicates that even at low initial SHMeMB monomer fraction (f_{SHMeMB} = 0.1 to 0.4), the fraction of SHMeMB radicals ($f_{r,SHMeMB}$) is very high. AM radicals are very reactive compared to SHMeMB radicals, given the high reactivity ratio (r_{AM}), and homopropagation and homotermination coefficients ($k_{p,AM}$ and $k_{t,AM}$) relative to SHMeMB. Once AM radicals are formed as a monomer unit or terminal radical unit, they are incorporated instantaneously into the polymer chain, while the lower reactivity of SHMeMB radicals to both termination and propagation events means that they remain in solution for longer before being polymerized. Therefore, there is always a high fraction of SHMeMB radicals in solution in comparison to fraction of AM radicals; even at f_{SHMeMB}=0.1, $f_{r,SHMeMB}$ is greater than 99% (see Appendix F Table A. 6), such that SHMeMB-SHMeMB termination is the dominant termination event.

To see whether the reactivity ratios values estimated at 50°C are also valid at higher temperatures, SHMeMB monomer composition drifts at initial monomer fraction f_{SHMeMB}=0.3 were simulated with and without depropagation at 50°C and compared with simulated monomer composition drifts with depropagation at higher temperatures as shown in Figure 37. An Arrhenius relationship was derived from previously estimated k_{dep} values (reported in Table 12 at 75 and 90°C) in order to estimate k_{dep} values of 10.4 and 18.4 s^{-1}, at 50 and 70°C, respectively. As seen in Figure 37, the effect of depropagation is to decrease the consumption rate of SHMeMB in the system, therefore leading to a slightly larger increase in the SHMeMB monomer fraction with temperature at increased temperature. However, the simulated effect of temperature on the composition drift is smaller than that observed experimentally in Chapter 5.1. At higher initial monomer composition of SHMeMB, the effects of depropagation would be more noticeable. Therefore, monomer composition drifts at f_{SHMeMB}=0.6 were also simulated (although not experimentally obtained); however, as seen in Figure 37, the effect of depropagation with increased temperature is only slightly more apparent. The very minor effect of temperature on the simulated composition drifts compared

to experiment suggests that the system reactivity ratios are temperature dependent, or that depropagation in the system is more prominent that estimated from the homopolymerization data.

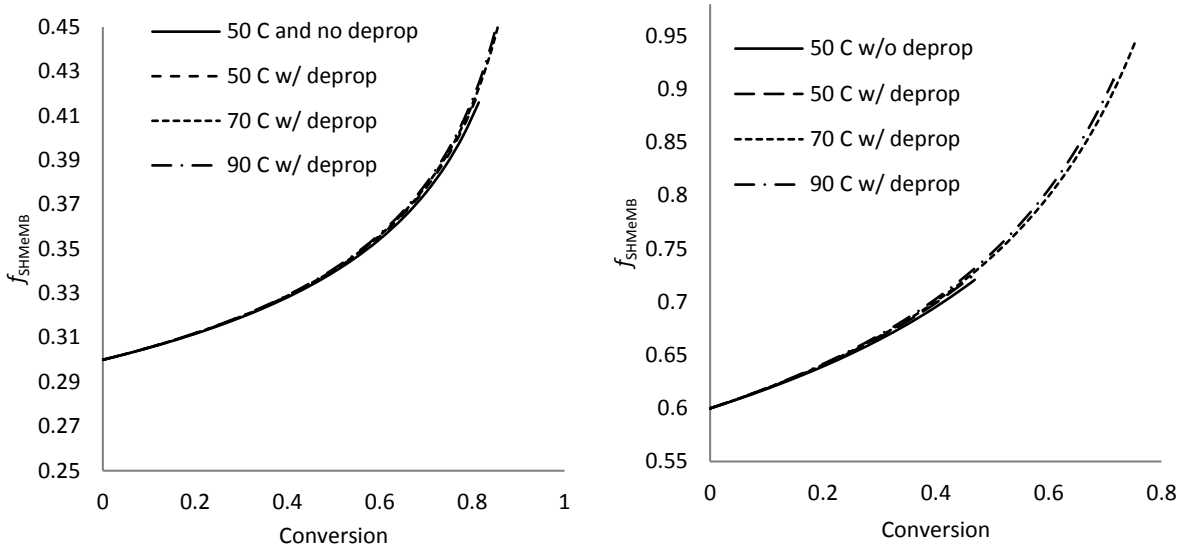

Figure 37: Simulated SHMeMB monomer composition drift of SHMeMB:AM copolymerization at initial monomer fraction f_{SHMeMB}=0.3 (left) and f_{SHMeMB}=0.6 (right) with 15 wt% monomer and 0.5 wt% V-50.

In summary, the estimates of SHMeMB:AM copolymerization k_t values indicated that termination in the system is dominated by $k_{t,SHMeMB}$ due to the high fraction of SHMeMB radical species, with the estimated k_t values at 50°C in good agreement with the estimated $k_{t,SHMeMB}$ value. The termination coefficient of SHMeMB is similar in magnitude compared to NaAA [71], which indicates that termination is slowed down due to repulsion of charges near the radical site rather than steric hindrance provided by SHMeMB monomer. However, the system reactivity ratios estimated at 50°C do not fully capture the influence of depropagation on SHMeMB composition drift in SHMeMB:AM copolymerizations observed at higher temperatures.

6 Conclusions and Recommendations

A bio-derived monomer, MeMBL, was saponified using NaOH to form SHMeMB, a fully ionized and water-soluble monomer. Ring-closure of SHMeMB is believed to be acid-catalyzed, but does not occur at pH = 7 or higher. SHMeMB was successfully copolymerized by radical polymerization in aqueous solution with AM at different molar ratios and BIS crosslinker to synthesis superabsorbent hydrogels, following a strategy used to previously synthesize SHMB:AM hydrogels [23]. As the synthesis was slightly modified by increasing monomer concentration, initiator content, and reaction time due to reactivity difference between SHMeMB:AM and SHMB:AM, the materials could not be directly compared. However, at f_{SHMeMB} = 0.4 and 0.6, the water absorbency of these hydrogels was greater than that of equivalent SHMB:AM hydrogels, likely due to their lowered conversion and hence less crosslinked network. At f_{SHMeMB} = 0.2, these hydrogels were less absorbent than f_{SHMB}=0.2 hydrogels as a result of a more tightly crosslinked network resulting from the increased initiator and monomer concentrations used during the synthesis. SEM images showed that pore sizes increased with increased SHMeMB content due to electrostatic repulsion of the charged groups, and that increased crosslinker levels led to more dense networks. Furthermore, mechanical tests confirmed that increasing AM content also increased mechanical strength of the hydrogels. Therefore, absorbency and mechanical strength of these materials are highly tunable by adjusting molar composition and crosslinking content.

To determine the reactivity of SHMeMB and AM in a copolymerization system, *in-situ* NMR studies were done to study polymer composition as a function of initial monomer composition at 50°C, 15 wt% monomer, and 0.5 wt% V-50 initiator. Reactivity ratios determined using low conversion data (r_{SHMeMB}=0.12 and r_{AM}=1.10) were in reasonable agreement with those estimated using the integrated Mayo-Lewis equation (r_{SHMeMB}=0.17 and r_{AM}=0.95). PLP-SEC studies were done to determine k_p^{cop} of SHMeMB:AM and SHMB:AM copolymers at 5, 10, and 15 mol% of SH(Me)MB at 10 wt% total monomer in aqueous solution at 60°C, with the study confirming significant differences in reactivity between the two

systems. Subsequently, k_p values for SHMeMB and SHMB homopolymerization at 60°C were estimated assuming terminal model kinetics as 25 and 165 L/mol·s, respectively, further confirming the difference in reactivity between the two monomers. These studies showed that polymerization rates of SHMeMB and SHMB are very slow, especially in comparison to AM, which has a k_p of 110 000 L/mol·s at the same temperature [28].

The difference in reactivity between SHMeMB and SHMB led to further kinetic studies to explore the effects of depropagation and added salt on polymerization rate. A plateau in conversion was observed for SHMeMB:AM copolymerizations done at 3:7 and 4:6 molar ratios and elevated temperatures, with monomer composition drift occurring at a faster rate as temperature increased as AM was incorporated faster than SHMeMB and SHMeMB monomers became more prone to depropagation. Homopolymerizations of SHMeMB at 75 and 90°C provided further evidence of depropagation, as conversion reached a lowered equilibrium value at the higher temperature. Upon the addition of salt, SHMeMB homopolymerization rate decreased at 75°C, but not at 90°C due to the dominating effect of depropagation over the screening of charges provided by counterions.

The experimental data was fitted to models developed in PREDICI in order to estimate termination (k_t) and depropagation (k_{dep}) rate coefficients, assuming a constant k_p value of 25 L/mol·s independent of temperature. The k_t values were estimated to be ~10^5 L/mol·s, similar in magnitude to those reported for NaAA [71] and NaMAA [78], and a k_{dep} of 21 s^{-1} was estimated at 75°C. The finding that $k_{t,SHMeMB}$ is similar to k_t of NaAA [71] indicates that electrostatic repulsion of charged radical species, rather than steric hindrance from bulky substituents, is the reason for slow termination. The addition of salt and increase in monomer concentration both increased k_p but had a greater effect on estimated values of k_t, showing that addition of salt had a similar effect to an increased concentration of ionized monomer on polymerization rate. The knowledge gathered from parameter estimations was then implemented to estimate k_t values for SHMeMB:AM copolymerizations, which were found to be much lower than the known value of 10^8 L/mol·s

for $k_{t,AM}$ but similar in magnitude (~10^5 L/mol·s) to the estimates of $k_{t,SHMeMB}$. This result suggests that k_t in the SHMeMB:AM copolymerization system is largely dominated by $k_{t,SHMeMB}$ because of the large fraction of charged SHMeMB radicals.

In summary, this study showed that SHMeMB:AM superabsorbent hydrogels can be synthesized and compared to SHMB:AM hydrogels, with both copolymers exhibiting superior water absorbency compared to conventional sodium acrylate hydrogels. Insights regarding polymerization kinetics of SHMeMB were gained by applying the knowledge from other water-soluble and ionized monomers, with depropagation and the effect of ionic strength and monomer concentration both considered to interpret the experimental trends observed. However, there are still unanswered questions to be investigated further. PLP-SEC experiments were limited due to lack of time at PISAS, and it would be very helpful to conduct experiments at higher temperatures for SHMeMB:AM copolymers to experimentally determine the Arrhenius relationship for k_p. A complete set of SHMeMB:AM copolymerizations at varying compositions should also be done at higher temperatures using the *in-situ* NMR technique to better understand whether reactivity ratios change with temperature. Both studies would also provide more insight regarding the influence of depropagation on the polymerization behaviour of the system. It is also worth investigating whether SHMeMB:AM copolymerization follows terminal or penultimate model chain-growth kinetics, and to independently verify the k_t .estimates perhaps using the SP-PLP-EPR technique. With increased confidence in the kinetic parameters, the copolymerization model could then be used to guide experimental conditions to produce hydrogels with controlled properties.

7 References

[1] V. Kadajji and G. Betageri, "Water Soluble Polymers for Pharmaceutical Applications," *Polymers,* vol. 3, pp. 1972-2009, 2011.

[2] D. Vedoy and J. Soares, "Water-soluble polymers for oil sands tailing treatment: A Review," *The Canadian Journal of Chemical Engineering,* vol. 93, pp. 888-904, 2015.

[3] B. Rivas, E. Pereira, M. Palencia and J. Sánchez, "Water-soluble functional polymers in conjunction with membranes to remove pollutant ions from aqueous solutions," *Progress in Polymer Science,* vol. 36, pp. 294-322, 2011.

[4] A. N. Syed, W. W. Habib and A. M. Kuhajda, "Water-Soluble Polymers in Hair Care," in *Water Soluble Polymers*, Boston, MA, Springer, 2002, pp. 231-244.

[5] Y. Hayashi, D. Lu and N. Kobayashi, "Application of Ultra-High Molecular Weight Amphoteric Acrylamide Copolymers to Detergents," in *Water Soluble Polymers*, Boston, MA, Springer, 2002, pp. 245-250.

[6] E. M. Ahmed, "Hydrogel: Preparation, characterization, and applications: A review," *Journal of Advanced Research,* vol. 6, pp. 105-121, 2015.

[7] U. B. Nurmatov, N. Tagiyeva, S. Semple , G. Devereux and A. Sheikh, "Volatile organic compounds and risk of asthma and allergy: a systematic review," *European Respiratory Review,* vol. 24, pp. 92-101, 2015.

[8] J. P. Dawson, B. J. Bloomer, D. A. Winner and C. P. Weaver, "Understanding the Meteorological Drivers of U.S. Particulate Matter Concentrations in a Changing Climate," *American Meteorological Society,* pp. 521-532, 2014.

[9] B. Nimana, C. Canter and A. Kumar, "Energy consumption and greenhouse gas emissions in the recovery and extraction of crude bitumen from Canada's oil sands," *Applied Energy,* vol. 143, pp. 189-199, 2015.

[10] P. Cashin, K. Mohaddes, M. Raissi and M. Raissi, "The differential effects of oil demand and supply shocks on the global economy," *Energy Economics,* vol. 44, pp. 113-134, 2014.

[11] R. Auras, L.-T. Lim, S. E. Selke and H. Tsuji, Poly(lactic acid): Synthesis, Structures, Properties, Processing, and Applications, Hoboken: John Wiley & Sons, 2011.

[12] K. Sudesh, H. Abe and Y. Doi, "Synthesis, structure and properties of polyhydroxyalkanoates: biological polyesters," *Progress in Polymer Science,* vol. 25, pp. 1503-1555, 2000.

[13] J. Zhao and H. Schlaad, "Synthesis of terpene-based polymers," in *Bio-synthetic Polymer Conjugates*, Springer Berlin Heidelberg, 2013, pp. 151-190.

[14] Y. Kato, H. Yoshida, K. Shoji, Y. Sato, N. Nakajima and S. Ojita, "A facile method for the preparation of α-methylene-γ-butyrolactones from tulip tissues by enzyme-mediated conversion," *Tetrahedron Letters,* vol. 50, pp. 4751-4753, 2009.

[15] R. R. Gowda and E. Y.-X. Chen, "Sustainable polymers from Biomass-Derived α-Methylene-γ-Butyrolactones," *Encyclopedia of Polymer Science and Technology,* pp. 1-37, 2013.

[16] C. Hutchinson and E. Leete, "Biosynthesis of α-methylene-γ-butyrolactone, the cyclized aglycone of tuliposide A," *Journal of the Chemical Society D: Chemical Communications*, vol. 0, pp. 1189-1190, 1970.

[17] L. E. Manzer, "Catalytic synthesis of α-methylene-γ-valerolactone: a biomass-derived acrylic monomer," *Applied Catalysis A: General*, vol. 272, pp. 249-256, 2004.

[18] M. K. Akkapeddi, "Poly(a-methylene-y-butyrolactone) Synthesis, Configurational Structure, and Properties," *Macromolecules* , vol. 12, pp. 546-551, 1979.

[19] J. Suenaga, D. M. Sutherlin and J. Stille, "Polymerization of (RS)-and (R)-a-Methylene-y-methyl-y-butyrolactone," *Macromolecules*, vol. 17, pp. 2913-2916, 1984.

[20] M. Ueda and M. Takahashi, "Radical-initiated homo- and copolymerization of α-methylene-γ-butyrolactone," *Journal of Polymer Science*, vol. 20, pp. 2819-2828, 1982.

[21] R. A. Cockburn, T. F. McKenna and R. A. Hutchinson, "An Investigation of Free Radical Copolymerization Kinetics of the Bio-renewable Monomer γ-Methyl-α-methylene-γ-butyrolactone with Methyl methacrylate and Styrene," *Macromolecules,* vol. 211, pp. 501-509, 2010.

[22] B. Mullen, M. Rodwogin, F. Stollmaier, D. Yontz and D. Leibig, "No Access New bio-derived superabsorbents from nature," *Green Materials*, vol. 1, pp. 186-190, 2013.

[23] J. Kollár, M. Mrlík, D. Moravčíková, Z. Kroneková, T. Liptaj, I. Lacík and J. Mosnáček, "Tulips: A Renewable Source of Monomer for Superabsorbent Hydrogels," *Macromolecules,* vol. 49, pp. 4047-4056, 2016.

[24] I. Lacik, S. Beuermann and M. Buback, "PLP-SEC Study into Free-Radical Propagation Rate of Nonionized Acrylic Acid in Aqueous Solution," *Macromolecules,* vol. 36, pp. 9355-9363, 2003.

[25] I. Lacik, S. Beuermann and M. Buback, "PLP-SEC Study into the Free-Radical Propagation Rate Coefficients of Partially and Fully Ionized Acrylic Acid in Aqueous Solution," *Macromolecular Chemistry and Physics,* vol. 205, pp. 1080-1087, 2004.

[26] S. Beuermann, M. Buback, P. Hesse and I. Lacik, "Free-Radical Propagation Rate Coefficient of Nonionized Methacrylic Acid in Aqueous Solution from Low Monomer Concentrations to Bulk Polymerization," *Macromolecules,* vol. 39, pp. 184-193, 2006.

[27] I. Lacik, L. Ucnova, S. Kukuckova, M. Buback, P. Hesse and S. Beuermann, "Propagation Rate Coefficient of Free-Radical Polymerization of Partially and Fully Ionized Methacrylic Acid in Aqueous Solution," *Macromolecules,* vol. 42, pp. 7753-7761, 2009.

[28] I. Lacik, A. Chovancova, L. Uhelska, C. Preusser, R. A. Hutchinson and M. Buback, "PLP-SEC Studies into the Propagation Rate Coefficient of Acrylamide Radical Polymerization in Aqueous Solution," *Macromolecules,* vol. 49, pp. 3244-3253, 2016.

[29] M. Buback, R. G. Gilbert, G. T. Russell, D. J. T. Hill, G. Moad, K. F. O'Driscoll, J. Shen and M. A. Winnik, "Consistent values of rate parameters in free radical polymerization systems. II. Outstanding dilemmas and recommendations," *Journal of Polymer Science Part A: Polymer Chemistry,* vol. 30, pp. 851-863, 1992.

[30] F.-D. Kuchta, A. M. van Herk and A. L. German, "Propagation Kinetics of Acrylic and Methacrylic Acid in Water and Organic Solvents Studied by Pulsed-Laser Polymerization," *Macromolecules,* vol. 33, pp. 3641-3649, 2000.

[31] C. Preusser, A. Chovancova, I. Lacik and R. A. Hutchinson, "Modeling the Radical Batch Homopolymerization of Acrylamide and Aqueous Solution," *Macromolecular Reaction Engineering,* vol. 10, pp. 490-501, 2016.

[32] C. Preusser and R. A. Hutchinson, "An In-Situ NMR Study of Radical Copolymerization Kinetics of Acrylamide and Non-Ionized Acrylic Acid in Aqueous Solution," *Macromolecular Symposia*, vol. 333, pp. 122-137, 2013.

[33] J. E. Schier and R. A. Hutchinson, "The influence of hydrogen bonding on radical chain-growth parameters for butyl methacrylate/2-hydroxyethyl acrylate solution copolymerization," *Polymer Chemistry*, vol. 7, pp. 4567-4574, 2016.

[34] D. Li, N. Li and R. A. Hutchinson, "High-Temperature Free Radical Copolymerization of Styrene and Butyl Methacrylate with Depropagation and Penultimate Kinetics Effects," *Macromolecules*, vol. 39, pp. 4366-4373, 2006.

[35] Z. Szablan, M. H. Stenzel, T. P. Davis, L. Barner and C. Barner-Kowollik, "Depropagation Kinetics of Sterically Demanding Monomers: A Pulsed Laser Size Exclusion Chromatography Study," *Macromolecules*, vol. 38, pp. 5944-5954, 2005.

[36] J. Penelle, J. Collot and G. Rufflard, "Kinetic and thermodynamic analysis of methyl ethacrylate radical polymerization," *Journal of Polymer Science*, vol. 31, pp. 2407-2412, 1993.

[37] J. Brandrup, E. Immergut and E. Grulke, Polymer Handbook, 4th Edition, New York: John Wiley & Sons, 1999.

[38] L. Morris, T. Davis and R. Chaplin, "Radical copolymerization propagation kinetics of methyl ethacrylate and styrene," *Polymer*, vol. 42, pp. 941-952, 2001.

[39] M. Ueda, M. Takahashi, Y. Imai and C. U. Pittman, "Synthesis and homopolymerization kinetics of α-methylene-δ-valerolactone, an exo-methylene cyclic monomer with a nonplanar ring system spanning the radical center," *Macromolecules*, vol. 16, pp. 1300-1305, 1983.

[40] M. Buback, R. G. Gilbert, R. A. Hutchinson , B. Klumperman, F.-D. Kuchta, B. G. Manders, K. F. O'Driscoll, G. T. Russel and J. Schweer, "Critically evaluate rate coefficients for free-radical polymerization, 1. Propagation rate coefficient for styrene," *Macromolecular Chemistry and Physics,* vol. 196, pp. 3267-3280, 1995.

[41] S. Beuermann, M. Buback, T. P. Davis, R. G. Gilbert, R. A. Hutchinson, O. F. Olaj, G. T. Russell, J. Schweer and A. M. van Herk, "Critically evaluated rate coefficients for free-radical polymerization, 2. Propagation rate coefficients for methyl methacrylate," *Macromolecular Chemistry and Physics,* vol. 198, pp. 1545-1560, 1997.

[42] S. Beuermann, M. Buback, T. P. Davis, R. G. Gilbert, R. A. Hutchinson, A. Kajiwara, B. Klumperman and G. T. Russell, "Critically evaluated rate coefficients for free-radical polymerization, 3. Propagation rate coefficients for alkyl methacrylates," *Macromolecular Chemistry and Physics,* vol. 201, pp. 1355-1364, 2000.

[43] S. Beuermann and M. Buback, "Rate coefficients of free-radical polymerization deduced from pulsed laser experiments," *Progress in Polymer Science,* vol. 27, pp. 191-254, 2002.

[44] O. F. Olaj and I. S. Bitai, "Solvent Effects on the Rate Constant of Chain Propagation in Free Radical Polymerization," *Chemical Monthly,* vol. 130, pp. 731-740, 1999.

[45] V. Kabanov, D. Topchiev and T. Karaputadze, "Some Features of Radical Polymerization of Acrylic Acid and Methacrylic Acid Salts in Aqueous Solutions," *Journal of Polymer Science,* vol. 42, pp. 173-183, 1973.

[46] N. F. Wittenberg, C. Preusser, H. Kattner, M. Stach, I. Lacik, R. A. Hutchinson and M. Buback, "Modeling Acrylic Acid Radical Polymerization in Aqueous Solution," *Macromolecular Reaction Engineering,* vol. 10, pp. 95-107, 2016.

[47] S. Beuermann, M. Buback, P. Hesse, S. Kukuckova and I. Lacik, "Propagation Kinetics of Free-Radical Methacrylic Acid: The Effect of Concentration and Degree of Ionization," *Macromolecular Symposia,* vol. 248, pp. 23-32, 2007.

[48] I. Rintoul and C. Wandrey, "Polymerization of ionic monomers in polar solvents: kinetics and mechanism of the free radical copolymerization of acrylamide/acrylic acid," *Polymer,* vol. 46, pp. 4525-4532, 2005.

[49] W. Cabaness, T. Yen-Chin Lin and C. Párkányi, "Effect of pH on the reactivity ratios in the copolymerization of acrylic acid and acrylamide," *Polymer Chemistry,* vol. 9, pp. 2155-2170, 1971.

[50] A. Paril, A. Alb, A. Giz and H. Çatalgil-Giz, "Effect of medium pH on the reactivity ratios in acrylamide acrylic acid copolymerization," *Journal of Applied Polymer Science,* vol. 103, pp. 968-974, 2007.

[51] A.-R. Mahdavian, M. Abdollahi and H. R. Bijanzadeh, "Kinetic Study of Radical Polymerization. III. Solution Polymerization of Acrylamide by 1H-NMR," *Journal of Applied Polymer Science,* vol. 93, pp. 2007-2013, 2004.

[52] F. R. Mayo and F. M. Lewis, "Copolymerization. I. A Basis for Comparing the Behavior of Monomers in Copolymerization; The Copolymerization of Styrene and Methyl Methacrylate," *Journal of the American Chemical Society,* vol. 66, pp. 1594-1601, 1944.

[53] V. E. Meyer and G. G. Lowry, "Integral and Differential Binary Copolymerization Equations," *Journal of Polymer Science,* vol. 3, pp. 2843-2851, 1965.

[54] C. Preusser, I. H. Ezenwajiaku and R. A. Hutchinson, "The Combined Influence of Monomer Concentration and Ionization on Acrylamide/Acrylic Acid Composition in Aqueous Solution Radical Batch Copolymerization," *Macromolecules,* vol. 49, pp. 4746-4756, 2016.

[55] J. Barth, W. Meiser and M. Buback, "SP-PLP-EPR Study into Termination and Transfer Kinetics of Non-Ionized Acrylic Acid Polymerized in Aqueous Solution," *Macromolecules,* vol. 45, pp. 1339-1345, 2012.

[56] J. Schrooten, "Investigations into the Propagation and Termination Kinetics of the Radical Polymerization of Polar Monomers in Aqueous Solution," Ph.D. Thesis, University of Gottingen, 2013.

[57] H. Kattner and M. Buback, "Termination and Transfer Kinetics of Acrylamide Homopolymerization in Aqueous Solution," *Macromolecules,* vol. 48, pp. 7410-7419, 2015.

[58] C. Preusser, "Kinetics and modeling of free radical aqueous phase polymerization of acrylamide with acrylic acid at varying degrees of ionization," Ph.D. Thesis, Queen's University, 2015.

[59] K. Ivin, "Thermodynamics of addition polymerization," *Angewandte Chemie,* vol. 12, pp. 487-494, 1973.

[60] G. G. Lowry, "The effect of depropagation on copolymer composition. I. General theory for one depropagating monomer," *Polymer Chemistry,* vol. 42, pp. 463-477, 1960.

[61] P. Wittmer, "Copolymerization in the presence of depolymerization reactions," *Advances in Chemistry Series,* vol. 99, pp. 140-174, 1971.

[62] N. Wittenburg, "Kinetics and Modeling of the Radical Polymerization of Acrylic Acid and of Methacrylic Acid in Aqueous Solution," Ph.D. Thesis, University of Gottingen, 2013.

[63] Wako Pure Chemical Industries Ltd, "V-50," 2013. [Online]. Available: http://www.wako-chem.co.jp/kaseihin_en/waterazo/V-50.htm. [Accessed 2017].

[64] D. L. Safranski and K. Gall, "Effect of chemical structure and crosslinking density on the thermo-mechanical properties and toughness of (meth)acrylate shape memory polymer networks," *Polymer,* vol. 49, pp. 4446-4455, 2008.

[65] J. Trompette, E. Fabregue and G. Cassanas, "Influence of the Monomer Properties on the Rheological Behavior of Chemically Crosslinked Hydrogels," *Journal of Polymer Science: Part B: Polymer Physics,* vol. 35, pp. 2535-2541, 1997.

[66] W.-F. Lee and P.-L. Yeh, "Superabsorbent Polymeric Materials. III. Effect of Initial Total Monomer Concentration on the Swelling Behaviour of Crosslinked Poly(sodium acrylate) in Aqueous Salt Solution," *Journal of Applied Polymer Science,* vol. 64, pp. 2371-2380, 1997.

[67] Q. Tang, J. Wu, J. Lin, Q. Li and S. Fan, "Two-step synthesis of polycrylamide/polyacrylate interpenetrating network hydrogels and its swelling/deswelling properties," *Journal of Material Science,* vol. 43, pp. 5884-5890, 2008.

[68] C. Kandow, P. Georges, P. Janmey and K. Beningo, "Polyacrylamide hydrogels for cell mechanics: steps toward optimization and alternative uses," *Methods Cell Biology,* vol. 83, pp. 29-46, 2007.

[69] S. He, F. Zhang and W. Wang, "Synthesis of Sodium Acrylate and Acrylamide Copolymer/GO Hydrogels and Their Effective Adsorption for Pb2+ and Cd2+," *Sustainable Chemistry and Engineering,* vol. 4, pp. 3948-3959, 2016.

[70] P. Drawe, M. Buback and I. Lacik, "Radical Polymerization of Alkali Acrylates in Aqueous Solution," *Macromolecular Journals,* vol. 216, pp. 1333-1340, 2015.

[71] J. Barth and M. Buback, "Termination and Transfer Kinetics of Sodium Acrylate Polymerization," *Macromolecules,* vol. 45, pp. 4152-4157, 2012.

[72] W. Wang and R. A. Hutchinson, "Study of Butyl Methacrylate Depropagation Behavior Using Batch Experiments in Combination with Modeling," *Industrial and Engineering Chemistry Research,* vol. 48, pp. 4810-4816, 2009.

[73] D. E. Henton, C. Powell and R. E. Reim, "The Decomposition of Sodium Persulfate in the Presence of Acrylic Acid," *Journal of Applied Polymer Science,* vol. 64, pp. 591-600, 1997.

[74] Wako Pure Chemical Industries Ltd, "VA-086," 2013, 2017. [Online]. Available: http://www.wako-chem.co.jp/kaseihin_en/waterazo/VA-086.htm.

[75] P. Drawe, "Kinetic of the Radical Polymerization of Ionic Monomers in Aqueous Solution: Spectroscopic Analysis and Modelling," Ph.D. Thesis, University of Gottingen, 2016.

[76] H. Kattner, P. Drawe and M. Buback, "Chain-Length-Dependent Termination of Sodium Methacrylate Polymerization in Aqueous Solution Studied by SP-PLP-EPR," *Macromolecules,* vol. 50, pp. 1386-1393, 2017.

[77] I. Ezenwajiaku, "Kinetics and modeling of radical polymerization of water-soluble cationic monomers," Ph.D. Thesis, Queen's University, 2017.

[78] J. Barth and M. Buback, "SP-PLP-EPR Study into the Termination Kinetics of Methacrylic Acid Radical Polymerization in Aqueous Solution," *Macromolecules,* vol. 44, pp. 1292-1297, 2011.

8 Appendices

A. Characterization of MeMBL and SHMeMB

Structure of MeMBL ring was confirmed using NMR as shown in Figure A. 1.

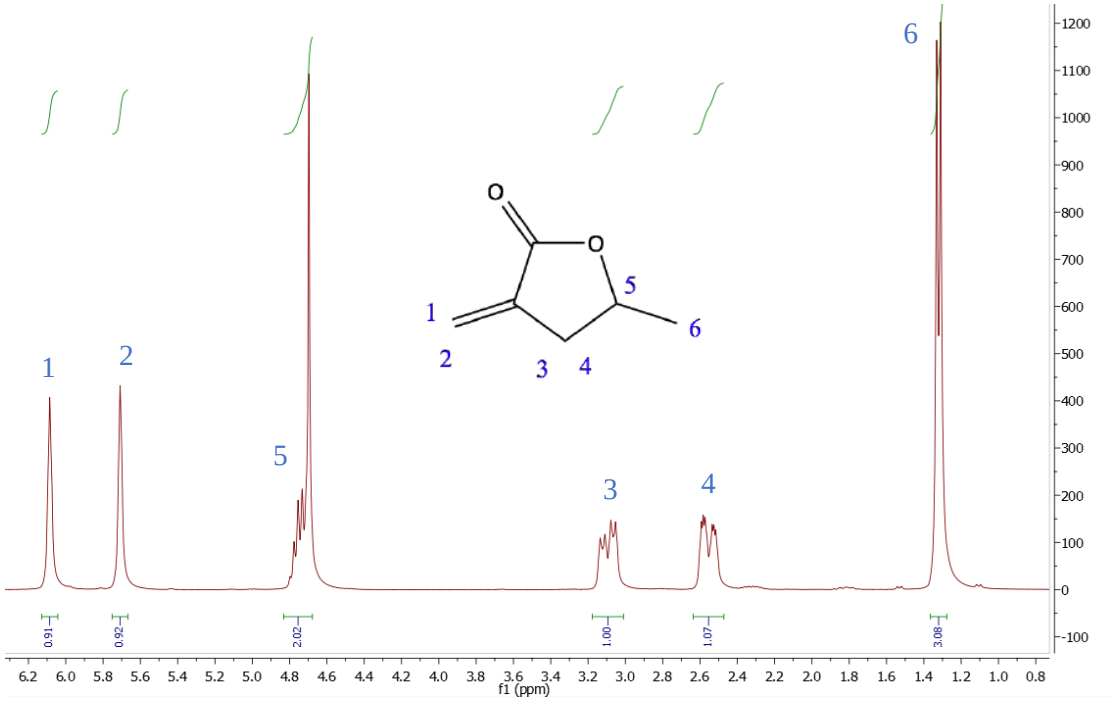

Figure A. 1: NMR spectra (500 MHz) of MeMBL in DMSO solvent (4.7 ppm) at room temperature.

Table A. 1: Proton assignment of MeMBL NMR spectra in Figure A. 1.

Proton Label	Shift (ppm)	Multiplicity	Justification
1	6.1	Doublet	Geminal proton split by H_2 on double bond
2	5.7	Doublet	Geminal proton split by H_1 on double bond
3	3.1	Doublet of doublet of doublet	Geminal proton – large splitting by H_4, and small splitting by H_5
4	2.55	Doublet of doublet of doublet	Geminal proton – large splitting by H_3, and small splitting by H_5
5	4.75	Multiplet*	Split by H_6 methyl group and H_3 and H_4
6	1.3	Doublet	Methyl group split by H_5

After saponification of MeMBL, structure of the opened ring, SHMeMB, was confirmed by NMR in Figure A. 2.

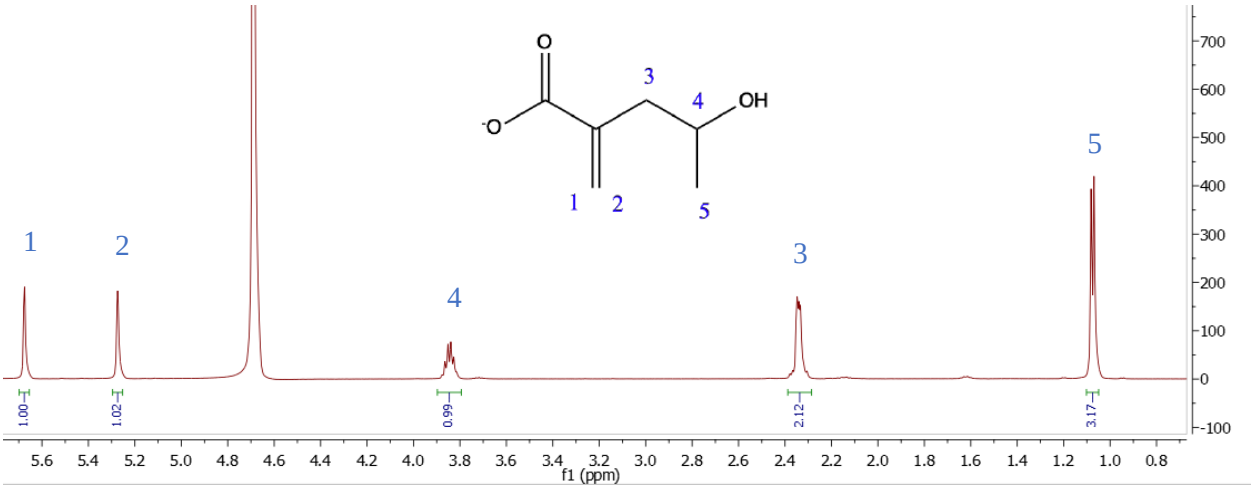

Figure A. 2: NMR spectra (500 MHz) of SHMeMB in D_2O (4.7 ppm) at room temperature and pH=7.

Table A. 2: Proton assignment of SHMeMB NMR spectra in Figure A. 2.

Proton Label	Shift (ppm)	Multiplicity	Justification
1	6.1	Doublet	Geminal proton split by H_2 on double bond
2	5.7	Doublet	Geminal proton split by H_1 on double bond
3	2.3	Multiplet	Two equivalent protons split by H_4, H_1 and H_2
4	3.85	Sextet	Split by H_5 methyl group and both H_3 protons
5	1.07	Doublet	Methyl group split by H_4

NMR spectra of equimolar SHMeMB and AM shows positions of respective monomer peaks before polymerization in Figure A. 3. At 50°C, peaks are slightly shifted to the left when compared to spectra at 25°C.

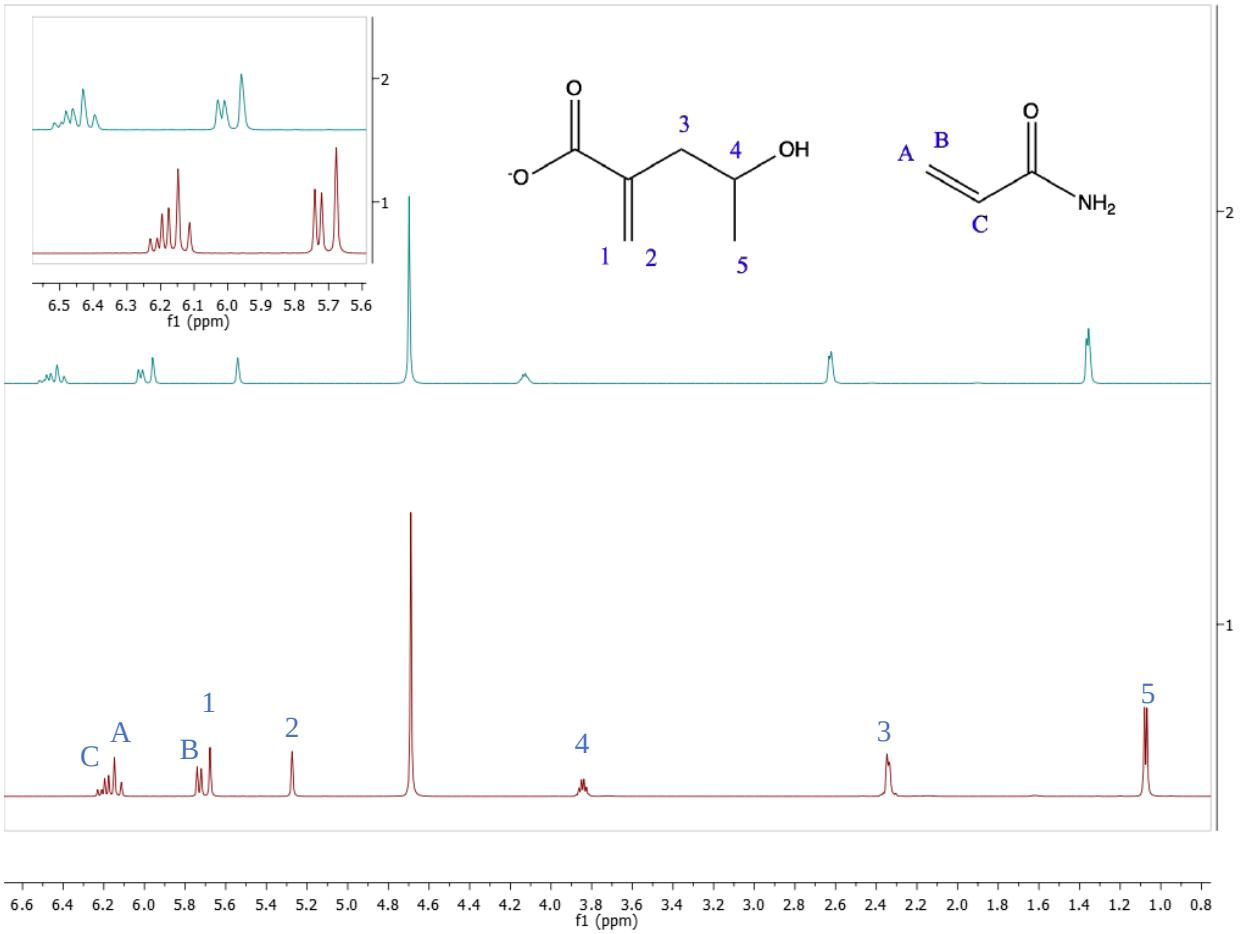

Figure A. 3: NMR spectra (500 MHz) of equimolar SHMeMB and AM at 25°C (bottom) and 50°C (top) in D_2O (4.7 ppm) and pH=7.

Table A. 3: Proton assignment of AM protons at 50°C in Figure A. 3.

Proton Label	Shift (ppm)	Multiplicity	Justification
A	6.4	Doublet	Geminal splitting by H_B on doublet bond and trans- to H_C
B	6.2	Doublet	Geminal splitting by H_A on doublet bond and cis- to H_C
C	6.48	Doublet of doublet	Split by H_A and H_B

B. Ring-closure of SHMeMB under acidic conditions

Homopolymerizations of SHMeMB at pH=5 for both 50 and 75°C are shown in Figure A. 4, where the red spectra represents the water phase in D_2O and the green spectra represents the organic phase in DMSO. In the red spectra in Figure A. 4 (bottom), the methylene proton peaks at 5.75 and 6.15 ppm and multiplets at 2.6, 3.1, and 4.8 ppm belong to MeMBL. For NMR spectra of SHMeMB, the green spectra for the organic phase clearly showed broad proton peaks, which represent polymer protons. MeMBL peaks were observed at 75°C in the water phase, but not at 50°C even though there was polymer precipitate at both temperatures. This could indicate that there was ring-closure of SHMeMB but the amount of MeMBL formed at 50°C was very little and they all polymerized into poly(MeMBL). In addition, any remaining MeMBL monomer would have been in the organic phase, which was subsequently removed by the freeze-drying process. At 75°C, there was more MeMBL formed and some of the residual MeMBL monomer was dissolved in the water phase.

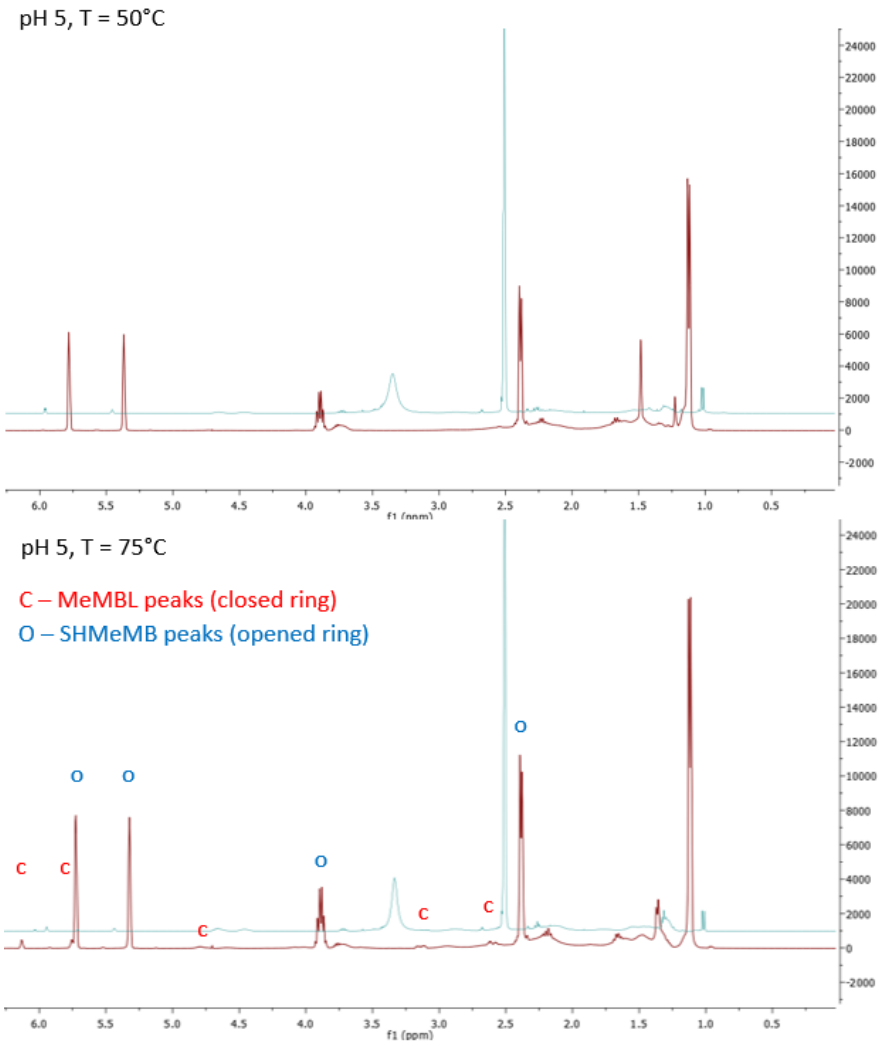

Figure A. 4: NMR analysis of SHMeMB homopolymerizations at pH=5 after 16 hours and 15 wt% monomer at 50°C with 1 wt% V-50 (top) and 75°C with 1 wt% KPS (bottom). The red spectra is of the water-soluble phase in D_2O and the green spectra is of the organic phase in DMSO.

At a lower pH=4, NMR spectra for both 50 and 75°C are shown in Figure A. 5. Similarly, there was no evidence of MeMBL peaks in the water phase at 50°C, but there were MeMBL peaks in the water phase at 75°C.

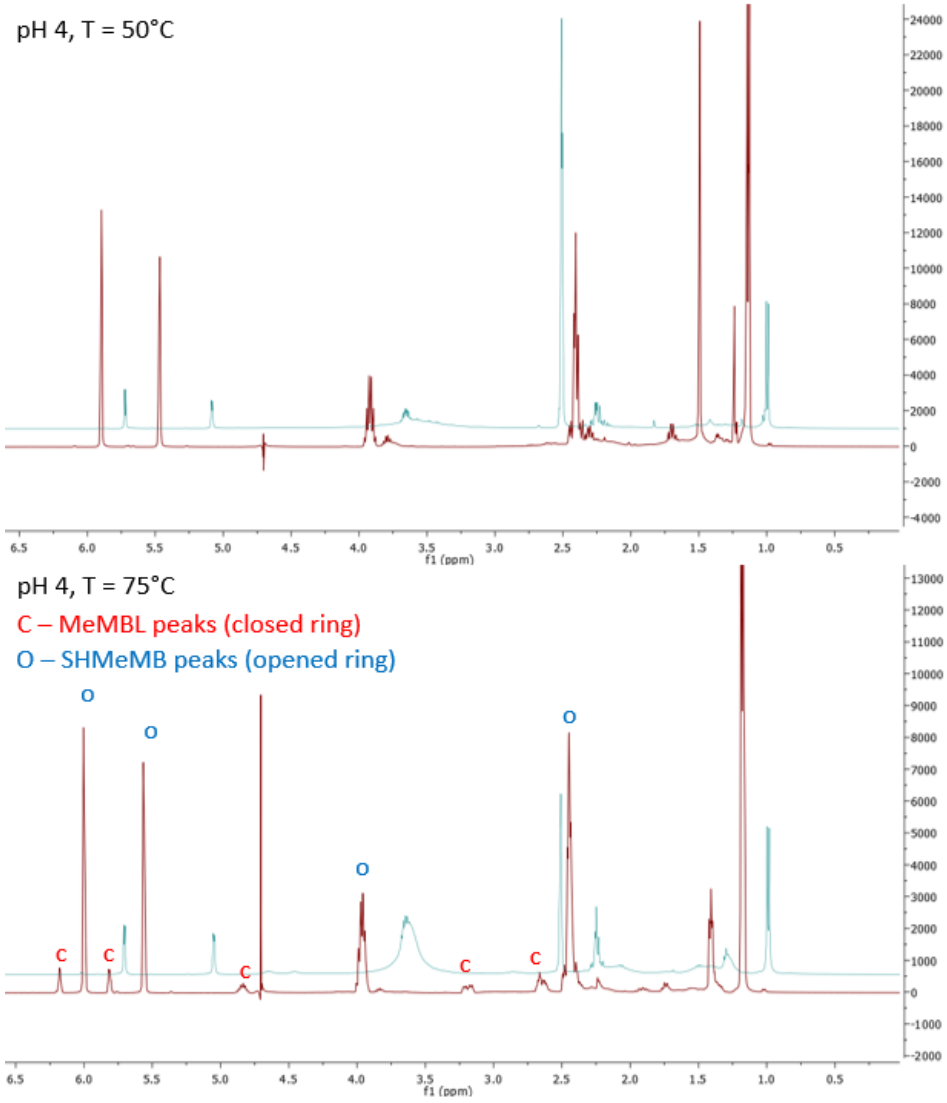

Figure A. 5: NMR analysis of SHMeMB homopolymerizations at pH=4 after 16 hours and 15 wt% monomer at 50°C with 1 wt% V-50 (top) and 75°C with 1 wt% KPS (bottom). The red spectra is of the water-soluble phase in D_2O and the green spectra is of the organic phase in DMSO.

C. PLP-SEC experiments

Preliminary PLP-SEC results of SHMeMB:AM with f_{SHMeMB}=0.1 are shown in Figure A. 6.

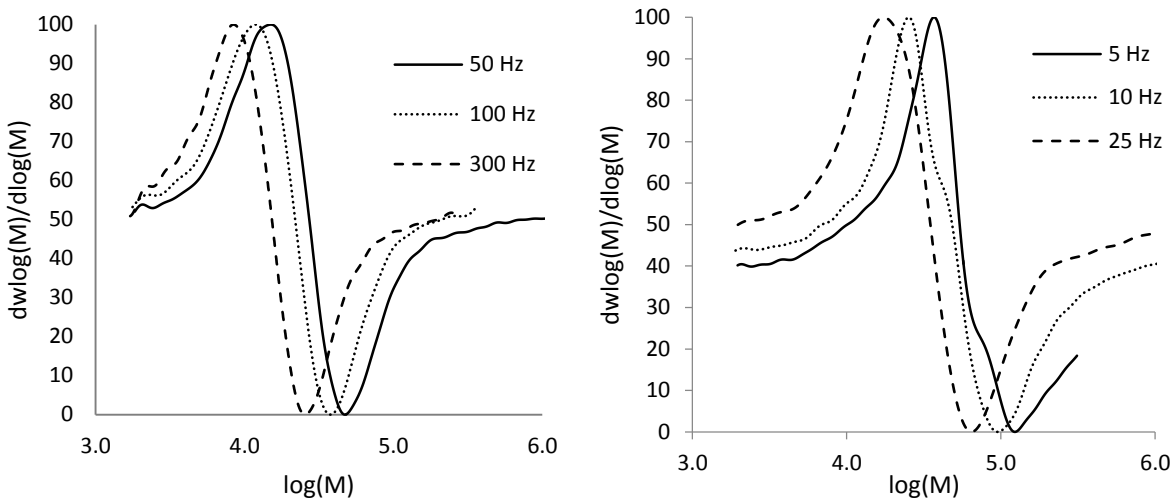

Figure A. 6: PLP-SEC results of SHMeMB:AM copolymers with f_{SHMeMB}=0.1, number of pulses=1000, 10 wt% monomer, 3.4 mmol/L LiTPO, and 60°C.

Initiator content was increased and PLP-SEC results are shown in Figure A. 7.

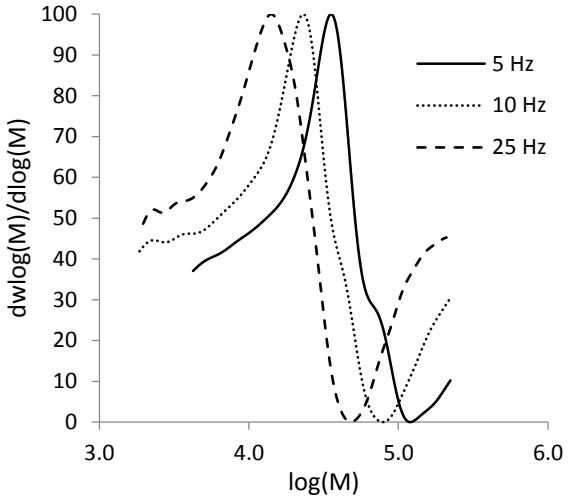

Figure A. 7: PLP-SEC results of SHMeMB:AM copolymers with f_{SHMeMB}=0.1, number of pulses=1000, 10 wt% monomer, 6.8 mmol/L LiTPO, and 60°C.

Table A. 4: Copolymer composition of SHMeMB:AM copolymers (F_{SHMeMB}) at low conversion (<10%) at from batch studies with varying feed comonomer compositions (f_{SHMeMB}).

f_{SHMeMB}	F_{SHMeMB}
0	0
0.11	0.088
0.197	0.164
0.267	0.216
0.383	0.285
0.487	0.318
0.534	0.372
0.8	0.539
1	1

D. Monomer concentration of SHMeMB and AM at different temperatures

SHMeMB and AM monomer consumption at different molar ratios and temperatures are shown in Figure A. 8.

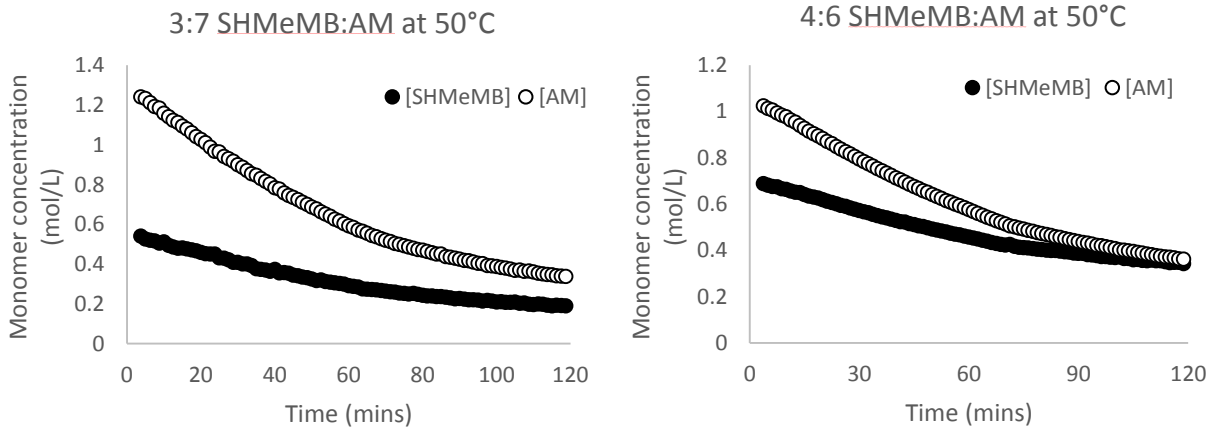

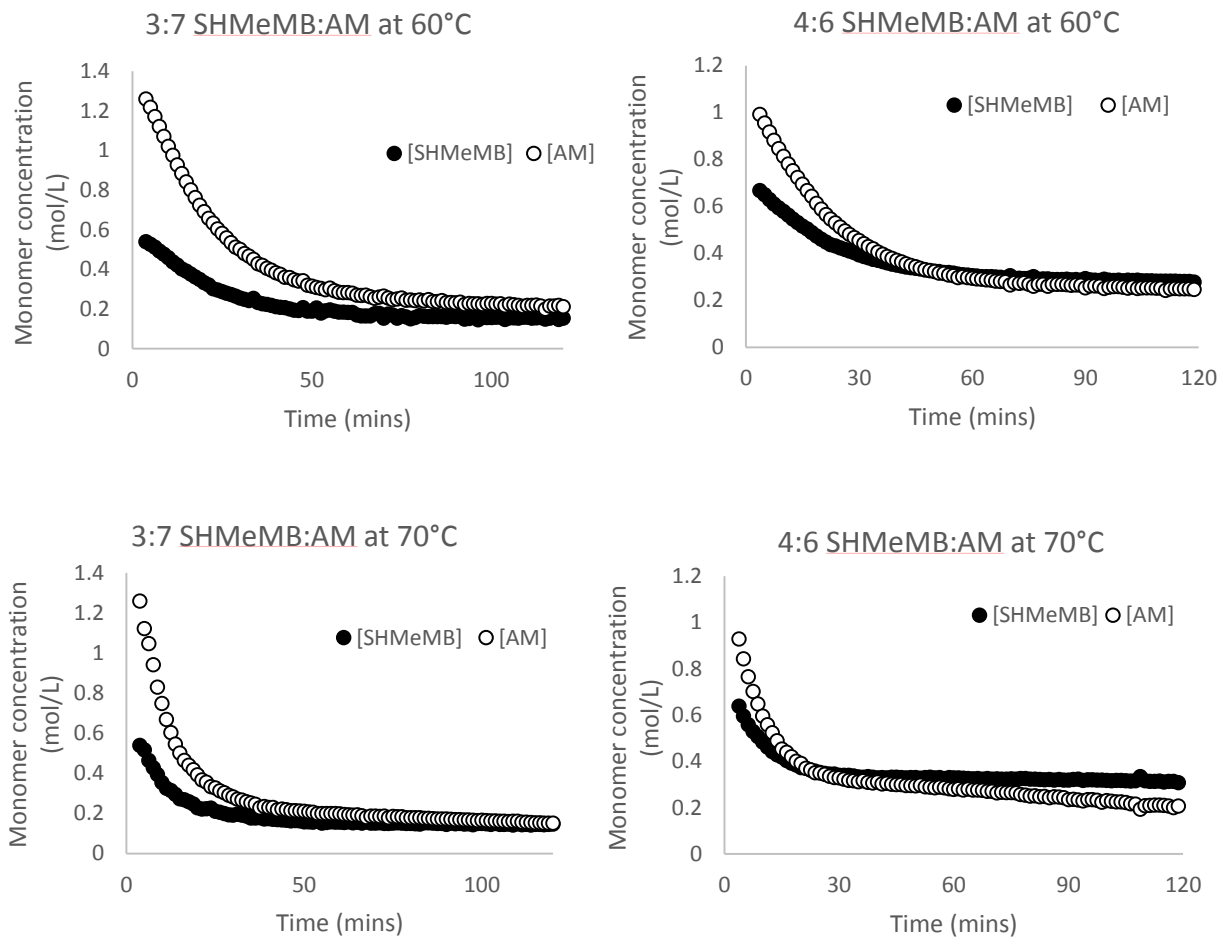

Figure A. 8: SHMeMB and AM concentration as a function of reaction time at 3:7 and 4:6 SHMeMB:AM molar ratios at 15 wt% monomer and 0.5 wt% V-50 at varying temperatures.

E. 3:7 SHMeMB:AM copolymerizations at with V-50 and V-86

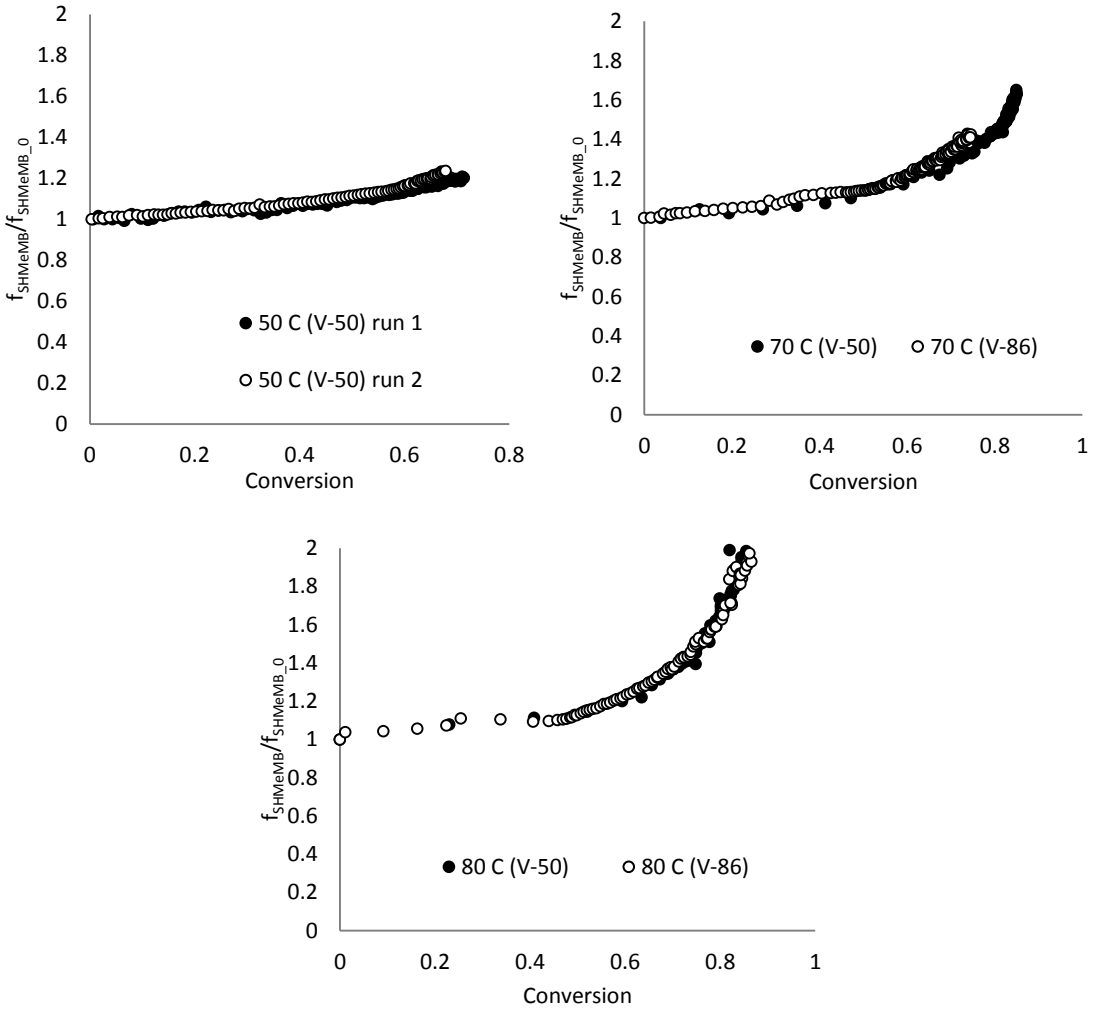

Figure A. 9: SHMeMB:AM copolymerizations at 15 wt% monomer at varying temperatures to compare composition drift between V-50 and V-86 initiators.

F. SHMeMB:AM conversion profiles with parameter estimation

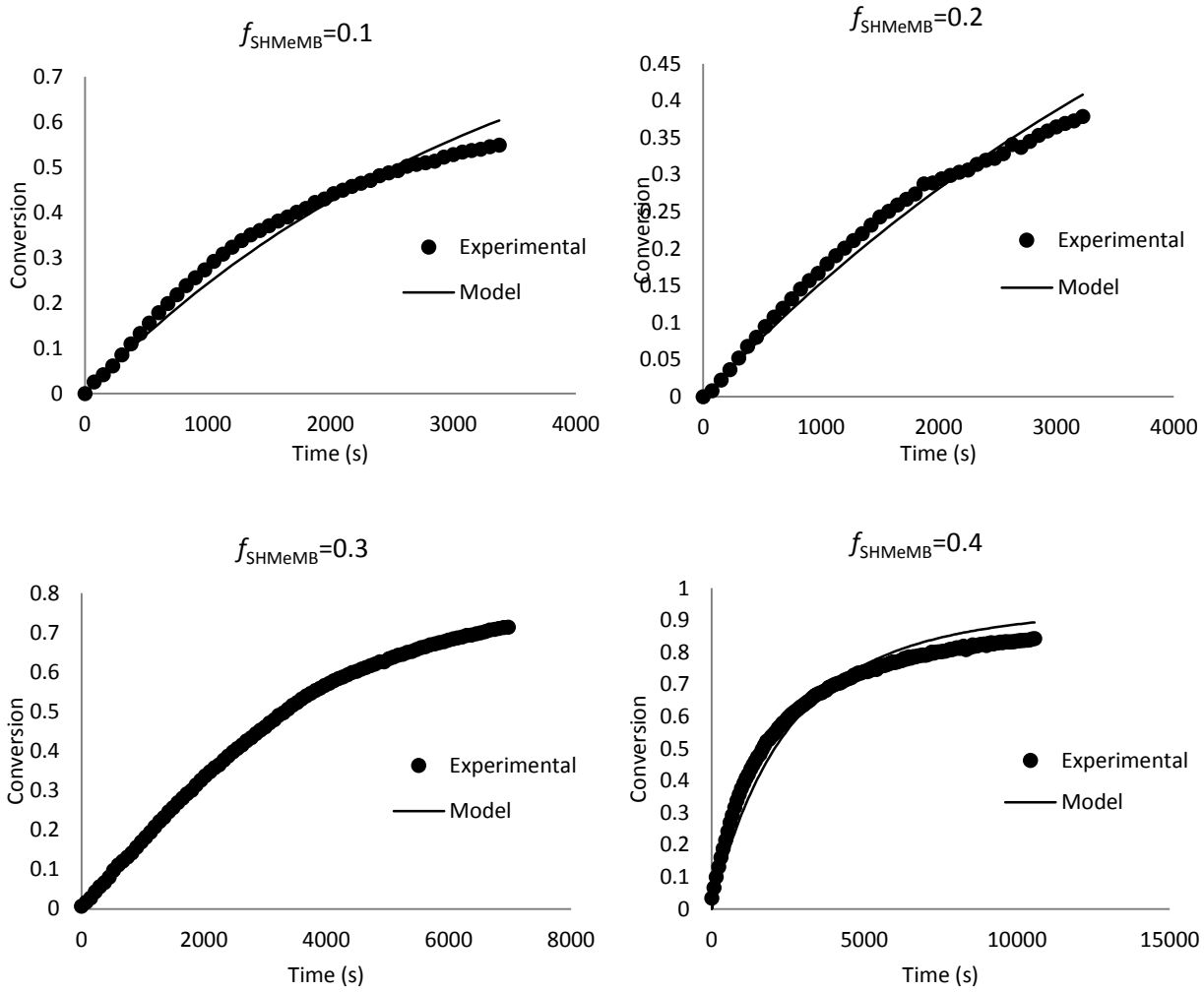

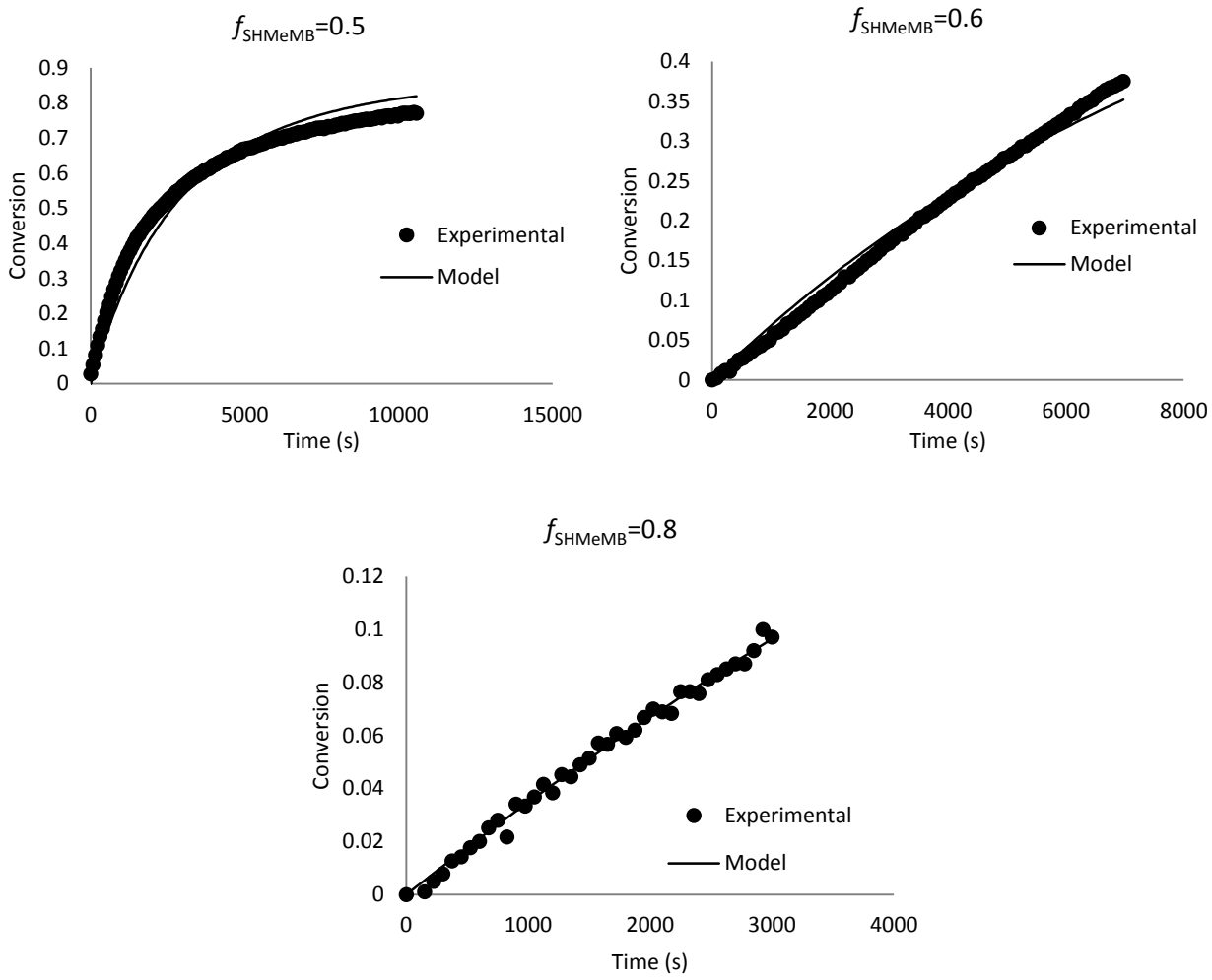

Figure A. 10: Conversion profiles of SHMeMB:AM copolymerizations at 15 wt% monomer concentration and 0.5 wt% V-50 at different molar compositions. The solid line represents simulated conversion to estimate k_t.

For all the copolymerization simulations, a $k_{p,AM}$ value of 86037 L/mol·s calculated at 15 wt% AM was used, even though it changes at different molar ratios of SHMeMB:AM. The $k_{p,AM}$ values were calculated at different total AM wt% in the copolymerizations as shown in Figure A. 10. However, changes in k_p^{cop} are negligible when calculated using the range of $k_{p,AM}$ values. SHMeMB:AM copolymerization with f_{SHMeMB}=0.8 at 50°C and 15 wt% monomer was also simulated using a $k_{p,AM}$ value of 104911 L/mol·s, The value of k_t was estimated to be 6.94 x 10^5 ± 2.55 x 10^4 L/mol·s, as opposed to 6.96 x 10^5 ± 2.56 x 10^4 L/mol·s

when using a $k_{p,AM}$ value of 86037 L/mol·s. Both values are very similar and within their 95% confidence intervals. This further shows that it is was adequate to assume one value for $k_{p,AM}$, as this did not affect the estimated values of k_t.

Table A. 5: Propagation rate coefficients of acrylamide calculated as a function of AM concentration for SHMeMB:AM copolymerization at 15 wt% and 50°C.

f_{SHMeMB}	AM wt%	$k_{p,AM}$ (L/mol·s)
0.1	12.8	89040
0.2	10.8	91810
0.3	8.9	94393
0.4	7.3	96791
0.5	5.8	99028
0.6	4.5	101118
0.8	2.1	104911

Table A. 6: Simulated SHMeMB and AM radical species concentration for estimation of k_t of SHMeMB:AM copolymerizations at 15 wt% with 0.5 wt% V-50 at 50°C.

f_{SHMeMB}	[SHMeMB*] (mol/L)	[AM*] (mol/L)	$f_{r,SHMeMB}$
0.1	1.88×10^{-7}	2.59×10^{-12}	0.999986224
0.2	2.23×10^{-7}	2.00×10^{-12}	0.999991031
0.3	4.60×10^{-7}	3.00×10^{-12}	0.999993478
0.4	1.14×10^{-6}	1.14×10^{-11}	0.99999
0.5	1.30×10^{-6}	2.12×10^{-11}	0.999983693
0.6	4.00×10^{-7}	2.11×10^{-12}	0.999994724
0.8	4.20×10^{-7}	1.68×10^{-12}	0.999996